# Surface Modification by Deposition and Thermal Decomposition of Transition Metal Cluster Halides

PhD Thesis
to the attainment of the academic grade of
doctor rerum naturalium (Dr. rer. nat.)
from the Mathematical and Sciences Faculty
of the University of Rostock

presented by
Ester Sala Bosch
born on the $20^{\text{th}}$ April 1982 in Olot (Spain)
from Rostock

Rostock, $2^{\text{nd}}$ September 2009

# Acknowledgement

# Declaration

I herewith apply irrevocably to take an oral examination in the form of a public scientific colloquium with examination character.

I herewith affirm that this work has been written and edited by myself without any help from others and that I have not used any other source than the ones mentioned in this work.

I herewith declare that this work has so far been submitted neither to the Faculty of Mathematics and Natural Sciences at the University of Rostock nor to any other scientific institution for the purpose of a PhD.

Rostock, $2^{nd}$ September 2009

Ester Sala Bosch

# Erklärung

Ich beantrage hiermit unwiderruflich, die mündliche Prüfung in Form eines öffentlichen wissenschaftlichen Kolloquiums mit Prüfungscharakter abzulegen.

Ich versichere hiermit an Eides statt, dass ich die vorliegende Arbeit selbstständig angefertigt und ohne fremde Hilfe verfasst habe, keine außer den von mir angegebenen Hilfsmitteln und Quellen dazu verwendet habe und die den benutzten Werken inhaltlich und wörtlich entnommenen Stellen als solche kenntlich gemacht habe.

Außerdem erkläre ich, dass diese Arbeit bisher von mir weder bei der Mathematisch-Naturwissenschaftlichen Fakultät der Universität Rostock noch bei einer anderen wissenschaftlichen Einrichtung zum Zweck der Promotion eingereicht wurde.

Rostock, 2. September 2009

Ester Sala Bosch

# Curriculum Vitae

|  |  |
|---|---|
| Birth date | 20.04.1982 |
| Birth place | Olot (Spain) |

| | |
|---|---|
| 1988-1994 | **Primary Education** - Escola Pia (Olot, Spain). |
| 1994-1998 | **Secondary Education** - I.E.S. Montsacopa (Olot, Spain). |
| 1998-2000 | **Baccalaureate -** I.E.S. Montsacopa (Olot, Spain). |
| 2000-2005 | **MSc in Chemical Engineering -** Polytechnic University of Catalonia (UPC-ETSEIB, Barcelona, Spain). |
| 2005 | **Diploma Thesis in Chemical Engineering** - "Palladium catalysts on carbon nanofibers for gaseous phase hydrogenation". Erasmus Programme, Polytechnic Federal University of Lausanne (EPFL, Switzerland). |
| 2006-2009 | **PhD in Chemistry – New Materials** - "Surface Modification by Deposition and Thermal Decomposition of Transition Metal Cluster Halides". Marie Curie Fellowship, University of Rostock, Inorganic and Solid State Chemistry Department (Rostock, Germany). |

# Lebenslauf

| | |
|---|---|
| Geburtsdatum | 20.04.1982 |
| Geburtsort | Olot (Spanien) |
| | |
| 1988-1994 | **Grundschule** - Escola Pia (Olot, Spanien). |
| | |
| 1994-1998 | **Gymnasium** - I.E.S. Montsacopa (Olot, Spanien). |
| | |
| 1998-2000 | **Abitur -** I.E.S. Montsacopa (Olot, Spain). |
| | |
| 2000-2005 | **Diplom Chemieingenieurwissenschaft** - Polytechnische Universität Kataloniens (UPC-ETSEIB, Barcelona, Spanien). |
| | |
| 2005 | **Diplomarbeit Chemieingenieurwissenschaft** - „Palladium Katalysatoren auf Kohlenstoffnanofasern für Hydrierung in der Gasphase". Erasmus-Programm, Eidgenössische Technische Hochschule Lausanne (EPFL, Die Schweiz). |
| | |
| 2006-2009 | **Promotion in Chemie – Bereich: neue Materialien -** „Oberflächenveredelung durch Abscheidung und Thermische Zersetzung von metallischen Cluster-Halogeniden". Marie Curie Stipendium, Universität Rostock, Abteilung Anorganische und Festkörperchemie (Rostock, Deutschland). |

# Abstract

To date, numerous methods for surface treatment constitute very important industrial processes of widespread use in a variety of engineering applications. A new, promising line of investigation is the use of transition metal cluster compounds to modify surfaces. In this work the use of metal-rich niobium halide cluster compounds with the formula $M_4^I[Nb_6Cl_{18}]$ ($M^I$ = Na, K or Rb) as precursor to achieve pure metallic niobium particles on the surface of a variety of metallic and non-metallic substrates has been investigated. To that effect, the influence on the particle size and morphology of the different deposition and decomposition methods as well as the precursor materials has been studied.

Niobium, like other transition metals, has refractive properties such as high melting point, high hardness and high tensile strength. This niobium coating is intended to modify the properties of the bulk material used as substrate, especially mechanical and thermal properties. Therefore, the hardness increase and the abrasion resistance of the resulting new coating composed of small niobium particles have been tested.

# Kurzdarstellung

Bis heute wurden bereits zahlreiche Methoden zur Oberflächenveredelung erforscht und haben an Bedeutung für die industrielle Anwendung gewonnen. Eine neue, viel versprechende Methode zur Optimierung der Eigenschaften von Oberflächen ist die Anwendung von Übergangsmetallclustern. In dieser Arbeit wird die Anwendung metallreicher Halogenidcluster mit der Formel $M_4^I[Nb_6Cl_{18}]$ ($M^I$ = Na, K, Rb) als Vorläufer für die Abscheidung metallischer Niob Partikel auf den Oberflächen verschiedener metallischer und nicht metallischer Substrate studiert. Demzufolge wurde der Einfluss der verschiedenen Abscheidungs- und Zersetzungsmethoden auf die Partikelgröße und Morphologie untersucht.

Durch die refraktären Eigenschaften des Niobs (wie zum Beispiel hohe Schmelztemperatur, hohe Härte oder hohe Bruchkraft) sollen die Eigenschaften des Substrates verbessert werden. Besonderer Augenwert liegt auf den mechanischen und thermische Eigenschaften. Deshalb wurden die Härte und die Abrasionsbeständigkeit der neuen beschichteten Proben gemessen.

x

# Nomenclature

bcc      Body centered cubic crystallograohic cell

CAMI    Coated Abrasive Manufacturers Institute, now part of the Unified Abrasives Manufacturers' Association.

CPA      Chirped Pulse Amplification

CVD      Chemical Vapour Deposition

DSC      Differential Scanning Calorimetry

EDX      Energy Diffractive X-ray Spectroscopy. Also known as EDS or EDXRF

FEPA    Federation of European Producers of Abrasives. Also designing the ISO standard 6344.

GC       Gas Chromatographer

HB       Hardness by Brinell

HK       Hardness by Knoop

HR       Hardness by Rockwell

HV       Hardness by Vickers

NIR      Near Infrared

NUV      Near Ultraviolet

PVD      Physical Vapour Deposition

SEM      Scanning Electron Microscope or Microscopy

SIT       Substrate Impregnation Technique

SIT-4    SIT method 4. Substrate Impregnation Technique with evaporation of the solvent at room temperature.

SIT-5    SIT method 5. Substrate Impregnation Technique with evaporation of the solvent in the sand bath (120°C)

SIT-6    SIT method 6. Substrate impregnation technique without evaporation of the solvent (atmospheric pressure and room temperature)

SIT-7    SIT method 7. Substrate Impregnation technique without evaporation of the solvent and pressure reduction (air removal, room temperature)

SIT-8    SIT method 8. Substrate Impregnation Technique without evaporation of the solvent, pressure reduction and deposition in a sand bath (air removal and 120°C)

SST      Cluster Solution Spreading Technique

SST-1  SST method 1. Cluster Solution Spreading and further drying in air (atmospheric pressure and room temperature).

SST-2  SST method 2. Cluster Solution Spreading and further drying using an ultra-sound bath (atmospheric pressure and room temperature)

SST-3  SST method 3. Cluster Solution Spreading and further drying using external heat (laboratory dryer, atmospheric pressure)

UV-Vis  Ultraviolet-visible

# Contents

# Chapter 1

# Introduction

## 1.1 Importance of materials and surface modification

In a much wider way than we usually realize, materials are present in our everyday life. Since the Prehistory, the need for better and stronger materials has always existed. Even early civilizations, as for example the Bronze or Iron Ages, based their developments in the domination of new materials and processing methods [1].

Surfaces are also of extreme importance since all interactions of the material with its environment (e.g. mechanical, thermal or chemical loads) have their origin in the surface [2]. In regard to this, surfaces must fulfil a series of functions in order to preserve the bulk material from the external loads. These functions include corrosion and wear resistance, defined tribological, optical and decorative behaviour and matched interface behaviour. The most important ones to be controlled by surface technology are typically corrosion and wear resistance.

Consequently, various methods for surface and material modification have been studied and several of them have become extremely important within the years. From the first baked pottery pieces and painted surfaces to the latest state-of-the-art coating processes, such as physical vapour deposition (PVD) or chemical vapour deposition (CVD), surface improvement has enjoyed significant industrial interest along the years, mainly for technical purposes, but also as decorative modifications [3].

In recent years the term advanced material has become increasingly adopted. This type of materials is used in high technological applications and is strictly designed in regard to the application they must fulfil. The most common examples can be found in computers, aircraft or rocketry [1].

As a subset of these *advanced materials*, the terms *nano-material* and *nano-science* have attracted recently the interest of many scientists. The main peculiarity of this kind of materials is that they behave differently compared to the bulk material. As expected, also *advanced* and *nano-scaled materials* have found their applications into the field of surface improvement

and surface modification. As examples, a series of materials with the properties of the Lotus effect® [4, 5] or several sorts of commercialized hardened car paints [6] are cited.

As seen in Fig. 1.1, the methods of surface modification and improvement can be divided into coating technologies, in which a layer of an external material is deposited on the substrate to be modified, and surface modification, in which some changes (chemical or physical) are applied to the substrate.
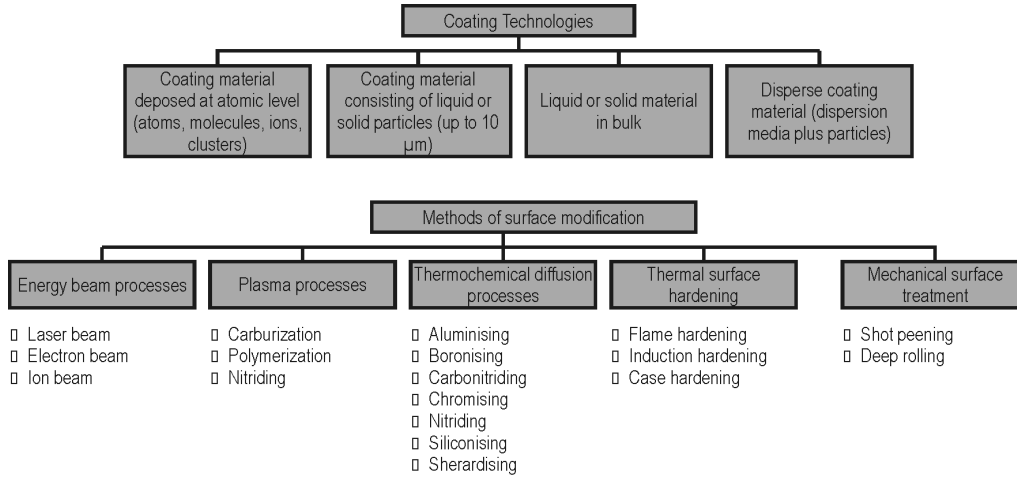


**Figure 1.1**: Classification of the known coating and surface modification processes. Extracted from [3].

## 1.2   Refractory metals

As known, some elements from groups 4 to 7 in the periodic table are called refractory metals. These metals have, among other important properties, high melting points and high tensile strengths. In a strict definition, only five elements can be considered as refractory materials: niobium, molybdenum, tantalum, tungsten and rhenium. Other wider definitions count up to ten elements, including also titanium, vanadium, chromium, zirconium and hafnium.

Thanks to this combination of properties, these metals and also some of their compounds have found very important and also very divergent applications. Two extremely important examples are their use in catalysis, mainly not as single metals but as supported metal compounds or mixed metal particles [7, 8] or as wear and thermal coatings, in the form of metallic thin films [9, 10].

### 1.2.1   Niobium[1.1]

Niobium is not a very common metal in the upper Earth layer, with an abundance in the crust of about 20 ppm [11]. Despite this fact, it can be found in all continents. It usually

---

[1.1]The information in this section is extracted from [11, 12].

appears not in a free state but in combination with tantalum. The most common mineral from which niobium can be obtained is the pyrochlore. It is usually found in the nature as niobates ($NbO_3^-$), which can be transformed using a multi-step reaction process into niobium pentoxide ($Nb_2O_5$) and finally to elementary Nb through a reduction with carbon monoxide.

The metal was discovered in 1801 by the English chemist Charles Hatchett and firstly named Columbium, although this was probably a mixture of Nb and Ta. The name niobium, coming from Niobe, the daughter of Tantalus in the Greek mythology, was officially adopted by the IUPAC in 1950.

The main producer of niobium is Brazil, with about 60 % of the total element amount and an annual production that has risen up in the last couple of years, going from 45'000 tones in 2004 to 70'000 tones in 2007 [13]. Also Canada, Nigeria and Zaire are large Nb producing countries.

Niobium belongs to group 5 of the periodic table, and is in many ways similar to the elements in group 4. It can react with almost all non metals at high temperature. Although it can exhibit all oxidation states from +5 to -1, the most stable state is +5. It has a slightly higher electronegativity than Zr and, due to the lanthanide contraction, has an almost identical size as Ta, although the latter is much heavier. As a consequence of the extra d electron in comparison with zirconium, the metal-metal bonds in the bulk are very strong. For that reason the melting and boiling points and enthalpy of atomization are much higher than for other elements with an atomic number similar to the that of niobium.

Metallic niobium is hard and has light grey metallic colour and a typical metal bcc structure and with a strength similar to that of steel. It also features high ductility and malleability, which implies that it can be very easily mechanically modified. Despite not being a noble metal, it has an extremely good corrosion resistance, thanks to its oxide passivation layer. Because of that, only hydrofluoric and hot concentrated sulphuric acid can damage the metal. It reacts easily with alkali bases. The optical microscope picture of the surface of the metal is shown in Fig. 1.2.
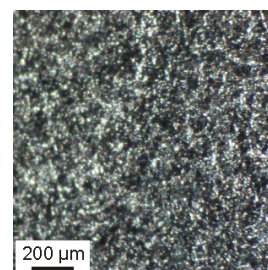


**Figure 1.2**: Niobium surface.

Due to its chemical stability, it is used as valuable material for chemical devices (spatulas, crucibles or husks) as well as instruments for surgeons and dentists (bone nails, clamps, implants or trephines). Niobium is also used as component in super alloys for applications requiring high heat, abrasion and corrosion resistance, as for example gas turbines. It can be also used to ennoble steel or in welded joints to increase strength. Some other common applications can be found in X-ray and electron guns, in getter elements in vacuum pumps or in thermal sensors.

### 1.2.2 Principles of cluster chemistry

From a chemical point of view, an interesting property of niobium and some other refractory metals (among other early transition elements as well) is the facility to form cluster compounds.

A cluster molecule represents in Chemistry an aggregate of at least two metal atoms with strong metal-metal bonds between them. They have an intermediate character between a molecule and a bulk solid. These metallic atoms are usually arranged in geometrical patterns (e.g. most commonly an octahedron with 6 metal atoms) and are stabilized by a ligand sphere. The term cluster was first introduced by F. Albert Cotton in the early 60s [14–16], and has aroused considerable interest since then[1.2].

**(a)**



**(b)**



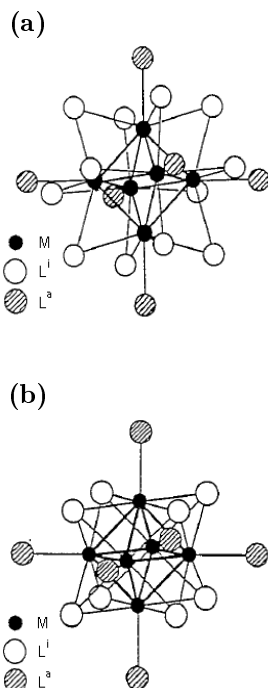**Figure 1.3**: Structures of the cluster units with octahedral metal cores (extracted from [19]).
(a) Cluster unit $[M_6L_{12}^iL_6^a]^n$.
(b) Cluster unit $[M_6L_8^iL_6^a]^n$.

The metallic units (M) that form the cluster core are usually surrounded by non-metal ligands (L) such as, for example, chlorido ($Cl^-$) or sulphido ($S^{2-}$) ligands. A first classification that can be done is between inner ($L^i$) and outer ($L^a$) ligands, which was introduced by Schäfer and von Schnering [20]. This classification describes inner ligands as non-metallic atoms bonded to two or more metal atoms in the cluster core and outer ligands as the ones bonded only to one metal atom in the cluster core.

In addition to this classification, another one can also be made depending on the bonding mode of the inner ligands to the metal core. In this case, two possible arrangements exist for the ligand atoms. On the one hand, the elements of the group 4 and 5 of the periodic table tend to have ligands bridging two metal atoms over the octahedral edges. In this case, this arrangement leads to a cluster with the general chemical formula $[M_6L_{12}^iL_6^a]^n$ (see Fig.1.3a). On the other hand, the elements in group 6 and 7 tend to have ligands bridging three metal atoms over the faces, what leads to clusters with the chemical formula $[M_6L_8^iL_6^a]^n$ (see Fig. 1.3b) [19, 21–30]. In both cases n can be positive, negative or neutral depending on the oxidation state of the metal core and the ligands.

Such cluster materials have some very interesting applications, also in the world of the advanced and nano-materials, for example their uses in catalysis, as precursors for catalytic metallic particles on inert substrates [31–33], in the design of magnetic and luminescent materials [34], or as ultra-low friction materials [35].

## 1.3  Particle deposition processes

Numerous particle deposition methods have been studied in the past [3]. Examples of these are the mentioned CVD and PVD, which allow the deposition of thin films on surfaces.

---

[1.2]The term "cluster" is used in various ways. In physics, it often refers to a small ligand-free particle of atoms, see for example ref. [17]. In coordination chemistry, "cluster" can often refer to multinuclear coordination compounds without direct metal-metal bonds. See for example ref. [18].

The work described in this thesis focuses on the methods using particle deposition from a precursor (e.g. halides, oxides or complex molecules), and not on the vapour phase techniques. Such processes have been known and successfully used since many years [32, 36]. Their use is especially common in the field of catalysis to achieve either mono-metallic or hetero-metallic catalysts [37].
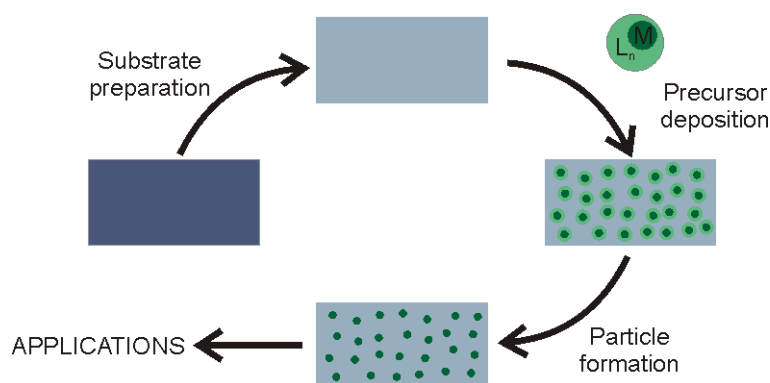


**Figure 1.4**: Scheme of the main steps of the synthesis of supported metal particles. According to [38].

The process has typically four basic preparational steps [38], which are shown in the scheme in Fig. 1.4. These steps are:

- Preparation of the substrate: All foreign species from the substrate are removed in order to increase the number of functional sites where the precursor particles can be deposited. This can be carried out for example using calcination, oxidation or cleaning.

- Deposition of the precursor: the compounds of the desired coating metal (usually salts) are deposited on the surface of the chosen substrate.

- Particle formation: The precursor compound decomposes into its metallic form and the non-metallic part is removed (e.g. ligands). This can be carried out, for example, through reduction or thermal decomposition.

- Properties testing and possible applications: Through testing of the substrate and surface properties, the potential applications of the coating can be defined (e.g. catalysis, conductive coating or hardening coatings).

The easiness and high efficiency of this procedure justifies the use of a similar method for the deposition and decomposition of the cluster halides used in this work.

# Chapter 2

# Goals and working procedure

## 2.1  Goals

The main goal of this project is to develop a new surface modification method using niobium cluster materials. These compounds will be used as precursors from which metallic niobium particles will be produced. These particles are expected to modify the properties of the substrate due to their refractory metal behaviour.

For each step of the general process described in Fig. 1.4 (substrate preparation, precursor deposition, particle formation and measurement of the properties and application) similar procedures will be tested and optimized. With this multiple-step procedure, a good distribution of the metallic niobium particles (homogeneously distributed on the surface and similar in size, ideally in the nanometre range) is expected to be obtained on a variety of substrates (e.g. metals, glass). The final goal is to develop a procedure to effectively deposit nano-scaled niobium particles on the chosen substrates.

Niobium features, among other interesting properties, high hardness and melting point, both typical of its refractory metal character (see section 1.2). As a result of that, the niobium coating is expected to modify the mechanical properties or thermal properties of the bulk material used as substrate. Therefore, the last one of the project goals is to observe and analyse these changes in properties and define possible applications for the new niobium coating (e.g. abrasion resistance coatings or thermal barrier coatings).

## 2.2  Overview of the chosen process

Following a method similar to the one described in section 1.3, cluster particles can be deposited and metallic niobium can be obtained on the tested substrates. This process, shown in Fig. 2.1, has also four steps: the preparation of the coating precursor, the preparation of the substrates, the deposition of the coating precursor, and the cluster decomposition. Finally,

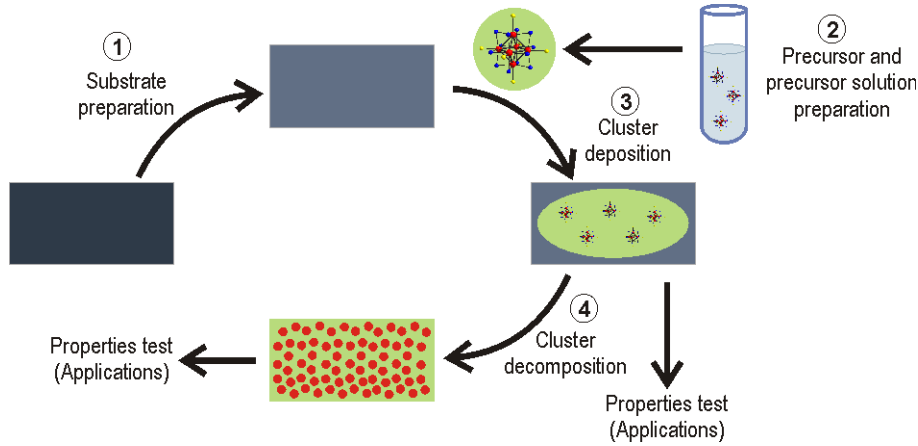also the improved properties of the new coated pieces are tested in order to define potential applications.



**Figure 2.1**: Main steps of the process to obtain metallic niobium particles on surfaces.

### 2.2.1   Preparation of the coating precursor

The preparation of the coating precursor, which is described in section 3.1, constitutes the first step of the process. In our case, the coating precursor is a known metal-rich niobium halide cluster compound with the chemical formula $M_4[Nb_6Cl_8]$ (with M being sodium, potassium or rubidium). This compound is chosen because of its easy synthesis process, its air stability and the fact that it is soluble in polar solvents. Moreover, the decomposition of these compounds is known to be possible at relatively low temperature [39]. The behaviour of the cluster compounds depending on the solvents is also described in section 3.1.

### 2.2.2   Preparation of the substrates

The second step of the process is the selection and preparation of the substrates on which the cluster will be deposited. These substrates are either in the shape of foils or in the shape of granules or chunks. For the foils, the preparation consists on cutting the material in pieces of the desired size and cleaning of these pieces with acetone in order to remove the grease and external particles from the surface. For the granule-shaped and chunk-shaped pieces, only the cleaning of their surfaces with acetone is carried out, no cutting is done on these pieces. These preparation processes, as well as the effect of the passivation oxide layer present on the surface of the substrates will be described in detail in section 3.2.

### 2.2.3   Deposition of the coating precursor

The deposition of the niobium cluster precursor on the substrates constitutes the third step of the process. This step will be thoroughly described in section 3.3, where the development

of the process on different substrates and different deposition methods is described. For this purpose, metallic substrates have been chosen from different groups of the periodic table (from the main groups and the transition metals). Substrates similar to niobium (with similar atomic number, e.g. zirconium and molybdenum) and substrates with irregular shapes (e.g. granules or chunks) will also be investigated. In order to study the deposition behaviour on non-metallic surfaces, glass substrates will be used. Finally, the growth behaviour and the deposition and formation mechanisms of the cluster particles on the substrate will be analysed and evaluated.

In order to study the appearance of the samples, they are analysed with a scanning electron microscope. SEM pictures are taken in order to study the size and distribution of the deposited particles, and EDX-graphs and chemical mappings are produced in order to characterize the distribution of the elements on the substrate.

The deposition of other niobium cluster compounds is also performed in order to investigate the effect of the ligands on the coating process. The clusters $[K(MeOH)_4]_2[Nb_6(OCH_3)_{18}]$ (niobium octahedral core with methanolate ligands in the inner and outer positions) and $[Nb_6Cl_{14}(H_2O)_4] \cdot 4\,H_2O$ (water-based cluster with a niobium octahedral core, Cl ligands in the inner position and Cl and aqua ligands in the outer positions) are used for that reason (see chapter 3.5).

### 2.2.4  Cluster decomposition

The fourth and last step of the process is described in section 3.4. In this step, the decomposition of the cluster particles on the surface is achieved and elemental metallic niobium particles are obtained.

As already described at the beginning of this chapter, the decomposition process of the cluster is known and a method based on this process will be used. This decomposition is achieved by applying energy to the cluster coated substrate. In this section, the differences between the two types of decomposition studied (heat and laser decomposition) will be described.

Finally, the observed differences in process behaviour depending on the substrate type and the precursor deposition method will be exposed, as well as the influence of the process parameters on the final metallic particles.

As in the case of the precursor deposition, the samples have been also analysed using SEM techniques. With the use of EDX and chemical mapping, the absence of chlorine and the alkali metal can be confirmed, and therefore the decomposition of the cluster can be assured.

Similar to the niobium precursor deposition, the decomposition of the methanolate-based and the water-based cluster have been studied. These results are shown as well in section 3.5.

### 2.2.5   Property tests and applications

As described in section 2.1, one of the goals of the project is to study the possible applications of these novel niobium-based coatings. To that purpose, the last chapter of this project is devoted to the description of the properties of these new coatings and their possible applications (see chapter 4).

Firstly, being metallic niobium very hard and featuring a high melting point, the coating could be expected to become a hardening / abrasion resistance coating. Therefore, this characteristic compared to that of the pure metal has been tested. The results are reported in section 4.2.

Secondly, in order to investigate the adhesion of the coating to the substrate, scratch tests have been conducted. The results are shown in section 4.3. With favourable results, the coating could find applications as a protection against abrasion or wear.

Finally, a good chemical adhesion of the precursor to the substrate along with a reduced particle size will lead to the application of these cluster particles as supported catalysts. Therefore, the catalytic effect of cluster particles deposited on glass has been investigated. These results obtained are found in section 4.1.

# Chapter 3

# Results and discussion

## 3.1 Preparation of the coating precursor

The first step of the coating procedure is the preparation of the cluster halide powder and the precursor solution. These procedures are described in the next sections.

### 3.1.1 Niobium cluster compounds

As described in section 1.3, a salt of the desired metal is required for the deposition and obtention of small metallic particles on surfaces. In the case of niobium, the most common compounds are halogenides (chlorides) and oxides. According to the work of Prokopuk and Shriver, chlorido ligands can be easily adsorbed on metallic surfaces [40], therefore the cluster $M_4^I[Nb_6Cl_{18}]$ ($M^I$ = Na, K, Rb) constitutes a good precursor for the deposition of niobium on surfaces.

With regards to the chlorides, niobium (V) chloride hydrolyzes easily in contact with air and moisture, and for this reason it must be handled in an inert atmosphere (e.g. in an argon box). A good alternative to these compounds are the niobium cluster chlorides with the chemical formula $M_4^I[Nb_6Cl_{18}]$ with $M^I$ being sodium, potassium or rubidium. These are the compounds that will be studied in this work as novel precursors for metallic niobium coatings. Moreover, these compounds already contain a metal particle in the core (octahedron of Nb atoms).

The compounds are obtained in the form of dark green powders (almost black to the naked eye), as shown in Fig. 3.1. The preparation of the niobium cluster chloride follows a solid state chemistry reaction at high temperature similar to the one described by Fleming et al. in the early sixties [23]. This process can be described by the reaction in equation 3.1. The chemical structure of the cluster anion is shown in Fig. 3.2.
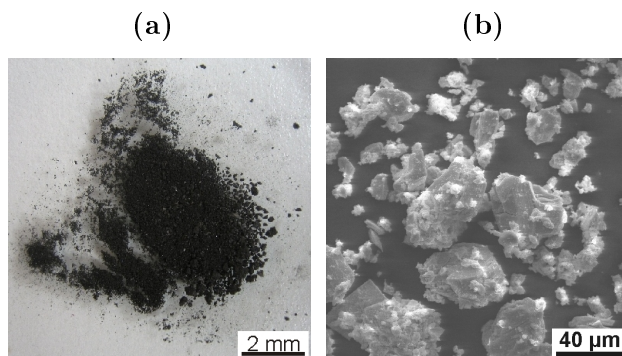
$$20\,M^ICl\,+\,14\,NbCl_5\,+\,16\,Nb\,\xrightarrow{\Delta}\,5\,M_4^I[Nb_6Cl_{18}] \qquad (M^I\,=\,Na,\,K,\,Rb) \qquad (3.1)$$
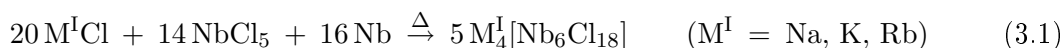
**Figure 3.1**: Niobium cluster chloride powder ($Rb_4[Nb_6Cl_{18}]$). **(a)** Photograph. **(b)** SEM Micrograph.

For the preparation of halide-based niobium cluster compounds, alkali chlorides $M^I Cl$ ($M^I$ = Na, K, Rb) are sublimed in a furnace at 810 °C (NaCl), 780 °C (KCl) or 720 °C (RbCl) during 4 to 5 hours under reduced pressure (approximately $10^{-6}$ mbar) and cooled down afterwards. This process is carried out in order to remove impurities and moisture in the chloride compounds. A quartz glass ampoule is filled with the alkali chloride (approximately 2 to 4 g depending on the alkali metal in the chloride), $NbCl_5$ (approximately 5 to 7 g depending on the alkali metal in the chloride) and approximately 3 g of metallic niobium (in excess). Due to the easy hydrolization of $NbCl_5$ in air, this process must take place inside the protective atmosphere of an argon glove box.

This glass ampoule is afterwards taken out of the glove box and sealed under high vacuum. The mixture is placed in a furnace for about a week. The temperature is increased in three steps: from room temperature to 350 °C (this last held during 2 days), than up to 500 °C (2 days), and finally to 800 °C (3 days).

In order to confirm the purity of the solid halide cluster compound, the dark green powder is analysed by X-ray powder diffraction using a GUINIER camera (Enraf-Nonius; Type: FR552) on X-ray photo film (Kodak® BioMax MR). For the measurements, the X-Ray tube (CuK$\alpha$ beam; $\lambda = 0.154056$ nm) works with a current of 27 mA and a voltage of 40 kV. The film is taken out of



**Figure 3.2**: Structure of the cluster anion $[Nb_6Cl_{18}]^{4-}$. The $i$ (inner) and $a$ (outer) notation is described in section 1.2.2 (extracted from the work of Schäfer and von Schnering [20]).

the camera after two hours of exposure and is afterwards developed and fixed using the products of the Eastman Kodak Company. The detection limit of crystalline phases is expected to lie by approximately 5 %.

With the use of this synthesis it is possible to easily obtain the cluster compound in very good yield (approximately up to 10 g per reaction). Furthermore, this compound is soluble in polar solvents and is air stable (no need to work under a protective atmosphere). The decomposition process of the cluster is also known, which gives the possibility to obtain metallic particles
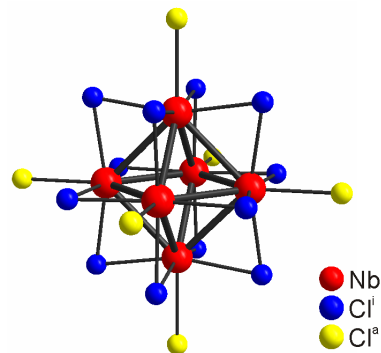
afterwards.

### 3.1.2 Preparation of the cluster solution

A precursor in liquid state is regarded as the best alternative to achieve a good distribution of the niobium precursor on the surface since, in this state, the precursor molecules are homogeneously distributed and can be homogeneously deposited. Therefore, a solution of the cluster chloride has been chosen as niobium precursor carrier for the deposition.

After synthesis and analysis, the cluster powder is dissolved in the chosen solvent. To this effect, a glass ampoule is filled with the cluster powder and the solvent and the air inside the ampoule is removed with the help of a vacuum pump. The ampoule is afterwards sealed and placed in a sand bath at approximately 110 °C during 24 to 48h. After this time, the majority of the cluster powder is dissolved. Undissolved products are filtered off with a filter paper with medium pore size. The formed saturated cluster solution contains approximately 10 mg of cluster per ml of solvent (approximately 6.50 to 8 $mol \cdot l^{-1}$)

The solvents that have been studied in this work are methanol, acetone, ethanol and water. The best results of solubility and subsequent particle distribution were achieved with the use of methanol. The resulting dark green solution is shown in Fig. 3.3. For the experiments, a constant precursor concentration was used in order to be able to compare and measure the dependence of the deposition on all other parameters.
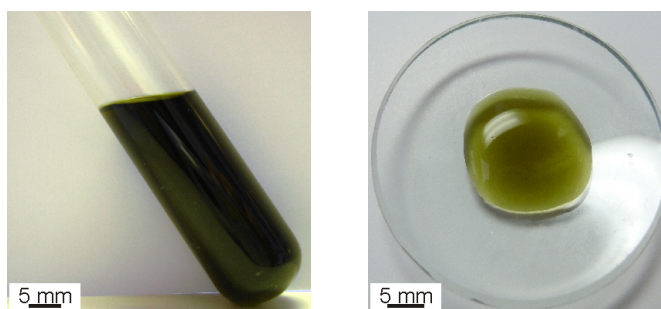


**Figure 3.3**: Cluster solution: $Rb_4[Nb_6Cl_{18}]$ in Methanol after filtration.

The use of acetone led mostly to a brown coloration of the solution. It has been reported in the literature that a brown coloration in a niobium cluster solution in methanol typically indicates an oxidation of the cluster core [41]. It is supposed that, since these cluster molecules are good reducers, they can easily reduce the ketone to alcohol and oxidize at the same time. This would explain the coloration observed, which would supposedly refer to a formation of the $[Nb_6Cl_{18}]^{3-}$ anion. The results achieved using the acetone solution typically featured small particle sizes (smaller than the ones obtained using a methanol solution) but a quite inhomogeneous macroscopic distribution of the deposited particles. For this reason, the use of acetone as solvent has not been further investigated.

Early research in our laboratory indicated that the outer chlorido ligands can be easily exchanged for methanolate ones in methanol under heating, obtaining $[\text{Nb}_6\text{Cl}_{12}(\text{CH}_3\text{OH})_4\text{Cl}_2] \cdot 6\,\text{CH}_3\text{OH}$ [42]. Since this cluster has similar properties to the one with only chlorido ligands and can also be decomposed with the help of energy, it supposes no problem for the aim of this work and no further analyses have been carried out to confirm the presence of this compound.

## 3.2    Preparation of the substrates

The chosen substrates for the deposition of the cluster have been metals (aluminium, copper, molybdenum and zirconium) as well as commercial laboratory glass. These substrate materials are used in the form of foils. With the use of these substrates small particle sizes and homogeneous distributions can be obtained. In order to study the deposition on substrates with more complicated surfaces, also materials in the form of chunks or grains (chromium, lead, tin and zinc). All substrates are cut and washed prior to use[3.1].

### 3.2.1    Acetone cleaning

Due to the hydrophobic character of grease molecules, polar solvents are repelled and consequently the deposition of the particles is reduced. This would lead to an inhomogeneous distribution of the precursor particles, both macroscopically and microscopically. In order to avoid this, the surface of the substrates is cleaned with acetone prior to use.

It has been confirmed that this acetone cleaning has no effects on the surface of the substrates other than the removal of the grease. No structural and / or morphological differences have been reported on the surface between the pre- and post-cleaning states. An example of the acetone treatment results is shown in the scanning electron microscope (SEM) micrographs in Fig. 3.4, where no differences can be seen on the surface structure of Zr before and after the treatment.

### 3.2.2    Effect of the passivation oxide layer on metals

As mentioned in section 2.2.2, the metals used as substrates in this work feature thin passivation layers on their surfaces. In order to study the effect of this layer on the distribution and sizes of the cluster particles, some experiments have been carried out in which the cluster solution is deposited on substrates that have been polished under an argon atmosphere[3.2]. Some examples

---

[3.1]Only metal foils and glass were cut prior to use. Chunks, grains and granules were used as received (after an acetone cleaning).

[3.2]Polished substrates refer to those from which the external layer of material is removed with the help of a sand paper under an argon atmosphere. The deposition is also carried out under the protective atmosphere or using Schlenk techniques.
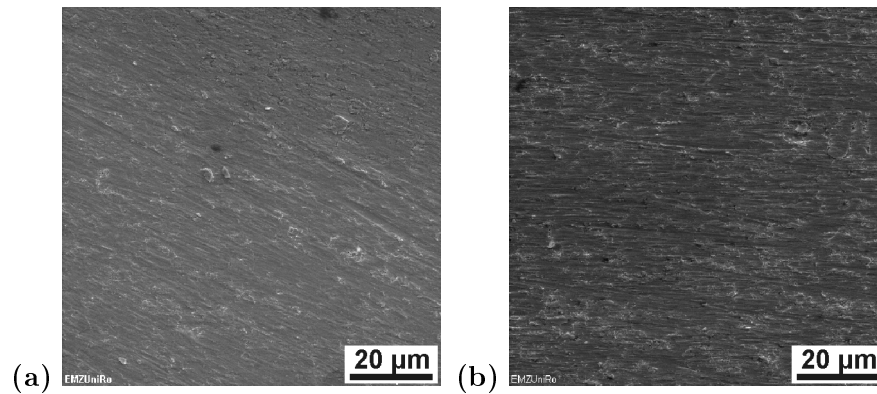
**Figure 3.4**: SEM micrographs of zirconium foils before deposition, **(a)** before the acetone cleaning and **(b)** after acetone cleaning.
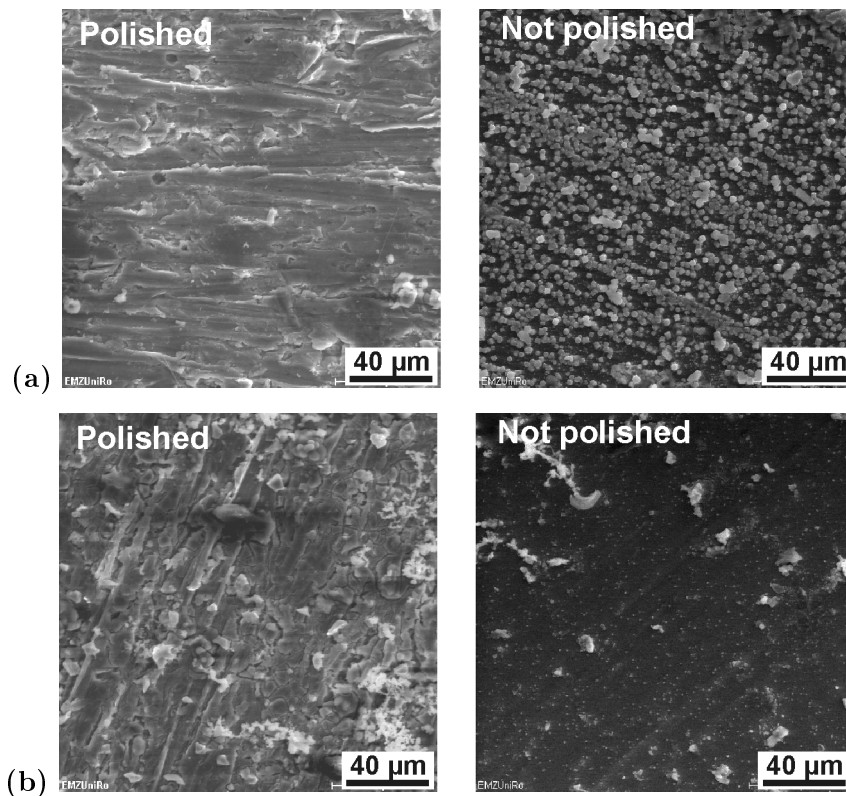


**Figure 3.5**: Deposition on polished surfaces. Effect of the polishing treatment on the deposition of the cluster particles using **(a)** *Solution Spreading Technique* (SST) and **(b)** *Substrate Impregnation Technique* (SIT).

of the deposition on polished substrates compared to the results of the deposition on untreated surfaces are shown in Fig. 3.5.

As it can be observed in the SEM pictures in Fig. 3.5, whenever the polishing is applied, the surface becomes rougher and more irregular. These superficial imperfections, instead of providing more locations where the precursor can attach to the surface, have been observed to effectively reduce the amount of material that can be deposited on the surface. This fact is also

confirmed by the decrease of the amounts of the deposited Nb, Cl and Rb to approximately 15 % to 20 % of the values of the not polished samples.

The lack of metal oxide on the surface could be another possible reason for this reduced amount of cluster deposited. However, due to the fact that the polishing pre-treatment did not yield any increase in the amount of deposited precursor, the investigations were not further continued and the hypothesis that the passivation layer can positively influence the deposition efficiency has not been confirmed. However, it has been demonstrated that surface preparation can play a very significant role for the success of the precursor deposition. Flat polished surfaces are the ones where the best results for precursor deposition have been observed and are the ones that have been used for the rest of the work.

## 3.3  Deposition of the halide based precursor

In order to obtain homogenously distributed nano-scaled cluster particles on the substrates, several process parameters have been varied and their influence on the deposition has been studied. The resulting distributions and sizes of the particles have been analysed with a scanning electron microscope. EDX and chemical mapping have been also performed on the samples in order to characterize the distribution of the elements on the surface.

### 3.3.1  Deposition methods

The tested deposition methods can be classified in two main groups that will be referred to as "*Solution Spreading Technique*" (SST methods **1**, **2** and **3**) and "*Substrate Impregnation Technique*" (SIT methods **4** to **8**). These methods are shown in the scheme in Fig. 3.6.
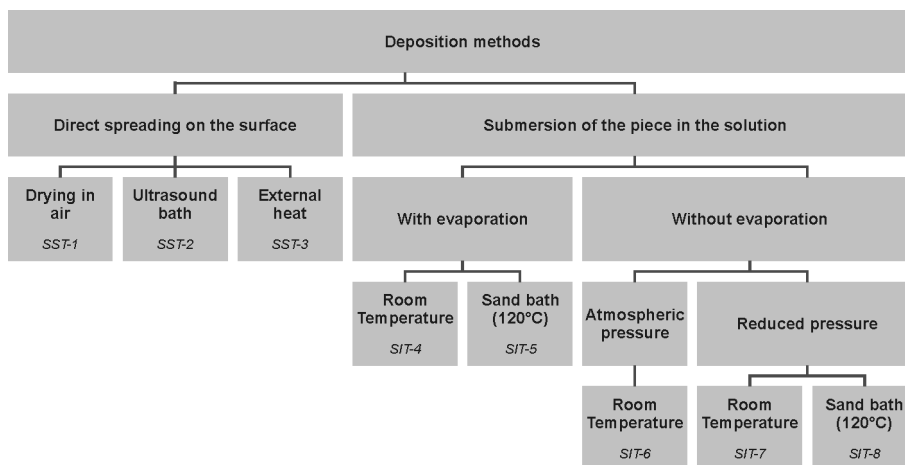


**Figure 3.6**: Methods for precursor deposition.

### 3.3.1.1 SST

Differences in the size, distribution and morphology of the deposited particles could be achieved by changing parameters such as temperature of the solution, pressure of the system or method of application of the carrier solution. The type of substrate has been also observed to play a significant role in the final appearance of the coated substrates.

**SST-1** Regarding the solution spreading technique (SST), the main process consists in bringing the solution directly on the surface of the substrate and evaporating the solvent to obtain cluster particles. This can be accomplished, for example, by simply letting the piece dry in air at room temperature. As described in sections 3.3.2, 3.3.3 and 3.3.4, when using this technique, the particles reach sizes between 1 µm and 5 µm with homogeneous distributions over the substrate. A scheme of this process is shown in Fig. 3.7.
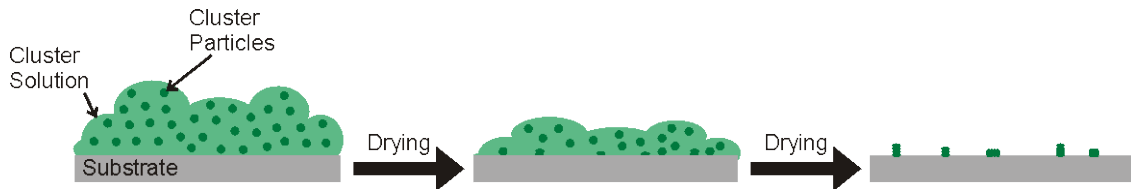


**Figure 3.7:** Solution spreading technique, drying in air at room temperature.

Concerning the experimental details, typically about 0.5 ml of the cluster solution are spread on the surface of the foils (approximately 2 x 3 cm, Al, Cu, Mo and Zr; approximately 1 x 1.2 cm, glass) and 5 to 10 drops (0.2 to 0.5 ml) on the surfaces of the grains, granules and chunks (Cr, Pb, Sn and Zn). The pieces are afterwards left drying in air overnight.

**SST-2** Some differences on the cluster particle sizes can be introduced with the use of an ultra-sound bath. The waves produced by the device produce an effect on the cluster particles in suspension that results on a more homogeneous deposition than in the case of SST-1. The comparison between the results of SST-1 with the results of SST-2 confirms that more homogeneous particle distributions and smaller particle sizes can be achieved with SST-2.

With regards to the experimental details, the deposition of the cluster solution for SST-2 is carried out in a similar manner as SST-1. For this deposition method, the pieces are placed inside a beaker, which is partially submerged in the ultrasound bath (without contact with the walls). The solution is brought onto the substrate and immediately afterwards the device is switched on. The pieces remain in the bath until they are completely dry.

**SST-3** Another possible parameter modification that can be tested is the variation of drying rate of the piece. This can be accomplished by applying heat to the pieces, for example, with the help of a laboratory hand dryer. With the increased temperature of the pieces, the solvent

evaporates faster and the particles, whose movement is faster due to the high temperature, tend to form smaller aggregates. Using this method, the particles reach sizes with an upper threshold of 1 μm, which are smaller than the sizes obtained by SST-1 and SST-2. The distributions are also more homogeneous than with SST-1 and SST-2.

The heat needed for this method is provided by a laboratory dryer (Steinel HL 1502 S, 1600W, air at approximately 200 °C). The solution is deposited on the surface in a similar manner as in SST-1 and immediately afterwards the external heat is applied for 1 to 2 minutes at a distance of about 10 cm, until the substrate is completely dry.

### 3.3.1.2   SIT

The second large group of deposition methods is the so called *"Substrate Impregnation Technique"* (SIT). With this method, the pieces are submerged in the cluster solution for a certain amount of time. This is similar to the process used by Prokopuk and Shriver in their work [40], in which they deposited monolayers of $[Bu_4N]_3[Nb_6Cl_{12}X_6]$ (X = F, Br, Cl, I) on gold and silver surfaces. Varying some parameters in the deposition method, some differences on the arrangement and size of the deposited particles can be achieved.

**SIT-4**   The first variation consists in the submersion of the sample in the cluster solution and a further evaporation of the solvent while the substrate is still immersed in it. A scheme of this process is shown in Fig. 3.8.
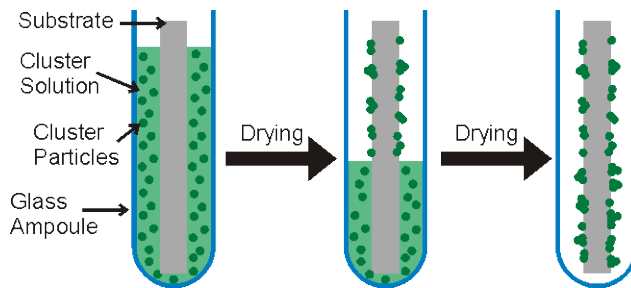


**Figure 3.8**: Substrate impregnation technique with solution evaporation.

Concerning the experimental details, in general for SIT, the substrates are placed inside a reaction tube and a quantity of cluster solution is added until the sample is completely covered (between 0.5 to 2 ml, depending on the substrate). For this methodology, the reaction tube is left open and the solution dries (evaporation of the solvent) overnight[3.3] in the extraction hood. Once the solvent is totally evaporated, the piece is taken out of the tube.

With the use of this treatment, a large amount of cluster precursor is deposited on the surface and the distribution as well as the size of the particles becomes quite inhomogeneous. Being

---

[3.3]The evaporation process has not lasted longer than 12h in any case.

the concentration of the cluster precursor solution used for all methods always the same, a possible explanation for this behaviour is just the large amount of solution applied over the substrate and, consequently, a large amount of cluster material. The abundance of deposited cluster precursor particles together with the very rapid evaporation of the solvent have the effect that the particle sizes grow larger, reaching mean size values between 2 and 10 µm.

**SIT-5** A second variation of the SIT method can be achieved by applying external heat during the evaporation of the solvent. In this case, the substrate pieces are also submerged in the solution and left overnight for evaporation of the solvent. However, this evaporation takes place in an open ampoule in a sand bath with a temperature of approximately 110 °C that provides the external heat. A scheme of this process is also presented in Fig. 3.8.

As in the case of SIT-4, the observed particle sizes the particle distribution are rather inhomogeneous. However, due to the higher temperature (compared to SIT-4), which leads to an increased mobility of the particles in solution and to a faster drying of the piece, the particle sizes are in general smaller than in the case of the evaporation at room temperature. In addition to that, another possible contributing factor for the smaller particles size would be the increased number of nucleation sites due to the increased temperature. This results in a larger amount of particles that can be deposited, which have consequently smaller particles sizes. In some occasions an extremely rapid drying can result in the formation of a clay-like covering of the piece, which leaves micro-cracks in the coating (an example for Al is shown in Fig. 3.12b). Overall, the upper and lower thresholds of the obtained particle sizes can be set at 800 nm and 3 µm respectively.

**SIT-6** Another subgroup of methods are the so called substrate impregnation techniques without evaporation of the solution. In this case the deposited particles are purely chemically bonded to the substrate and, therefore, the adhesion of the coating is higher. The first one of these methods is the SIT without evaporation of the solvent under atmospheric pressure and room temperature. The deposition using this method is achieved with the samples being placed in a closed reaction tube and left there for up to 50 days. A scheme of this process is shown in Fig. 3.9.
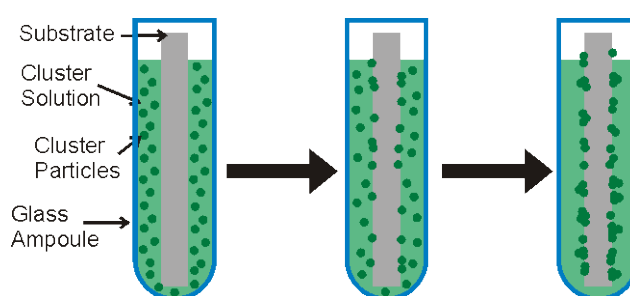


**Figure 3.9**: Substrate impregnation technique without solution evaporation, under atmospheric pressure (SIT-6) or under reduced pressure (SIT-7 and SIT-8).

In order to achieve this deposition, the uncoated samples are placed inside the reaction tube and the solution is added until the sample is completely covered (between 0.5 and 2 ml, depending on the substrate). The tube is covered with the lid and it is secured with Teflon band in order to avoid any evaporation of the solvent. After the chosen deposition time, the substrates are taken out of the tube and the excess of solution is carefully dried with absorbent paper.

Homogeneous distributions and small particle sizes can be achieved with the use of this method, especially for the case in which glass is used as a substrate (see Fig. 3.22, SIT-6), where mean particle sizes of 1 µm have been observed. For the case of the metals, the particle sizes obtained range between 1 and 3 µm. However, these tend to gather in larger groups of up to 10 µm. Due to the presence of air and moisture in the system, some substrates can be damaged in the process (as for example the surface of the copper substrates, see Fig. 3.10). Apparently, the oxygen present in the environment of the sample starts a surface degradation process that results in the damage of the surface of the substrate.



**Figure 3.10**: Oxidation process on a Copper substrate, due to the deposition of $Rb_4[Nb_6Cl_{18}]$ using SIT-6.

**SIT-7, SIT-8**   In order to avoid the oxidation of some pieces, the method SIT-7 has been developed, in which the substrate impregnation is carried out under reduced pressure. In this method the sample is placed in a glass ampoule and the solution is added until the sample is completely covered (between 0.5 and 2 ml, depending on the substrate). The air inside this tube is removed (reducing the pressure) with the help of a vacuum pump. Afterwards, the ampoule is sealed using a conventional glass burner with a high temperature flame. The piece stays in solution for up to 50 days.

Another change can be done in which the sample is exposed to external heat during the deposition time (SIT-8). This is achieved by placing the sealed ampoule that contains the substrate in a sand bath with a temperature of approximately 110 °C. As in the case of SIT-6, after the deposition time, the samples are taken out of the tube and the solution excess is dried carefully with absorbent paper. A scheme of both methods SIT-7 and SIT-8 is shown in Fig. 3.9.

With these methods homogeneous particle distributions can be achieved, especially with the use of the high temperature process. When SIT-8 is applied, the resulting particles are smaller and better defined than with SIT-7. The particle sizes for the deposition with external heat (SIT-8) vary from 800 nm to 4 µm, whereas those for the room temperature deposition (SIT-7) can reach up to 15 µm.

The oxidation of the samples can indeed be prevented by using SIT-7 and SIT-8, which is confirmed by the fact that no precipitated materials appear and the colour of the solution does

not change during the deposition time. However, it must be taken into account that the piece can slightly oxidize once taken out of the solution. In order to avoid that, the substrate must be immediately dried after deposition.

### 3.3.2 Deposition on metals[3.4]

The goal of this part of the work is to investigate the dependence of the deposition of the cluster precursor and the particle sizes on the type of substrates. A total of 4 different metallic foils have been used as substrates, which contain metals from the main groups and from the transition metal groups.

#### 3.3.2.1 Aluminium

Aluminium is a metal with a silver-white appearance and relative low density and hardness. It has very good electric and thermal conductivity. Despite its base metal character, it is not affected by air and moisture thanks to the passivation caused by an external oxide layer. This layer can also avoid the dissolution of aluminium in solvents between 4.5 and 8.5 in pH. However, if it comes in contact with strong acids or bases, the $Al_2O_3$ layer is chemically removed and the metal can be damaged. The untreated microstructure of the aluminium surface seen using optical microscope is shown in Fig. 3.11.
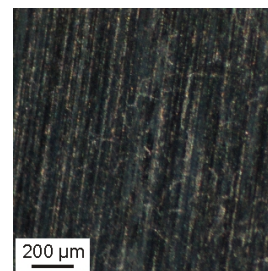


**Figure 3.11**: Al surface.

The metal is received in the form of a three-centimetre-wide and 0.3-millimetre-thick band (Merck, purity >99.9 %, trace metals, <0.02 %). The substrate is cleaned with some drops of acetone prior to use. Pieces of approximately 2 x 3 cm for the SST methods and 1 x 1 cm for the SIT methods are used.

The deposition on aluminium has provided interesting results when the solution spreading technique is used, especially SST-3, as shown in Fig. 3.12a. Homogeneous distributions have been achieved for all three SST methods. As it was expected, the best results with regards to particle size are achieved with the methods using external influences to evaporate the solvent (SST-2 and SST-3). In these cases, the smallest particles observed feature diameters from 400 nm to 2 µm and have been obtained with the SST-3 method. However, SST-1 is the method that allows the deposition of the biggest amount of cluster. The SST-2 method has been observed to be a compromise between the amount of cluster precursor deposited and size of the particles obtained.

---

[3.4]The descriptions of the metals in this section are extracted from [12].
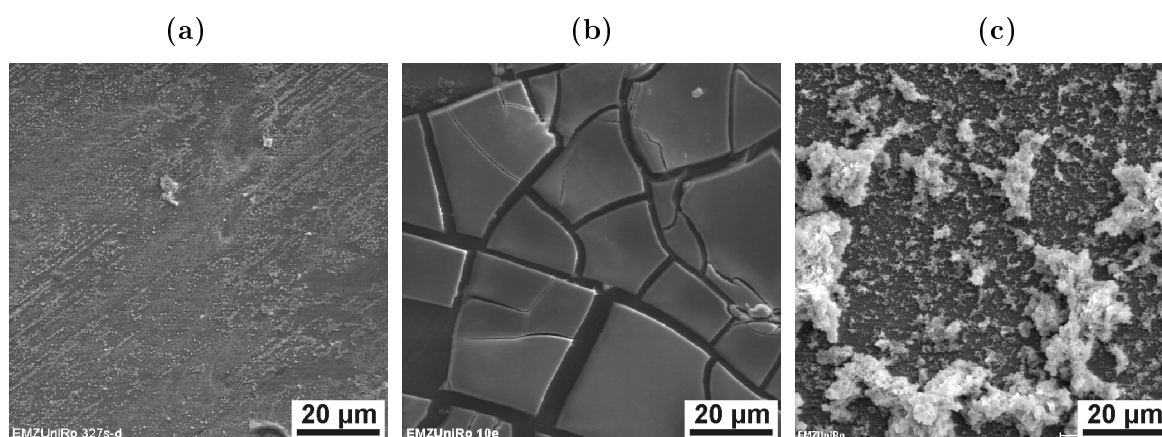
(a)                   (b)                   (c)



**Figure 3.12**: Cluster particles on aluminium deposited by **(a)** SST-3 **(b)** SIT-5 and **(c)** SIT-8.
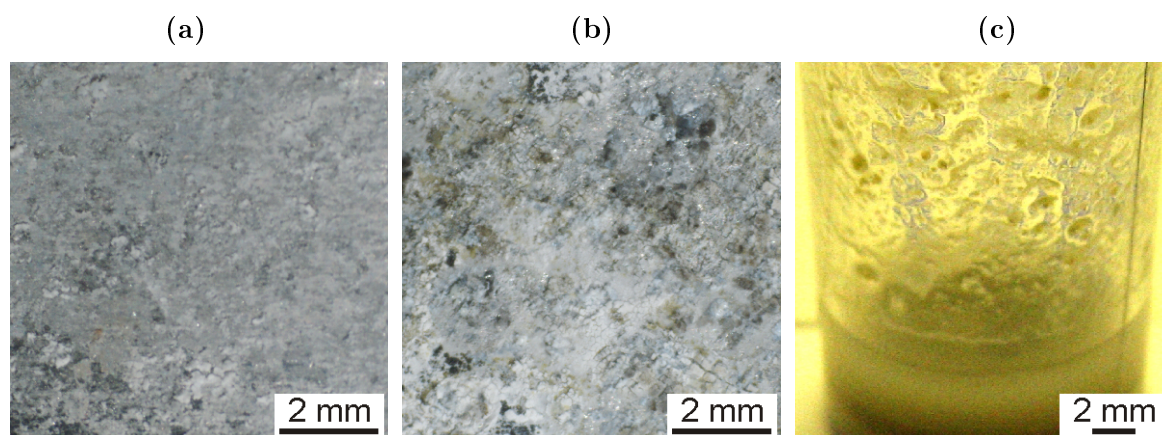
(a)                   (b)                   (c)



**Figure 3.13**: Deterioration of aluminium substrates during the deposition of $Na_4[Nb_6Cl_{18}]$ using SIT-8. **(a)**, **(b)** Partial deterioration of the surface. **(c)** White powder-like substance on the walls of the reaction tube coming from the decomposition of Al.

Regarding the SIT methods, the distribution of the particles is less homogeneous and particle aggregates are formed, reaching sizes up to 30 µm. An example of this phenomenon is shown in Fig. 3.12c. Nevertheless, the individual particles forming these aggregates are rather small, with sizes ranging from 800 nm to 2 µm. As commented in section 3.3.1, when an extremely fast evaporation of the solvent is used for this substrate (SIT-5), an homogeneous layer with some micro-cracks on the surface (clay-like substance) is obtained. This is probably due to the sand bath elevated temperature (approximately 110 °C) and the amount of solution rather than caused by the surface structure of aluminium. An example is shown in Fig. 3.12b. The fact that the amounts of Nb, Cl and the alkali metal in this continuous coverage showed by the EDX graphs were very low, makes it not suitable for the purpose of this work. Therefore, despite the good coverage of the substrate, it has been declined as coating procedure.

Due to the passivation layer and the rather inert character of $Al_2O_3$, almost no oxidation could be observed for the deposition on aluminium. However, in a few samples the metal has been damaged or completely turned into a white powder-like compound. Since this compound was

not of interest for this work, it has not been further investigated. Some examples are shown in Fig. 3.13.

#### 3.3.2.2 Copper

In a pure state, copper has a yellow-red appearance and is a relatively hard metal. It is also ductile and malleable and possesses, after silver and gold, the highest electrical and thermal conductivity among all metals. Thanks to its positive standard potential, copper has a high corrosion resistance. At room temperature, it does not react with hydrochloric, sulphuric, phosphoric and numerous organic acids, although it can be dissolved by nitric acid through a redox process. In contact with air, it slowly oxidizes to $Cu_2O$, which can be seen through a pink-red colour-



**Figure 3.14**: Cu surface.

ing of the Cu surface, and in contact with moist air, the product known as patina is formed ($CuSO_4 \cdot Cu(OH)_2$, $CuCl_2 \cdot Cu(OH)_2$), which can be identified through the characteristic green-grey colour. Since this is a not a soluble compound, this layer protects the copper from further deterioration. An optical microscope picture of the untreated microstructure of the copper surface is shown in Fig. 3.14.
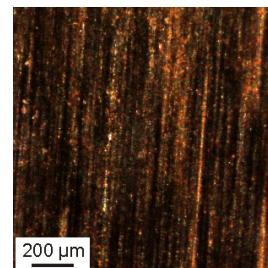
The metal is received in the form of a 0.1-millimetre-thick foil (Fisher Scientific, purity >99.9 %, trace metals <0.02 %). The substrate is cleaned with some drops of acetone prior to cluster deposition. Pieces of approximately 2 x 3 cm for the SST methods and 1 x 1 cm for the SIT methods are used.

With the use of copper substrates, the results achieved have been good with all techniques (see some examples in Fig. 3.15) except for SIT-5, where despite homogeneous distributions and small particle sizes, only a small quantity of material could be deposited. For all other
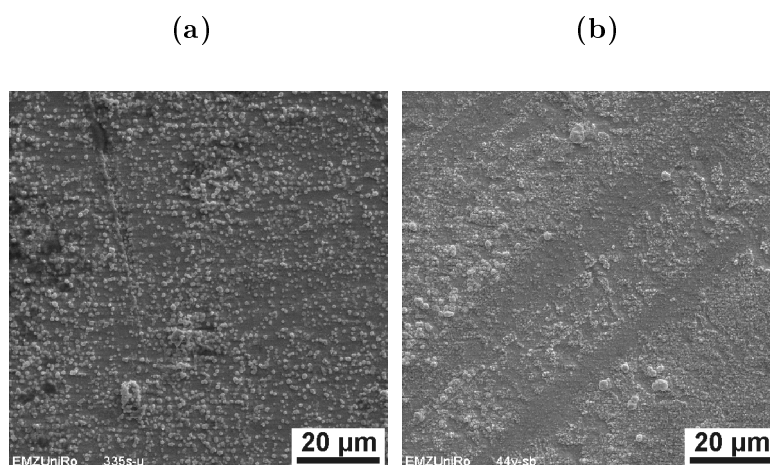
(a)          (b)



**Figure 3.15**: Cluster particles on copper deposited by **(a)** SST-2 and **(b)** SIT-8.

methods, highly homogeneous distributions and small particle sizes were achieved. These sizes range from 200 nm to 4 µm for the deposition using SST, achieving the best results with SST-2 and from 100 nm to 3 µm for the SIT, with the best results coming from SIT-7 and SIT-8.

Unlike all other metals studied in this work, all deposition methods work well with this metal. This can be due to the noble metal character of copper caused by its positive standard potential. It can be extracted from here that this noble metal character is confirmed to be favourable to the deposition of the cluster particles in the case of copper.

However, the substrate can be damaged using some of the methods in which the contact with moist air is present. This is especially the case with the use of the substrate impregnation technique with and without evaporation of the solvent, where the formation of compounds resulting on severe surface degradation has been observed (most probably oxides and chlorides, see Fig. 3.16). Using the SST, the drying of the piece is typically fast enough to avoid this effect, although it has also been observed in a few occasions, probably due to an excess of cluster solution. The nature and formation of these damaging compounds has not been further investigated since they were not of interest for this work.
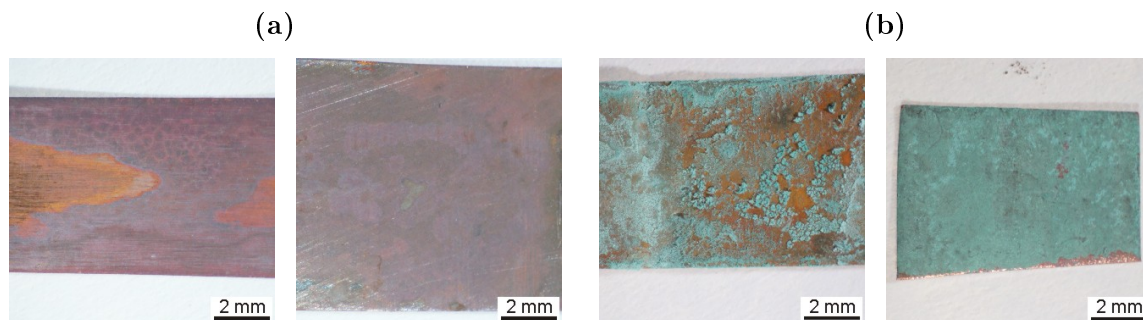


**(a)**                                                             **(b)**

**Figure 3.16**: Damaging of the substrates with deposited cluster using SIT-8. **(a)** Supposed formation of copper oxide during the deposition of $Na_4[Nb_6Cl_{18}]$. **(b)** Supposed formation of copper chloride during the deposition of $Na_4[Nb_6Cl_{18}]$.

### 3.3.2.3   Molybdenum
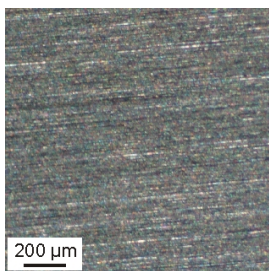


Molybdenum is a shiny blue-grey metal. It is very hard and brittle and it has a high electrical conductivity. Air, water, non-oxidizing acids and alkali bases do not damage the metal, thanks to its passivation layer. However, aqua regia, nitric acid and hot sulphuric acid corrode molybdenum. It is alloyable with iron, nickel, aluminium, chromium and lead among many other metals. In Fig. 3.17, the optical microscope picture of the untreated superficial microstructure of molybdenum is shown.

**Figure 3.17**: Mo surface.

The metal is received in the form of a 0.1-millimetre-thick foil (Sigma-Aldrich, purity >99.9 %, trace metals <0.02 %). The substrate is cleaned with some drops of acetone prior to cluster

deposition. Pieces of approximately 2 x 3 cm for the SST methods and 1 x 1 cm for the SIT methods are used.

Some results of the SST deposition methods on molybdenum are shown in Fig. 3.18a and 3.18b. As shown in these figures, the solution spreading methods give good results for this metal, following the general pattern described in section 3.3.1. Using all SST homogeneous distributions were achieved, with outstanding results for SST-3, with sizes up to 600 nm.
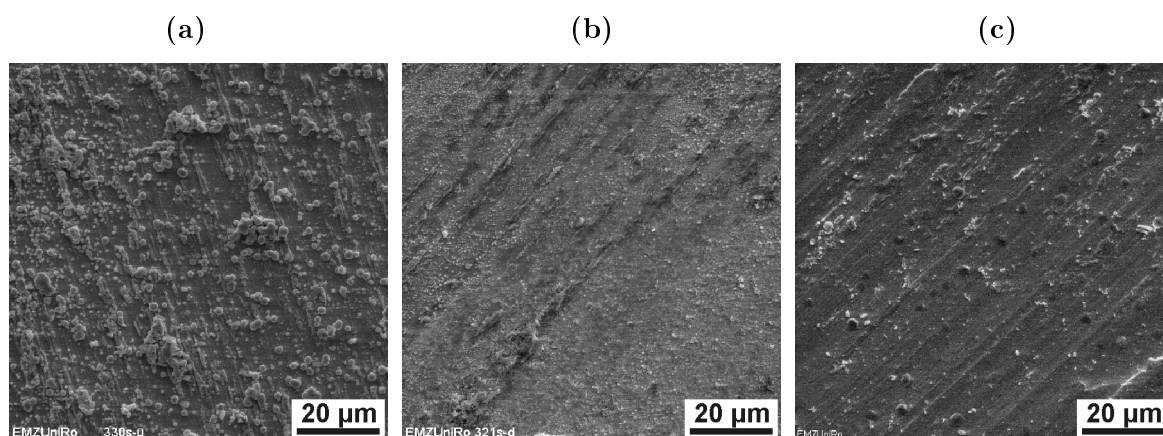
**(a)**               **(b)**               **(c)**



**Figure 3.18**: Cluster particles on molybdenum deposited by **(a)** SST-2, **(b)** SST-3 and **(c)** SIT-8.

On the contrary, the results obtained for the deposition using the SIT method were of poor quality. Here two different deposition behaviours could be observed. First, using the methods with solution evaporation, the deposited particles turn out to be extremely large (in reference to all other substrates), with diameters going up to 15 µm, especially for SIT-4, as expected (see section 3.3.1). Concerning the deposition using the SIT without solvent evaporation, the amount of deposited cluster was very low, although good distributions were achieved. This could have been a result of some remaining grease on the surface, which gives the molybdenum surface a certain roughness degree, as shown in the SEM micrographs in Fig. 3.18 (b and c). With regards to the particle size achieved with these methods, the particles grow up to 2.5 µm.

No oxidation or damaging of the substrate could be observed during deposition on molybdenum. The reason for that is the highly stable passivation layer on the surface of this metal, which also constitutes the most likely reason for the low amount of cluster deposited.

### 3.3.2.4   Zirconium

In its compact form, zirconium is a brilliant silvery metal, similar in appearance to steel, and has properties close to those of titanium. Thanks to its passivation layer, zirconium has an extremely high resistivity against corrosion produced by water, bases and most strong acids. However, at room temperature it can be damaged by aqua regia and hydrofluoric acid. Zirconium is black in its powder form and can be self ignited with a little heating, therefore it
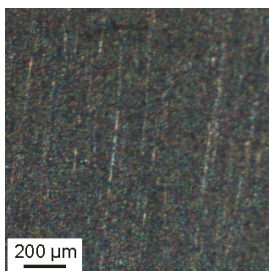
**Figure 3.19**: Zr surface.

is always stored in methanol or under an argon atmosphere. The untreated microstructure of the zirconium surface as seen using an optical microscope is shown in Fig. 3.19.

The metal is received in the form of a 0.25-millimetre-thick foil (Merck, purity >99.9 %, trace metals <0.02 %). The substrate is cleaned with some drops of acetone prior to cluster deposition. Pieces of approximately 2 x 3 cm for the SST methods and 1 x 1 cm for the SIT methods are used.

Some results of the deposition of the precursor particles on zirconium are shown in Fig. 3.20. As shown in the micrographs, the cluster can be deposited very homogeneously on Zr, using either spreading or impregnation techniques. For the case of the spreading techniques, good results were obtained using SST-3, where the material distribution was very homogeneous and the particle sizes were up to 1 µm. The results for SST-1 as well as SST-2 were also satisfying, although the particles grew larger than the SST with external heat applied (SST-3).
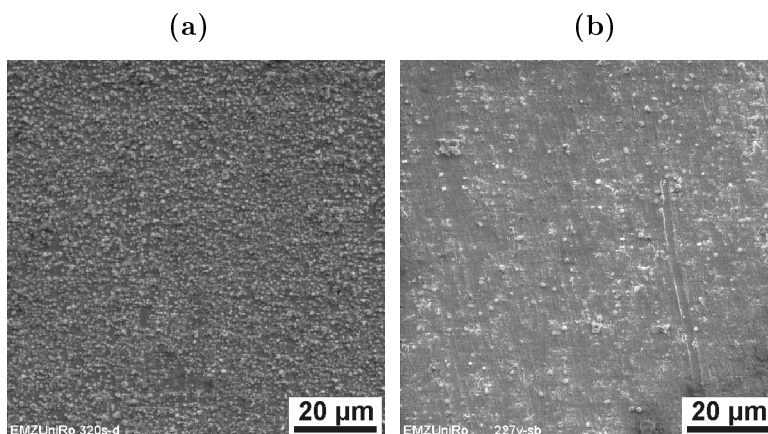
**(a)**                                                    **(b)**



**Figure 3.20**: Cluster particles on zirconium deposited by **(a)** SST-3 and **(b)** SIT-8.

Even smaller particles could be achieved with the use of the impregnation methods without solvent evaporation (SIT-6, SIT-7 and SIT-8), with deposited particles with a maximum diameter of 700 nm. Homogeneous distributions were also achieved using these methods. However, the amount of cluster deposited was, as expected, lower than with the SST, since with the use of the spreading method the complete cluster amount is deposited whereas using the impregnation methods only a part of the total cluster amount is found on the surface.

The results obtained with the methods SIT-4 and SIT-5 were, in contrast, of poor quality. As in all other substrates, the particles achieved large diameters up to 7 µm due to the rapid evaporation of the solvent in air or by external heating and the large amount of solution (meaning a large amount of cluster material). The deposited particles featured rather inhomogeneous distributions with both, SIT-4 and SIT-5.

No oxidation or damaging of the substrate has been observed for zirconium in any of the

deposition methods used. This is due to the high stability of the zirconium oxide that passivates the metal.

### 3.3.3 Deposition on glass

Commercial glass is a mixture of silicon, sodium and calcium oxides (71-75 % $SiO_2$, 12-16 % $Na_2O$ and 10-15 % CaO [43]) arranged in a two-dimensional net structure, similar to the one seen in Fig. 3.21. Depending on the chemical composition, the properties of glass can widely vary [44], for example, some amounts of Al and Pb can be found in commercial glass, helping enhance chemical durability [45]. In this kind of glasses, the Al and Pb ions are placed in a Si position and form therefore aluminium and lead oxides within the $SiO_2$ net structure of glass.

Commercial laboratory glass from microscope object slides is used for the experiments (Technisches Glas Ilmenau GmbH). The slides are cut using a



**Figure 3.21**: Ca-Na glass 2D-structure.

glass saw, typically into pieces of about 1 x 1.2 cm for all deposition methods. Two pieces are used for each deposition. The substrates are cleaned with some drops of acetone prior to use.

Some results for the deposition on glass are shown in Fig. 3.22. As in the case of the metallic substrates, for the deposition on glass two different behaviours can be observed depending on whether the method used is SST or SIT. The deposition using solution spreading has led to extremely ordered particle distributions in all cases. However, the particle sizes do depend on the detailed method used. As it was expected, the larger particles have been obtained using SST-1, with mean diameters of 7 µm, and the smallest particles have been obtained using SST-3, with mean diameter sizes of 600 nm. This behaviour is very similar to the one observed with the metallic substrates.

With regards to the deposition using substrate impregnation, the results were quite different from the ones with the metallic substrates. Uniform cluster distributions were achieved with all of the methods, except for SIT-4, probably due to the large amount of cluster solution deposited (see section 3.3.1). However, the particle sizes were observed to be very different, depending mainly on the technique used. The smallest particles have been obtained, as expected, with the methods without solvent evaporation. With these methods particles with maximal diameters of 500 nm were achieved. For the case of the SIT-5, the particles grew up to 2 µm, gathering in particle aggregates of about 5 to 10 µm. This same behaviour has also been observed for some metals.
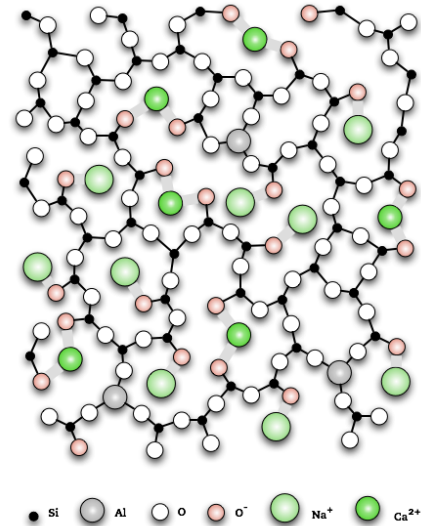
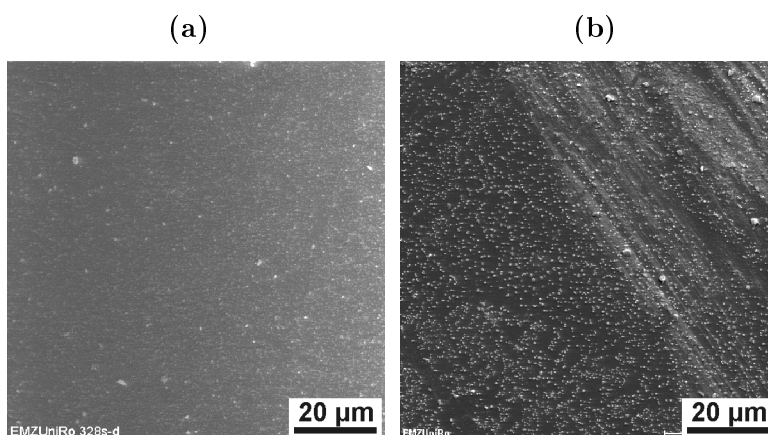(a)                                          (b)



**Figure 3.22**: Cluster particles on glass deposited by **(a)** SST-3 and **(b)** SIT-6.

As already commented, the deposition using substrate impregnation without evaporation of the solvent and under normal conditions (SIT-6) works very well with glass. In addition to that, it has been observed that this coating is extremely well adhered to the surface of the glass. Only strong acids or bases can remove the cluster particles on the surface. Since glass is an inert substrate, these samples would be adequate for use as catalyst, for example. Since a supported catalyst must also have the property to remain attached to the substrate after cleaning the rests of the reaction, the cleaning resistivity of the cluster particles on the surface has been tested. This substrate cleaning has been tested using water, methanol and acetone. The results of the cleaning for the first two (during 10 seconds, 1 day, and 10 days) are shown in Fig. 3.23. To perform these experiments, the coated substrates are submerged in the solvent inside a reaction tube (0.2 to 0.5 ml of solvent, to assure complete submersion of the substrate). The sample is left up to 10 days in the solvent. After this time, it is taken out of the tube and the excess of liquid is dried carefully with absorbent paper.

It can be extracted from these pictures that the cluster coating is well attached to the substrate considering it is completely re-dissolved only after 10 days submerged in methanol. Since the washing of the supported catalysts after reaction takes only a short time and the amount of cluster on the glass surface after the ten-second-cleaning is still large, it can be stated that this substrate would be adequate for heterogeneous catalysis (from the point of view of the adherence on the support). The results for these experiments will be described in section 4.1.

Inert surfaces are usually extremely flat, i.e. they do not have any sites in which particles can be deposited. With the etching of the surfaces the number of sites where the particles can be deposited is increased and consequently smaller and better distributed particles can be achieved. For that reason it has been tried to induce some irregularities to the glass surfaces submerging them in hydrofluoric acid prior to the cluster deposition. For that purpose, the piece is held approximately 10 seconds in the hydrofluoric acid and then washed with distilled water and placed during some minutes in the drying oven.
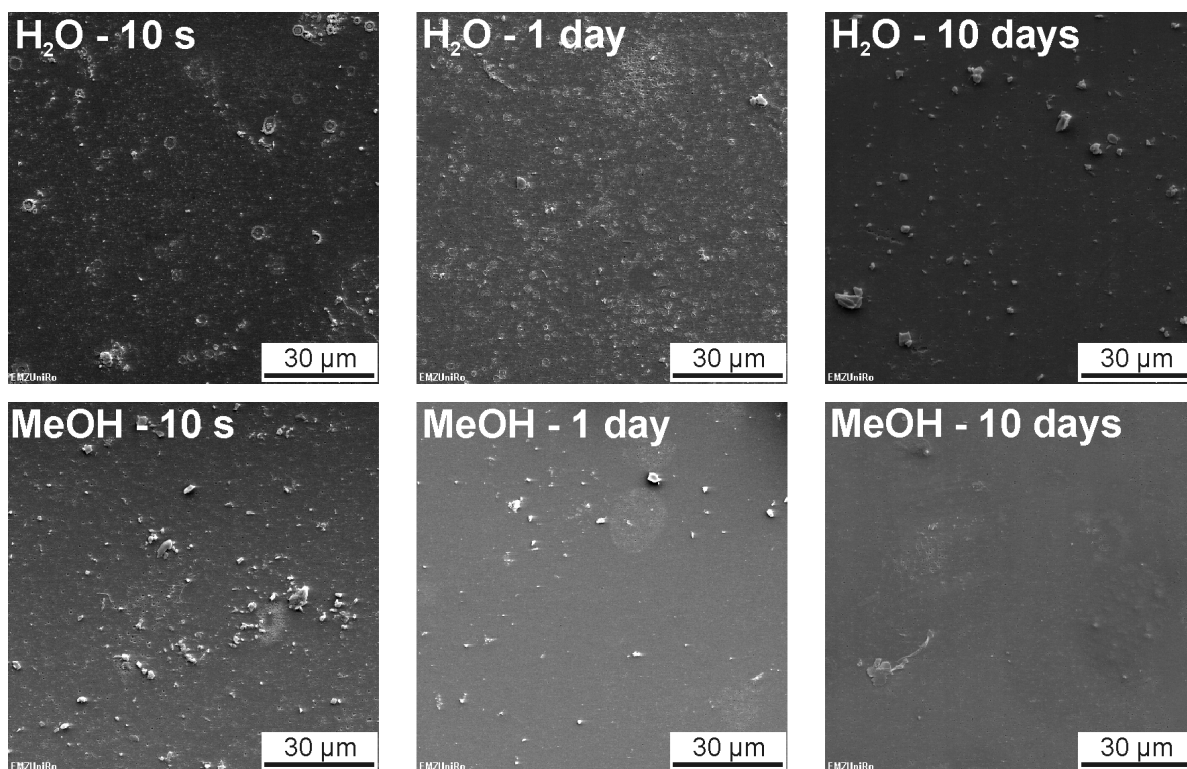
**Figure 3.23**: $Rb_4[Nb_6Cl_{18}]$ deposition on glass using SIT-6 during 10 days and cleaning afterwards.
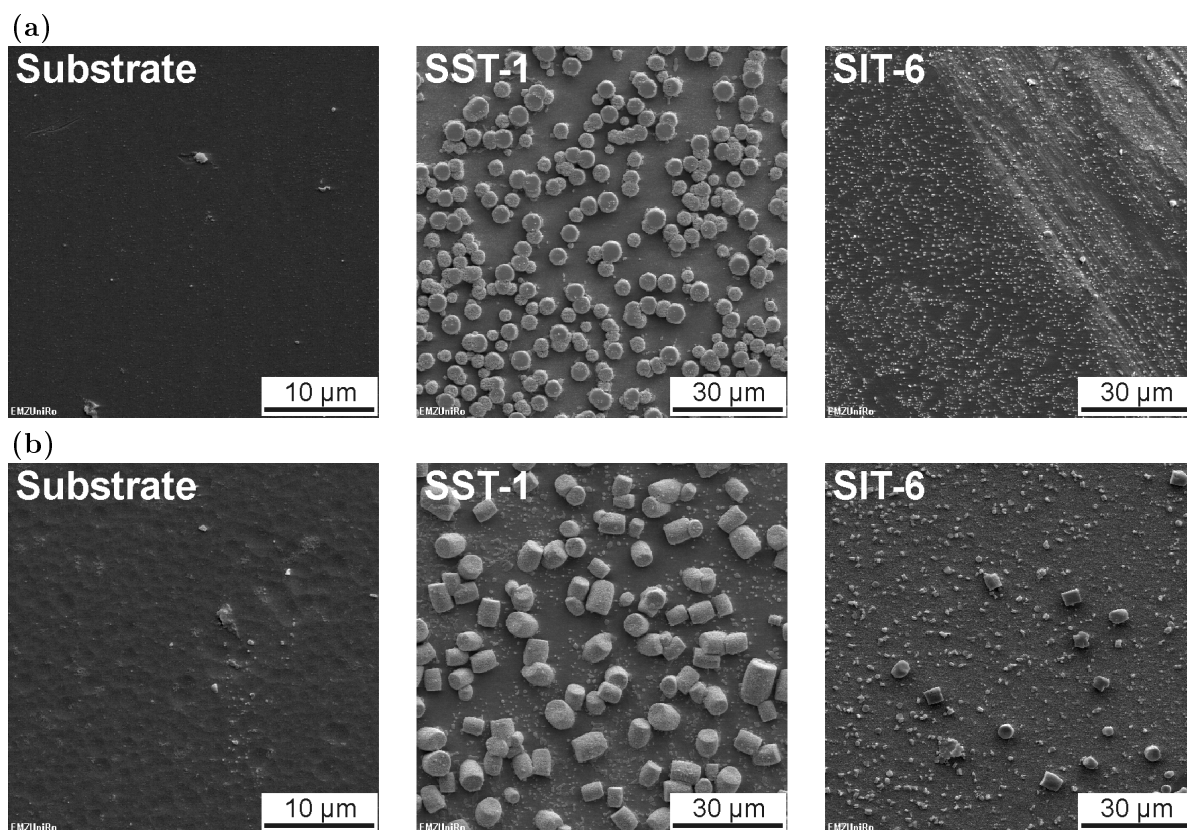


**Figure 3.24**: Effect of the HF treatment on glass and coated samples. **(a)** Untreated pieces and **(b)** Piece treated with HF.

An example of an etched substrate obtained with this method is shown in Fig. 3.24. It can be observed that the distributions and sizes of the deposited cluster particles are highly similar for both preparation methods. For the case of the SST-1, smaller particles are indeed achieved with the use of the HF-treatment, although larger particles up to 10 µm in diameter are also deposited. In the case of SIT-6, apart from some larger particles, the size of the particles is approximately the same with and without the use of the HF pre-treatment. It has been proven that this pre-treatment does not have any favourable effect on the particle size and distribution and, in consequence, has not been further applied or studied.

### 3.3.4   Deposition on irregular substrates

It has been proven that the deposition of cluster particles on foils provides good results. In order to investigate the efficacy of the method on irregular pieces the deposition will be carried out using chunks and granules as substrates. To this effect, chromium, lead, tin and zinc will be investigated.
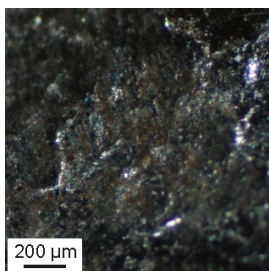
#### 3.3.4.1   Chromium



Figure 3.25: Cr surface.

Chromium is a silver-coloured, very hard and brittle metall. Despite its negative standard potential, it has an extremely good reaction inactivity and corrosion protection. It possesses also a very thin oxide layer on its surface, which acts as a passivation layer. Because of this, chromium is not affected by air at room temperature, water and most strong acids, although, it can be dissolved in hydrochloric and sulphuric acid. An optical microscope picture of the untreated surface microstructure of chromium is shown in Fig. 3.25.

The metal is received in the form of chunks of 5 to 50 mm (Merck, purity >99.99 %, trace metals <0.02 %). The substrate is cleaned with some drops of acetone prior to cluster deposition. For the SST methods a large chunk of about 1 g is used, spreading the solution over a flat surface. For the SIT methods, 3 to 5 small pieces with a total weight of approximately 1 g are used.

The best deposition results were shown on chromium with the use of SST, where all three methods have led to local homogenous distributions and small particle sizes, ranging from 500 nm to 4 µm and achieving high quantities of material deposited, as shown in Fig. 3.26a and 3.26b. However, on a general macroscopical view of the samples (see Fig. 3.27) and due to the uneven surface of the chromium chunks, the coating of the surface is not regular, which can be seen through the light (no covering) and dark zones (cluster covering) of the chunks.

Concerning the impregnation methods, the results were of rather poor quality, except for the deposition with SIT-8 (see Fig. 3.26c). For the methods SIT-4 to SIT-7, the general and
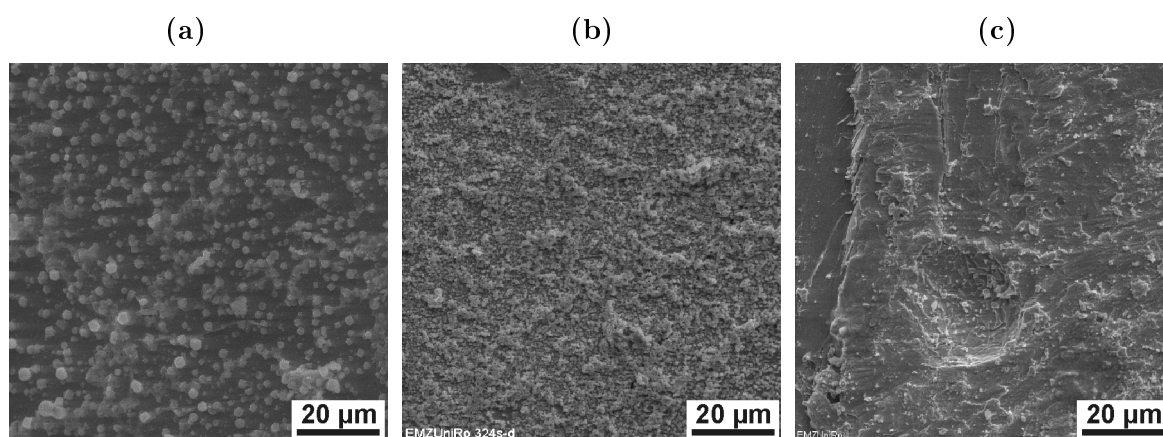
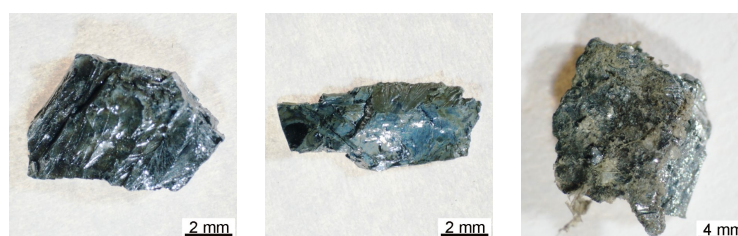**Figure 3.26**: Cluster particles on chromium deposited by **(a)** SST-1, **(b)** SST-3 and **(c)** SIT-8.



**Figure 3.27**: $Rb_4[Nb_6Cl_{18}]$ particle deposition on chromium using SST methods.

local distributions are extremely inhomogeneous and the particles have reached large sizes (approximately 5 to 20 µm). A possible explanation for that are the extremely inert conditions of the chromium oxide passivation layer on the surface of the metal. Nevertheless the use of the deposition by impregnation at high temperature and reduced pressure (SIT-8) leads to local homogeneous distributions with particle sizes going from 500 nm to 3.5 µm, as already commented. In this case, the high temperature enhances the reaction of the cluster molecules with the substrate and the particles can be deposited. Thanks to the highly inactive passivation layer, no oxidation or other damage of the substrate have been observed for this metal.

### 3.3.4.2 Lead

Lead is a very soft metal, with high malleability and low elasticity. It has also a low fusion point and a relatively high density (11.4 $g \cdot cm^{-3}$). Lead has a mat grey colour, which is due to a passivation lead oxide layer. Pure Pb (in an inert atmosphere) has a shiny blue-white appearance. In water, it reacts to lead hydroxide, forming layer of this compound on the surface that protects it from further corrosion. $CO_2$ in water, chlorine, hydrogen sulphide and hydrochloric, hydrofluoric, and sulphuric acids cannot solve lead, since a hydroxide passivation layer is formed that avoids a



**Figure 3.28**: Pb surface.

further reaction. The optical microscope picture of the untreated surface microstructure of lead is shown in Fig. 3.28.

The metal is received in the form of grains (Acros, purity >99.0 %, trace metals <0.05 %). The substrate is cleaned with some drops of acetone prior to cluster deposition. For the SST methods 4 grains with a total weight of approximately 300 mg are used. For the SIT methods, 10 grains are used, with a weight between 1.0 and 1.3 g.

As shown in Fig. 3.29a and 3.29b, the deposition of the niobium precursor on lead works rather well when using solution spreading techniques, although the results are quite unexpected. As described in section 3.3.1, with the use of SST, the cluster particles should grow smaller when external influences are applied during the drying (temperature, movement, etc.). In the case of lead, however, the deposition resulted in smaller particles for SST-1 (from 400 nm to 2 µm, no external modification on the drying) than with SST-3 (about 1.5 µm, heat applied during drying). This behaviour is due to the complex surface microstructure of the lead grain, since the same behaviour has been observed for tin, as will be seen next (section 3.3.4.3).

**(a)**                                   **(b)**                                   **(c)**
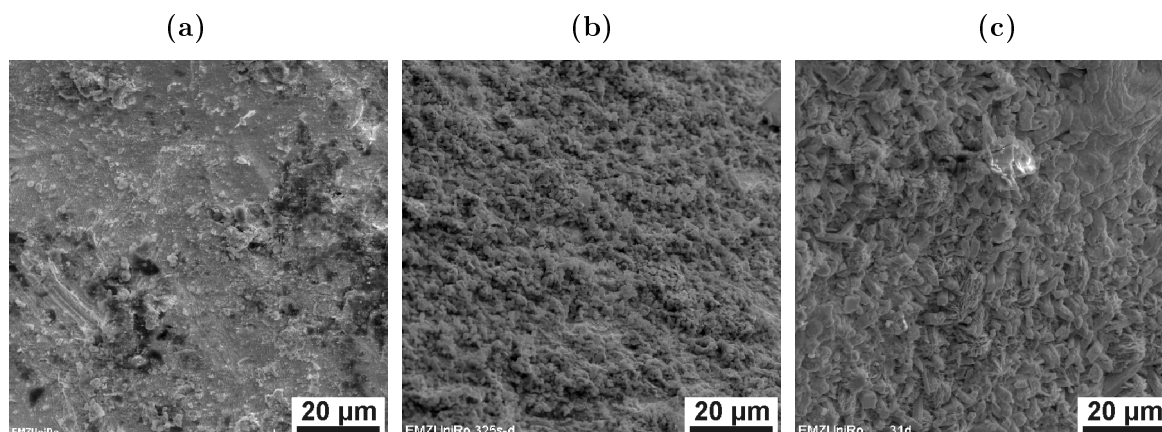


Figure 3.29: Cluster particles on lead deposited by (a) SST-1, (b) SST-3 and (c) SIT-4.

Concerning the substrate impregnation methods, the results are also quite good, especially for the methods SIT-4 and SIT-5 (see Fig. 3.29c), where homogeneous distributions with particle sizes from 300 nm to 3 µm are achieved. For the methods without evaporation of the solvent, small particles were also achieved, however not in homogeneous distributions, which is also due to the complex lead surface.

No structural changes or damaging of the substrates has been observed for lead substrates. On a few samples with cluster deposited using SIT methods, the troubling and brown colouration of the solution has been observed. This has been most probably due to precipitation of a lead compound, which indicates the damaging of the metallic surface. Due to the lack of importance for the whole process, the compound formed by the precipitation has not been further investigated.

### 3.3.4.3  Tin

Tin is a silver-white metal at room temperature and atmospheric pressure. It has a very low melting point (232 °C), very low hardness and is very ductile and malleable. Metallic tin can be damaged at low temperatures due to the transformation in Sn-powder (below 13 °C). In this point, a phase transition from α-Sn (grey tin powder) to β-Sn (silver-white tin) takes place, which is known as tin pest. As in the case of the other metals studied in this work, tin has a transparent surface passivation layer, which protects it against air and water corrosion. Mild acids and bases do not at-



**Figure 3.30**: Tin surface.

tack tin, which allows it to be used in tinned food packages. An optical microscope picture of the untreated superficial microstructure of tin is shown in Fig. 3.30.
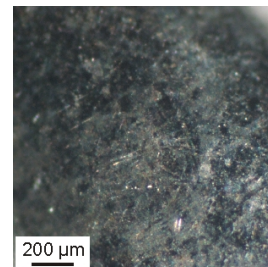
The metal is received in the form of granules of 1 to 4 mm (Fluka, purity >99.5 %, trace metals <0.02 %). The substrate is cleaned with some drops of acetone prior to cluster deposition. For the SST methods a large grain of approximately 200 mg is used, spreading the solution over a flat surface. For the SIT methods, 2 pieces are used, with a total weight of approximately 400 mg.

In Fig. 3.31 some results on the deposition on tin are shown. It has been observed that the behaviours of tin and lead are similar, which is expected since they belong to the same group in the periodic table. This can be confirmed from this figure and will be described in the following paragraphs.
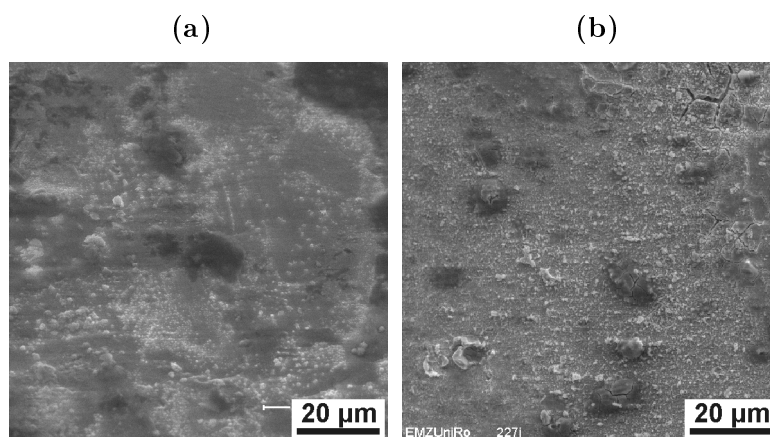
**(a)**　　　　　　　　　　**(b)**



**Figure 3.31**: Cluster particles on tin deposited by **(a)** SST-1 and **(b)** SIT-6.

The deposition by solution spreading showed very good results concerning distribution and particle sizes. In fact, this substrate exhibited the smallest mean particle sizes of all substrates, especially for SST-1, with diameters only up to 1 μm. In addition to that, unlike all other substrates except lead, tin showed similar particle sizes in all three SST methods although the amount of particles deposited was lowest for SST-1. This behaviour is caused, as in the case of lead, by the rather complex surface microstructure of tin (see section 3.3.4.2).

Regarding the substrate impregnation techniques, tin has shown good results in distribution and particle size if the deposition is carried out through the methods without solvent evaporation. Using these methods the particle sizes range from 200 nm to 1 µm, although the amounts of deposited cluster were rather low, most probably because of the high stability of the oxide passivation layer and the complex surface structure. The methods SIT-4 and SIT-5 (with solvent evaporation) have not provided good results. For the SIT-4 small particles were indeed achieved (up to 1.5 µm in diameter), but significantly larger ones too, with diameters up to 15 µm. The deposition using SIT-5 led to micro-cracks in the coating, which indicate the poor quality of the coating adhesion.

No severe damaging of the tin substrates has been observed for any of the methods used. In some occasions using the heating techniques the colour of the metal surface turned gold (see Fig. 3.32), which has been observed not only if SIT-5 is used, but also using SIT-8, This could be due to the presence of oxygen during the deposition caused by a poor sealing or reduction of the pressure.



**Figure 3.32**: $Na_4[Nb_6Cl_{18}]$ particles on tin. Gold colouring on the surface.

However this is unclear as it could be also caused by the cluster coating. Since it is not of interest for the results of this work, this subject has not been further investigated.
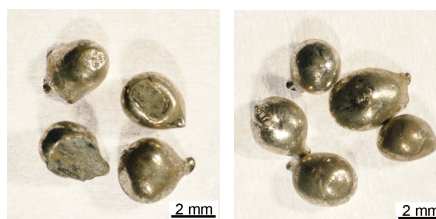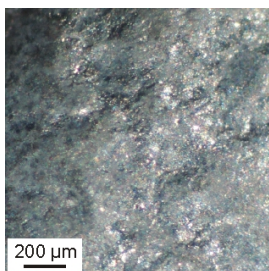
### 3.3.4.4  Zinc



**Figure 3.33**: Zinc surface.

Zinc is a blue-white metal with a very brilliant surface, usually covered by an oxide passivation layer that gives it a mat appearance. At room temperature zinc is quite brittle, but when heated up to 100-150 °C, it becomes soft and malleable, which allows an easy processing of the metal. It has also a high electrical conductivity. Zinc does not react with dry air and an oxidation begins only if heated above 200 °C. Opposite to that, if it comes in contact with moist air, a layer of a mixture of zinc hydroxide and zinc carbonate $(Zn_5(OH_6)_2(CO_3)_2)$ is produced, which protects the metal against a further corrosion. Mild acids and bases corrode the passivation layer and, due to the formation of strong bases during the process, the metal can be damaged. In Fig. 3.33, the optical microscope picture of the untreated microstructure of the zinc surface is shown.

The metal is received in the form of granules of about 3 to 5 mm in diameter (Riedel-de Haën, purity >99.5 %, trace metals <0.05 %). The substrate is cleaned with some drops of acetone prior to cluster deposition. For the SST methods a large grain of approximately 350 mg is used, spreading the solution over a flat surface. For the SIT methods, 2 pieces are used, with a total weight of approximately 700 mg.
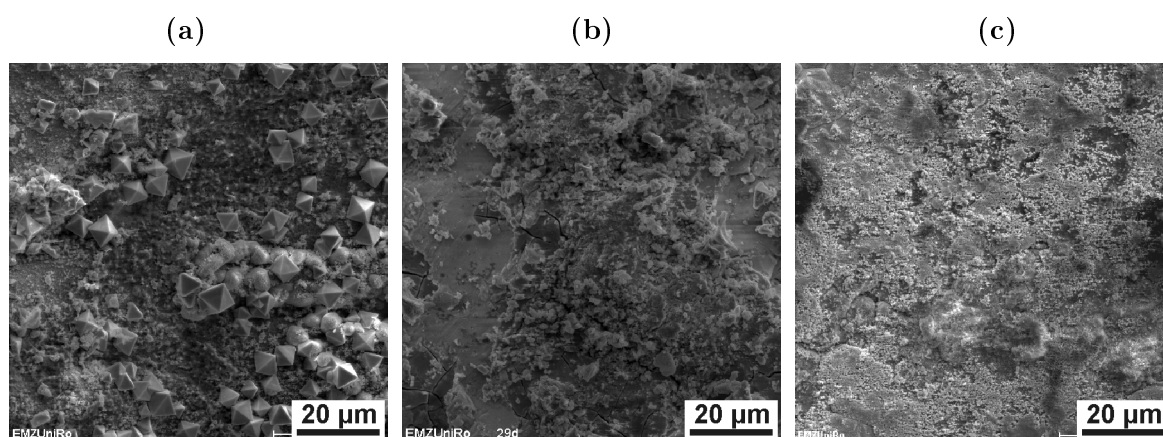
(a) (b) (c)



**Figure 3.34**: Cluster particles on zinc deposited by **(a)** SIT-4 and **(b)** SIT-6.

The results of the deposition using SST-1 were quite unexpected, since small octahedral crystalline particles of up to 7.5 µm were formed, whereas using SST-2 and SST-3 the behaviour was, despite the complex surface microstructure of zinc, similar to the one observed for all other substrates (see Fig. 3.34a). Apart from the octahedral particles, the deposited particles reached sizes up to 3 µm, while the particles for the methods with externally-influenced drying grew only up to 800 nm and gathered in large aggregates of 2 µm to 5 µm in diameter.

The use of the substrate impregnation techniques has led to good results, with homogeneously distributed cluster particles and small particle sizes, except for the case of SIT-7, where the amount of deposited particles was lower, most probably due to a deposition error (e.g. using a too low concentration) rather than problems caused by the properties of zinc. On overall, the upper and lower thresholds for the deposited particle sizes can be set by 300 nm and 1.5 µm respectively. As in the case of the solution spreading methods, these small particles tended to gather in aggregates of up to 7 µm in diameter, especially for SIT-4 and SIT-5 due to the rapid evaporation of the solvent. Some examples are shown in Fig. 3.34(b and c).

No damaging or severe oxidation of the surface has been observed due to the high stability of the ZnO that passivates the metal. However, in a few SIT samples the solution turned brown while remaining a clear solution. As indicated in section 3.1.2 this can be explained by a change in the charge of the cluster anion from -4 to -3 (oxidation).

### 3.3.5 Growth behaviours

Different growth behaviours can be observed in the samples, depending mainly on the deposition time and the substrate. These behaviours are consistent with the ones described by previous literature in this field [46, 47], which leads us to think that clusters with ligands follow the same growth patterns as ligand-free cluster assemblies. A sketch of the growth modes is shown in Fig. 3.35. Three different growing phases can be seen in this sketch: formation, early stage growing and late stage growing.
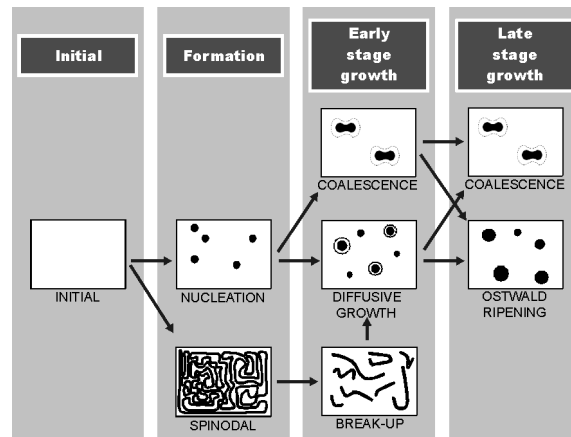
**Figure 3.35**: Overview of the cluster particle formation stages on surfaces, adapted from the work of Zinke-Allmang et al. [46].

After deposition of the precursor, the formation phase begins, with random nucleation and spinodal decomposition as dominating processes. In the nucleation process, cluster particles from the supersaturated liquid medium start to precipitate until the supersaturation in the solution is reduced. An example of this process is shown in Fig. 3.36a. In what concerns the process of spinodal decomposition, the particles are arranged forming branches, which is due to the low mobility of the particles in the solution. Fig. 3.36b shows an example of this growth mode. In both cases the particles have diameters up to 1 µm.
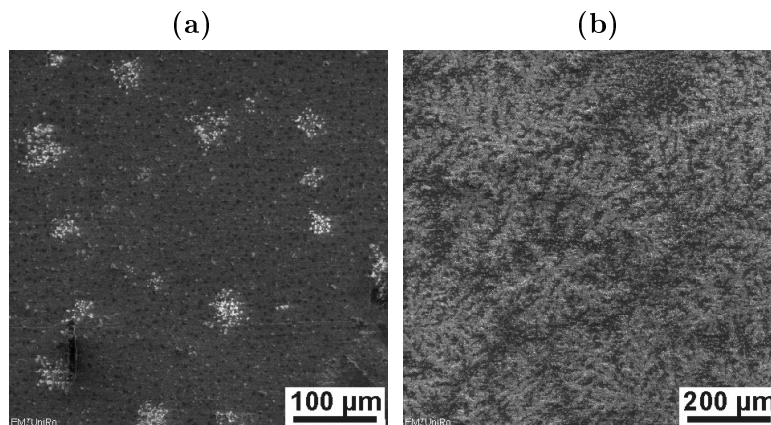


**Figure 3.36**: SEM Photographs of the dominating processes during the formation stage.  **(a)** Nucleation ($Na_4[Nb_6Cl_{18}]$ on Zr by SIT-8). **(b)** Spinodal Decomposition ($Rb_4[Nb_6Cl_{18}]$ on Al by SST-1).

After this phase, the system evolves to the early stage growth. This phase is only a transition between the formation and the late stage growth.  Three different mechanisms contribute to determine the evolution of the system: coalescence, diffusive growth and break-up of the spinodal structures. In Fig. 3.37a an example of the coalescence growth is shown. This process is driven by the amount of cluster on the surface. Smaller particles (with diameters of about 800 nm) gather together to form larger particles, with diameters up to 4 µm. Fig. 3.37b shows an example of diffusive growth. In this growth stage small particles adhere to large particles

to form larger ones, which, in our case, can reach up to 2 µm. Finally, the breaking of the spinodal networks to form larger particles can also take place. An example of this mechanism is shown in Fig. 3.37c, where the particles enlarge their sizes from 200 nm in branches up to 3 µm as "free" particles.
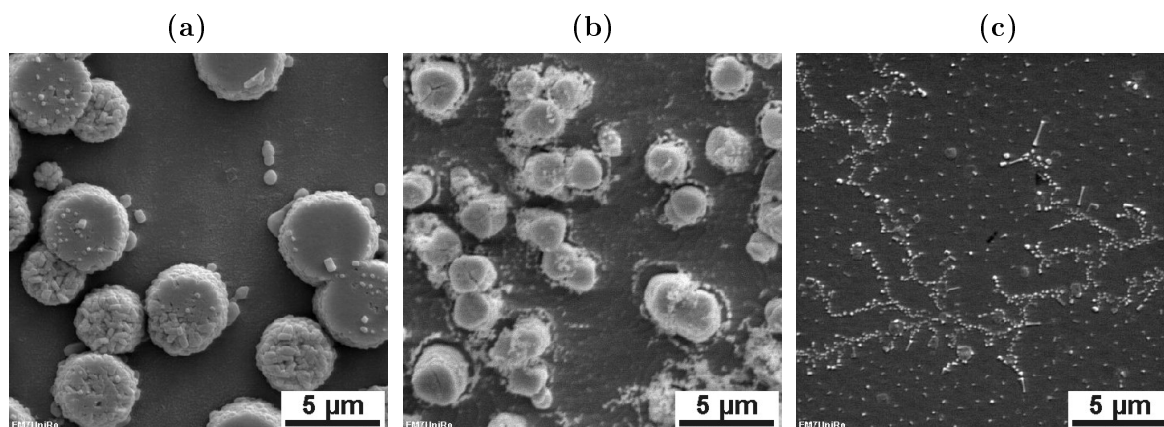
(a)            (b)            (c)



**Figure 3.37**: SEM Photographs of the dominating processes during the early stage growth. **(a)** Coalescence ($Na_4[Nb_6Cl_{18}]$ on glass by SST-1). **(b)** Diffusive Growth ($Na_4[Nb_6Cl_{18}]$ on Cu by SST-1). **(c)** Break-up of the spinodal structures ($Na_4[Nb_6Cl_{18}]$ on glass by SIT-6).

Direct ripening is the leading process in the late stage growth, but coalescence can also occur in this part of the growing process (See Fig. 3.38a). In this step the diffusional growth slows down and the cluster areas start to overlap. An example of this kind of growth mode has been shown in Fig. 3.38b. In this step the particles enlarge their sizes up to 5 µm.

(a)                    (b)
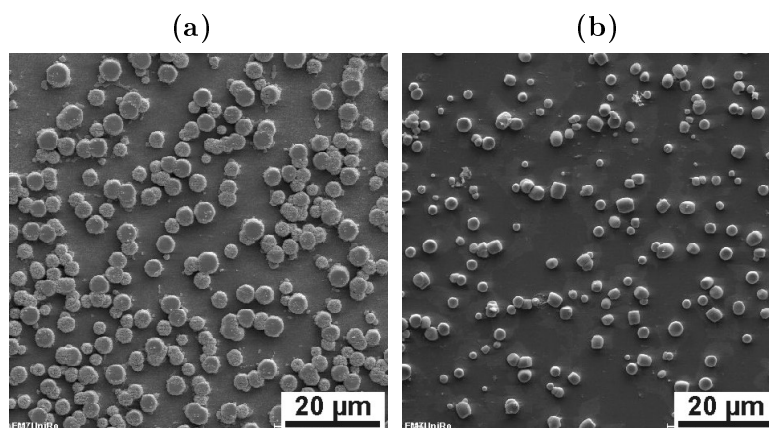


**Figure 3.38**: SEM Photographs of the dominating processes during the late stage growth. **(a)** Coalescence ($Na_4[Nb_6Cl_{18}]$ on glass by SST-1). **(b)** Ostwald ripening ($Rb_4[Nb_6Cl_{18}]$ on glass by SST-1).

### 3.3.6   Evaluation of the deposition methods

It has been shown in the last sections that the deposition of the cluster particles on the chosen substrates is indeed successful, especially on those shaped as foils. For them (Al, Cu, Mo, Zr and glass) homogeneous microscopic and macroscopic distributions and small particle sizes

could be achieved with almost all methods. With regards to the irregular-shaped substrates, it has been seen that the deposition is also successful, although in most of the cases homogeneous distributions and small particle sizes could be only achieved locally.

As seen in the micrographs shown in sections 3.3.2, 3.3.3 and 3.3.4 the solution spreading methods (SST) work well on all substrates. Fine examples of the cluster depositions in copper and aluminium are shown in the chemical mappings in Fig. 3.39, where green refers to Nb, blue to Cl and red to Rb. With regards to the distribution of the elements, it can also be seen in the same figure that there is no decomposition of the cluster during the solution preparation and deposition time (since the particles are formed by Nb and Cl).
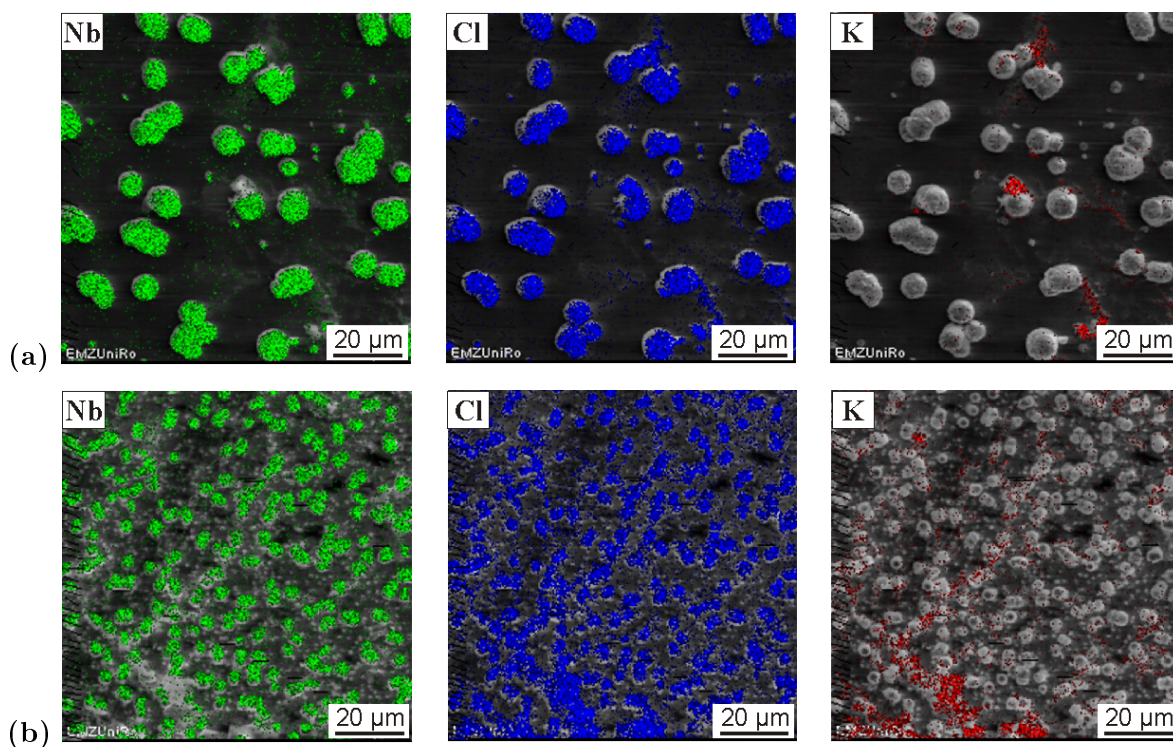


**Figure 3.39**: Cluster depositions using the solution spreading technique with drying in air (SST-1). $K_4[Nb_6Cl_{18}]$ deposition on **(a)** aluminium and **(b)** copper.

In some cases alkali chlorides can precipitate during the deposition time, which can be identified by the presence of potassium in the chemical mapping micrographs in Fig. 3.39. This process is mostly due to the ligand exchange process that takes place during the solution formation. In this process, 4 of the outer chlorido ligands are exchanged for methanol obtaining $[Nb_6Cl_{14}(MeOH)_4]$. In this process alkali chlorides are formed, following the reaction in 3.2.

$$M_4^I[Nb_6Cl_{18}] \ + \ 4\,MeOH \ \rightleftharpoons \ [Nb_6Cl_{14}(MeOH)_4] \ + \ 4\,M^I Cl \qquad (M^I \ = \ Na, \ K, \ Rb) \qquad (3.2)$$
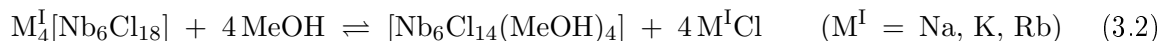
However, the cluster particles can also react with water coming from the solvent (methanol),

and alkali chloride particles can be formed, following the process shown in reaction 3.3. These chlorides precipitate afterwards.

$$M_4^I[Nb_6Cl_{18}] + 4\,H_2O \rightleftharpoons [Nb_6Cl_{14}(H_2O)_4] + 4\,M^ICl \qquad (M^I = Na, K, Rb) \qquad (3.3)$$
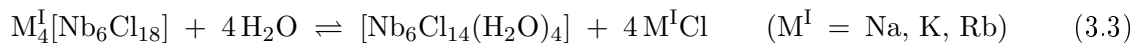
The examples in Fig. 3.39 show that the particles typically adopt the shape of small cylinders when SST-1 is used. As shown in the scheme in Fig. 3.7, during the evaporation of the solvent from the cluster solution, some small cylinders are formed on the surface of the substrate due to the stapling of the cluster molecules. Once the piece is completely dry, the cylinders can either remain vertically-arranged or cant over. Some examples of this can be found in Fig. 3.40. This is not the case when SST-2 or SST-3 are used, where the faster drying of the solvent does not provide enough time for the particles to grow and achieve a cylindrical arrangement. Instead, the particles remain spherical and of a small size. It has been found that the size of these cylindrical particles significantly depends on the substrate.
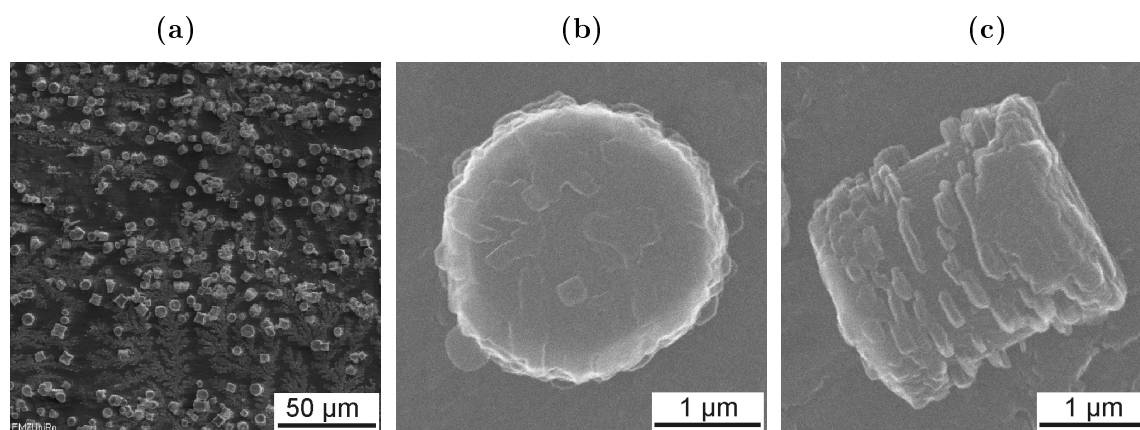
**(a)** **(b)** **(c)**



**Figure 3.40**: SEM micrographs of the formation of cylinders during cluster particle growth, all deposited by SST-1. **(a)** $Rb_4[Nb_6Cl_{18}]$ on Al. **(b)** Standing and **(c)** lying cylinder ($Rb_4[Nb_6Cl_{18}]$ on Zr).

With regards to the substrate impregnation technique, it has been shown that the methods that have provided the best results are SIT-6 for glass and some metallic substrates and SIT-7 and SIT-8 for all substrates. The chemical mapping micrographs of some of the samples treated with these methods can be found in Fig. 3.41 and 3.42.

On one side, it has been observed that the impregnation method without evaporation of the solvent and normal conditions (SIT-6) provides better results when used on glass than on metallic substrates. In this case the adhesion of the cluster particles to the substrate is also higher, which gives the glass a green-brown colour, perdurable even after cleaning of the surface. This behaviour is caused by the $Ca^{2+}$ and $Na^+$ cations in the chemical structure of glass (see Fig. 3.21), which act like anchors for the cluster anions in solution. Once the solvent has dried out, the cluster molecules remain anchored to the glass structure as $Ca_2[Nb_6Cl_{18}]$ or $Na_4[Nb_6Cl_{18}]$. An example of that is shown in Fig. 3.41, where green indicates Nb and blue Cl. The fact that the traces of the elements appear slightly shifted from the actual position
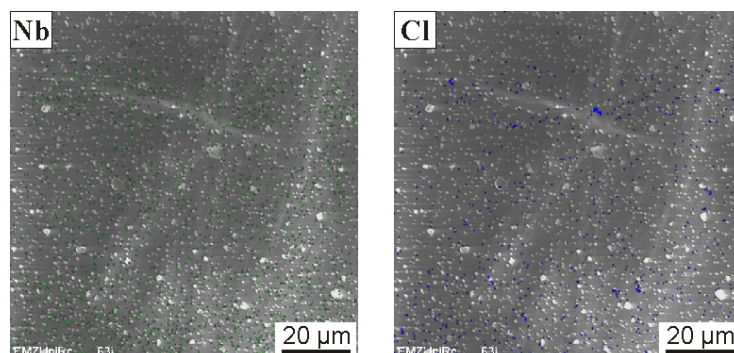
**Figure 3.41**: Cluster deposition on glass using the substrate impregnation technique without evaporation of the solvent and at atmospheric pressure (SIT-6).
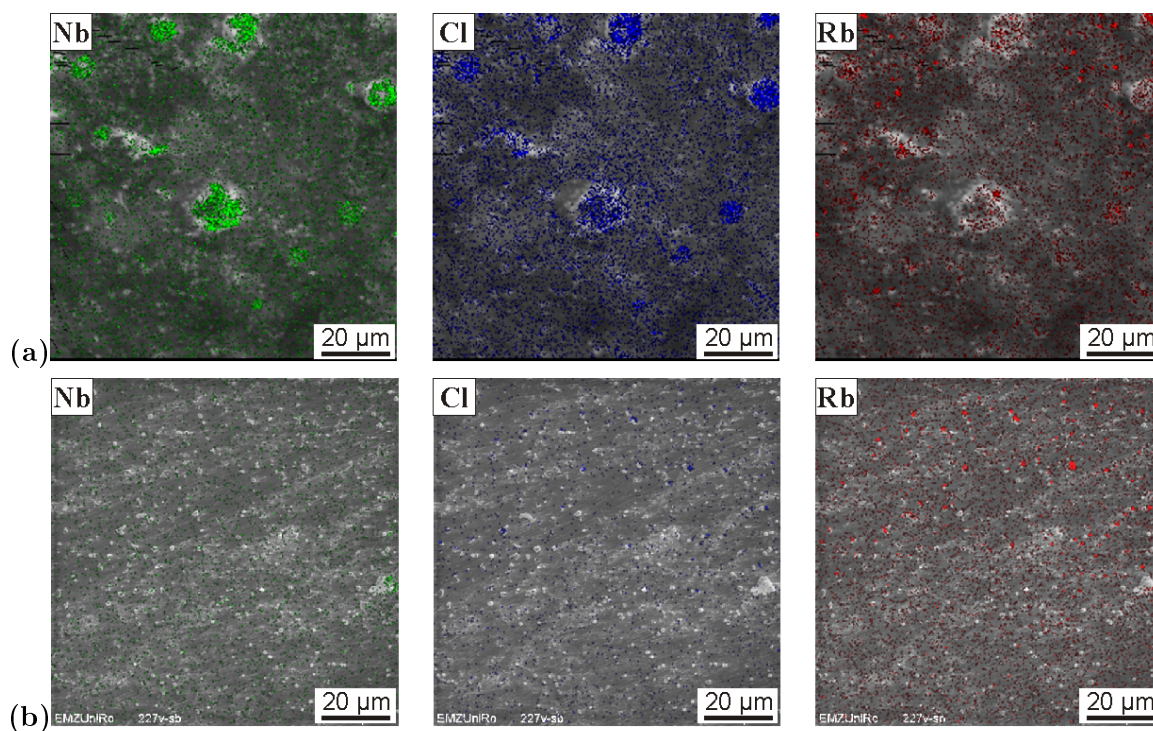


**Figure 3.42**: Cluster deposition using the substrate impregnation technique without evaporation of the solvent and under reduced pressure **(a)** $Rb_4[Nb_6Cl_{18}]$ deposition on copper (SIT-7). **(b)** $Rb_4[Nb_6Cl_{18}]$ deposition on zirconium (SIT-8).

of the particles is due to the non-conductive character of glass, which causes a rather irregular reflection of the electrons and, in consequence, a false position of the elements on the EDX map. Nevertheless, as observed in the figure, with the use of this method, a relatively large amount of cluster is deposited in homogeneously ordered distributions.

On the other side, SIT-7 and SIT-8 methods provide mostly homogeneous distributions of the particles as seen in Fig. 3.42. However, the use of this kind of method produces large particle size ranges (usually from a few nanometres to a few micrometers). Furthermore, the amount of cluster deposited by these methods is usually lower than the amount deposited by SST

methods. With regards to the distribution of the elements, unlike the case of the deposition by SST, in this case a certain degree of decomposition or restructuring of the niobium cluster takes place during the deposition of the cluster particles. As shown in the micrographs in Fig. 3.42, the amounts of Nb (green) and Cl (blue) are different. If the cluster particle deposited had not been structurally changed, the amount of matter for both elements should have been the same[3.5], so the traces of Nb and Cl should be the same. Since in some molecules the amount of Nb is larger than that of Cl, it can be stated that some restructuring of the cluster molecule has taken place. The most likely possibility is that a ligand exchange has been produced during the production of the solution, as introduced earlier in this chapter, which has no further effect on the decomposition of the cluster molecules, as has been described in section 3.1.2.

In some of the samples, the EDX graphs showed the presence of oxygen. This presence of oxygen could be also due to the already commented exchange of the chloride ligands for methanol ligands, according to the results of prior research in our laboratory [42]. This ligand exchange can explain the different proportion of Nb / Cl observed in some particles using the SIT-7 and SIT-8 methods[3.6]. Apart from that, the larger methanol outer ligands in the cluster would promote the anchorage of the molecule on the substrate, as reported by Braunstein et al. [48, 49], which also explains the rather adhesive character of the niobium cluster particles deposited by SIT methods. However, according to chemical mapping analyses, this oxygen comes also from the passivation layer present on the surface of the substrate metals. Therefore no definitive statement can be made concerning the ligand exchange process during the precursor solution formation.
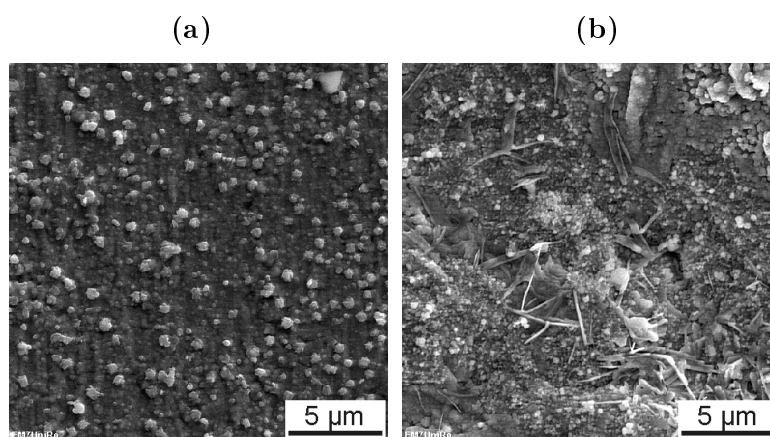
**(a)** **(b)**



**Figure 3.43**: SEM micrographs of the formation of spheres during the cluster particle growth, both deposited by SIT-8 (10 days). **(a)** $Na_4[Nb_6Cl_{18}]$ on zirconium. **(b)** $Na_4[Nb_6Cl_{18}]$ on zinc.

Similar to the case of the cylinder formation for the spreading methods (SST-1), the micrographs in Fig. 3.41 and Fig. 3.42 show that the deposition using the SIT techniques enhances

---

[3.5]Six atoms of Nb and eighteen atoms of chlorine are present in each cluster ion and the molecular weight of Nb is three times larger than that of chlorine. Therefore the amount (in weight) of each element in the molecule is approximately the same.

[3.6]The proportion is originally of 50 % (in $[Nb_6Cl_8]^{4-}$ cluster material). When chlorine ligands are exchanged for methanol ligands the amount of Cl is reduced and the factor Nb / Cl increases.
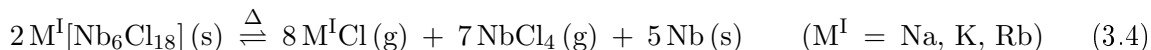
the formation of spherical particles. The sizes of these spheres have been found to be dependent on the substrate and the deposition methods, as in the case of the cylinders, but also on the time in solution. Some examples of the sphere formation are shown in Fig. 3.43.

## 3.4  Cluster decomposition

The last step of the process to obtain metallic niobium particles on substrate surfaces is the decomposition of the niobium cluster material. This process requires the injection of energy to the system. For this project two different energy sources have been studied, direct heating and laser light.

### 3.4.1  Decomposition through direct heating

By heating niobium cluster compounds to high temperature, according to Simon et al. [39], the chemical reaction represented in 3.4 takes place and metallic niobium can be gained again from the process, in addition to the alkali chloride and niobium chloride in gaseous phase.

$$2\,M^{I}[Nb_6Cl_{18}]\,(s) \stackrel{\Delta}{\rightleftharpoons} 8\,M^{I}Cl\,(g) \,+\, 7\,NbCl_4\,(g) \,+\, 5\,Nb\,(s) \qquad (M^{I} \,=\, Na,\, K,\, Rb) \qquad (3.4)$$

As already mentioned, energy is needed for the cluster decomposition (in this case in the form of heat). Therefore, the samples are heated up in a laboratory furnace during a few minutes. In the course of the decomposition, also $NbCl_4$ and the alkali chloride ($M^{I}Cl$, $M^{I}$ = Na, K, Rb) in gaseous state are formed. These compounds can be easily removed from the system using a vacuum pump, allowing only the solid metallic niobium to remain chemically bonded to the substrate.

Metals can easily oxidize when they are heated under atmospheric conditions, due to the oxygen and the moisture (water molecules) in the air. In this case, the use of reduced pressure is also highly helpful in minimizing or even avoiding this oxidation. No oxidation or damaging of the substrates has been noticed on any sample after the heating process.

The cluster thermal decomposition is carried out in a high vacuum installation. The pieces with already deposited precursor are placed in a quartz reaction tube under reduced pressure (approximately $10^{-5}$ mbar). With regards to the heating of the samples, two variations have been used: in the case of the samples without pre-heating (thermal shock), the furnace (Gero GmbH, Neuhausen) is heated up to the desired temperature (200 °C to 1100 °C depending on the substrate). Once this temperature is reached, the tube with the samples is introduced in the furnace. For the samples where pre-heating is applied, the heating rate is set in the device (5 to 25 °C · min$^{-1}$) and the sample is placed inside the furnace at room temperature (see scheme in Fig. 3.44).
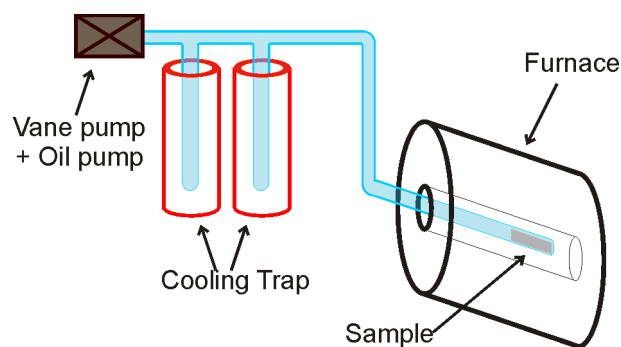
**Figure 3.44**: Scheme of the cluster decomposition process using the heating method (furnace).

After the heat treatment, the reaction tube with the piece is taken out of the furnace and left for cooling. The sample is maintained under vacuum in order to avoid any oxidation of the piece caused by the high temperature of the substrate in contact with air. Once cold, the sample is taken out of the tube.

Some examples of the results using heat decomposition are shown in Fig. 3.45 and 3.46, where green refers to Nb, blue to Cl and red to K / Rb. It can be observed in these figures that the heating method is indeed successful in decomposing the cluster compounds. After this process, only niobium particles (represented by the green spots) and no traces of chlorine or the alkali metal (blue and red respectively) are found[3.7].

With regards to the size of the particles, it has been found to be variable with the specifications of the precursor deposition process (especially the deposition method and the cluster type) and with the substrate. However, these particle sizes are directly related to those of the precursor particles, as it might be expected. Since no sintering has taken place, the sizes of the metallic niobium particles are always slightly smaller than those of the cluster particles. Overall, an upper threshold can be set at 5 µm for the diameter sizes of the particles deposited by SST and at 1 µm for those deposited by SIT.

Regarding the distribution and appearance of the particles, these have been found to be directly related to the decomposition process specifications, being the temperature, time and heating rate especially relevant. These dependences are presented in more detail at the end of this section (sections 3.4.1.1, 3.4.1.2, and 3.4.1.3).

Despite the encouraging results obtained using the heating process, this is not a practicable solution for all substrates. The tests have shown that, in order to achieve a good decomposition of the particles, a temperature above 600 °C must be applied. Therefore, this method cannot be used with substrates such as glass, tin or lead. As shown in the micrographs and EDX graphs in Fig. 3.47, the treatment has almost no effect on the samples if the temperature

---

[3.7]Some blue and red spots appear in all pictures, which correspond to the errors of the method. In the rubidium chemical mapping in Fig. 3.46, the amount of this element is noticeable (larger than an error amount), probably due to interaction of the energy line of the element with that of Si, which comes probably from the ampoule where the decomposition takes place ($L\alpha_{Rb} = 1,69\,keV$ and $K\alpha_{Si} = 1,74\,keV$).

**Figure 3.45**: Decomposition process of the $K_4[Nb_6Cl_{18}]$ particles on a copper substrate. **(a)** Cluster particles deposited on Cu before decomposition (SST-1). **(b)** Metallic Nb particles on Cu after decomposition (1 h at 900 °C).
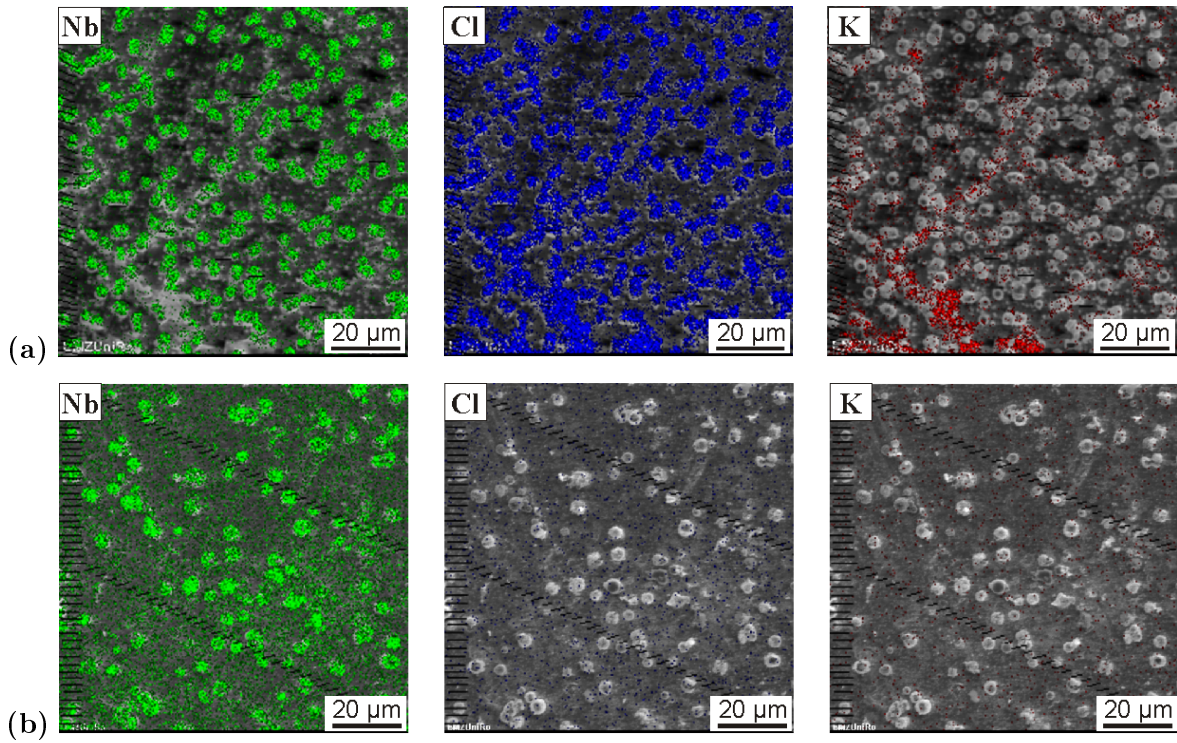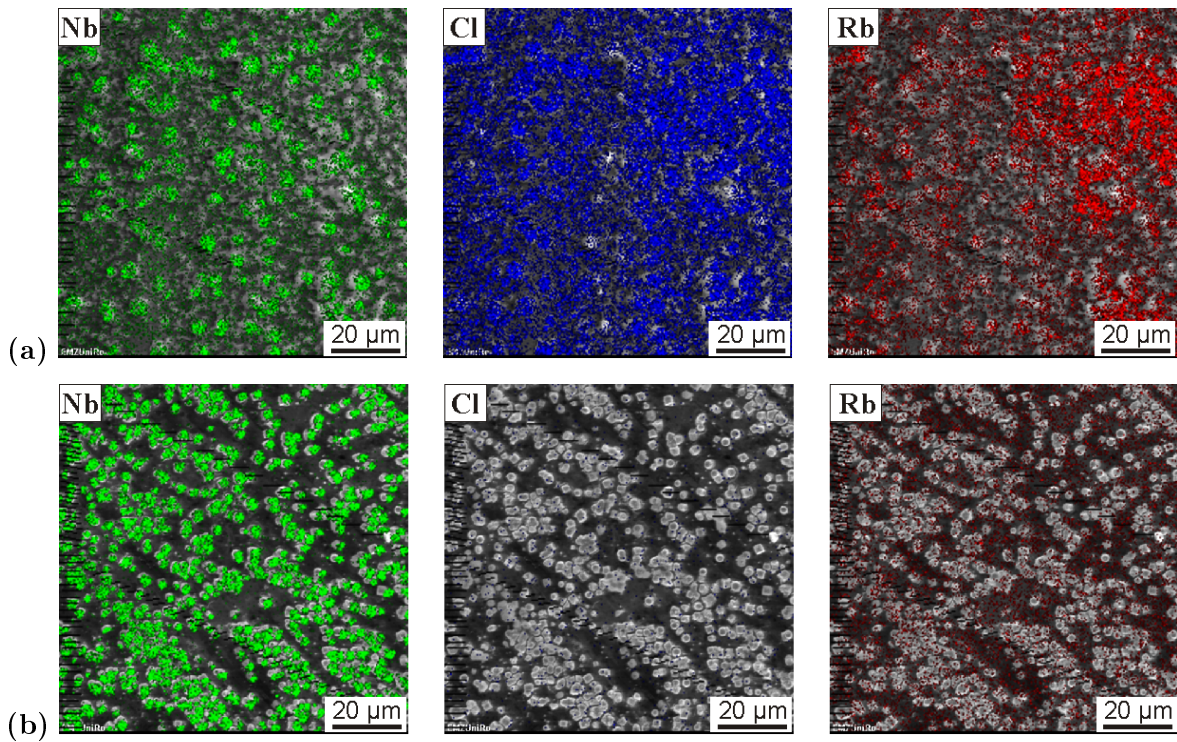


**Figure 3.46**: Decomposition process of the $Rb_4[Nb_6Cl_{18}]$ particles on an aluminium substrate. **(a)** Cluster particles deposited on Al before decomposition (SST-1). **(b)** Metallic Nb particles on Al after decomposition (1 h at 600 °C).

of the heating process is lower than 600 °C (chlorine and rubidium can be still found on the sample).
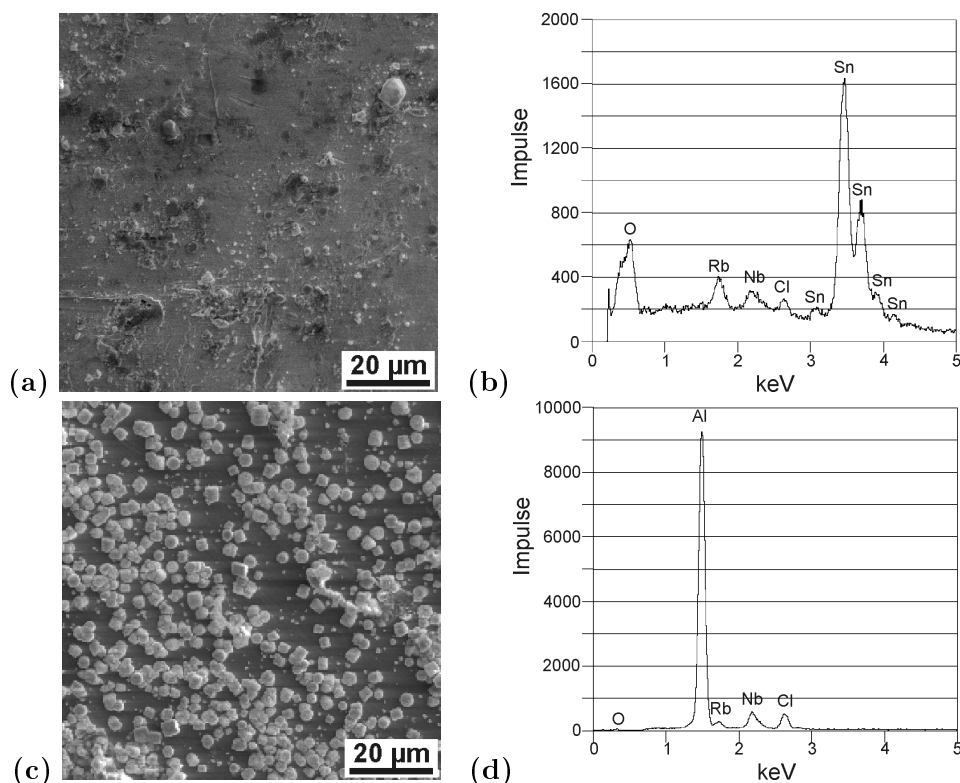


**Figure 3.47**: Heating process at a temperature lower than 600 °C. **(a)** SEM micrograph and **(b)** EDX graph of the $Rb_4[Nb_6Cl_{18}]$ particles deposited on tin (SST-1, 180 °C decomposition). **(c)** SEM micrograph and **(d)** EDX graph of the $Rb_4[Nb_6Cl_{18}]$ particles deposited on aluminium (SST-1, 400 °C decomposition).

#### 3.4.1.1   Heating time

As described previously, the appearance of the cluster after the decomposition depends mainly on the time spent at the decomposition temperature. Some results as well as the starting sample deposited by SST-1 are depicted in Fig. 3.48.

As seen in the micrographs in this figure, even very short times (e.g. 5 minutes) are sufficient to decompose the cluster particles and remove the chlorides from the environment of the sample (avoiding a further deposition of these compounds). Since no sintering of the particles takes place during this process, the distribution and sizes of the particles remain similar to the ones before the decomposition process, becoming only slightly smaller due to the chlorine loss.

However, when using long decomposition times, the particles tend to become smaller and more defined (see the micrograph after 4 hours of decomposition in Fig. 3.48). At first, this is due to a sintering process that gathers the remaining niobium particles occupying the space left by the chlorine and therefore reducing the size of the particles (see the micrograph after 30 minutes of decomposition in Fig. 3.48). Second, after the sintering process, the niobium particles on the

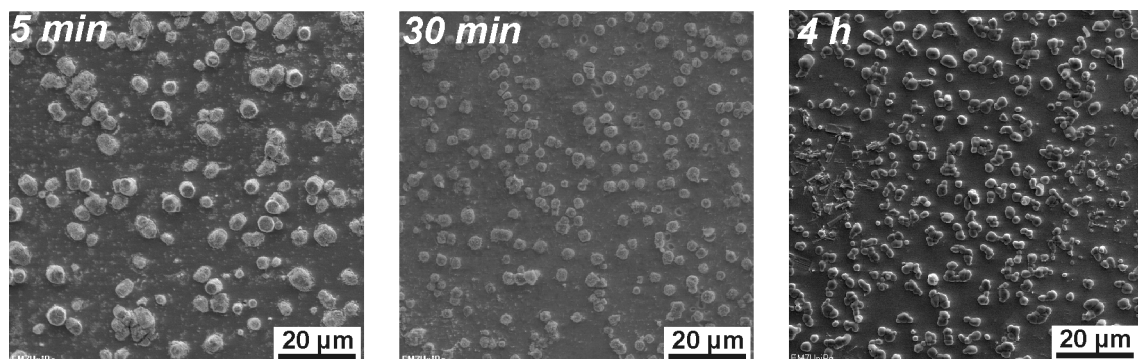substrate crystallize forming micro-needles (see the micrograph after 4 hours of decomposition in Fig. 3.48).



**Figure 3.48**: Dependence on time. Nb particles on copper. $Na_4[Nb_6Cl_{18}]$ particle deposition using SST-1.

### 3.4.1.2   Temperature

With regards to the temperature, several tests at different temperatures have been conducted. The results obtained indicate that the pieces must be heated at a minimum of 600 °C to achieve a complete decomposition of the cluster particles. However, this temperature must be kept below 900 °C for optimal results. As seen in the micrographs in Fig. 3.49, at temperatures higher than 900 °C the metallic particles are sintered and their sizes become larger (decomposition at 1000 °C in the figure).

With regards to the sizes of the particles, it is possible to observe in Fig. 3.49, that the sizes of the particles remain constant or very similar independently of the temperature used. In this particular case for copper the particle size seems to increase with the increasing temperatures, however this enlargement is also due to differences in the particle size of the initial precursor-coated samples.
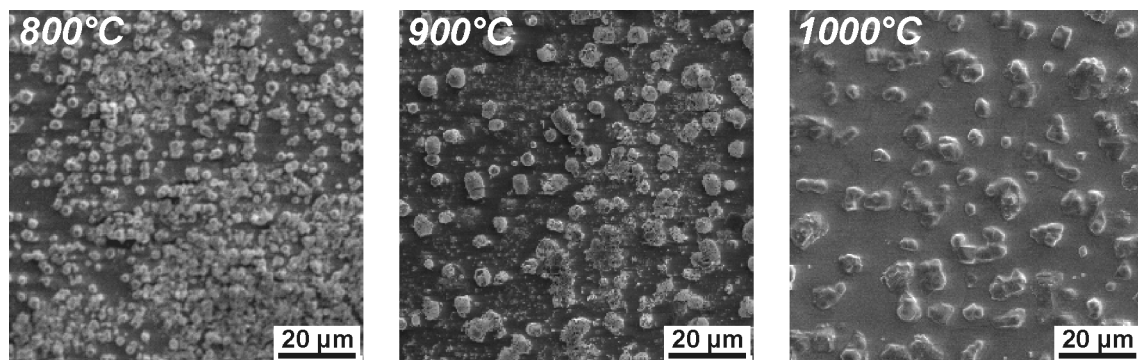


**Figure 3.49**: Dependence on the temperature. Nb particles on copper. $Na_4[Nb_6Cl_{18}]$ particle deposition using SST-1.

### 3.4.1.3  Heating rate

The heating rate defines the amount of time the sample remains in the furnace before the temperature of the sample changes from its initial value until it reaches the desired value. It is measured in $°C \cdot min^{-1}$. A heating rate of $\infty$ represents a thermal shock, i.e. the sudden introduction of the sample in the hot furnace, which has previously been set at the desired temperature.

As seen in the micrographs in Fig. 3.50, the results for all heating rates are very similar in terms of particle size and distribution. With regards to the particle sizes obtained, these are almost constant and similar to the starting precursor particles. The only difference observed is, however, due to a difference in the starting precursor-coated material rather than an effect of the method, like in the case of the dependence on temperature.

The distribution of the particles remains also very similar during the process, which leads us to think that the adhesion of the particles is quite strong, not allowing them to move with the increase of temperature or the thermal shock. Some small differences can be seen for this distribution in the samples in Fig. 3.50, although they are not relevant since they are caused as well by differences in the starting coated samples.
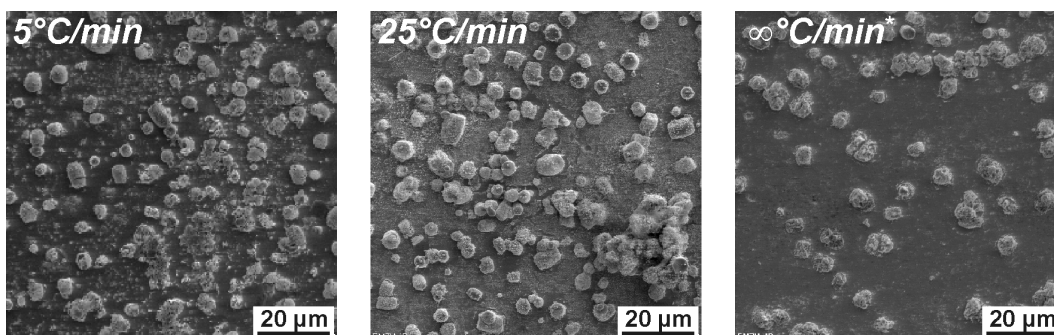


**Figure 3.50**: Dependence on the heating rate. Nb particles on copper. $Rb_4[Nb_6Cl_{18}]$ deposition using SST-1 and heating 10 minutes at 900 °C (once this is reached).

### 3.4.2  Decomposition using laser light

As introduced in section 3.4.1, the direct heating of the samples to decompose the cluster particles is only practicable for substrates with a melting temperature above 650 °C. Therefore, it is necessary to investigate alternative energy sources that can be used for substrates with low melting points.

A possible source of energy is a laser. In this case, the energy needed to decompose the niobium-chlorine bonds in the cluster can be applied in a very localized manner without damaging the underlying substrate. Consequently, the decomposition reaction 3.4 introduced in section 3.4.1 would also take place and volatile $M^I Cl$ ($M^I$ = Na, K, Rb) and $NbCl_4$ would also be obtained and removed from the environment of the sample.
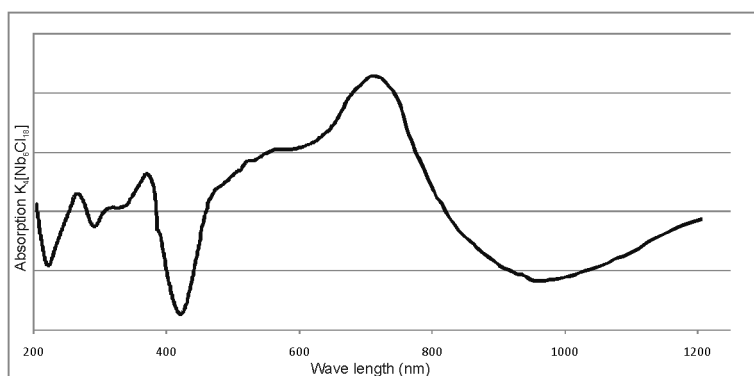
**Figure 3.51**: Absorption spectrum of solid $K_4[Nb_6Cl_{18}]$. Adapted from [23].

The efficiency of this process will be maximized if the laser beam used is of the same wavelength than the maximum on the absorption spectrum of the cluster compound. A review of previous work [23, 50] indicates that this wave length lays within the visible zone of the light spectrum, as seen in Fig. 3.51. Precisely, the solid compound has an absolute absorbance maximum at approximately 710 nm (visible light, red) and two other local maxima at approximately 370 and 270 nm respectively (near ultraviolet, NUV).

The experiments using a laser as energy source have been carried out in the laboratories of Prof. Dr. Lochbrunner in the Institute of Physics at the University of Rostock. The samples are placed inside a chamber where vacuum is applied with an oil pump, as seen in the scheme in Fig. 3.52. With this process, the chlorides in vapour phase that are produced during the decomposition process can be extracted.



**Figure 3.52**: Scheme of the cluster decomposition device using laser light (UV-Vis).

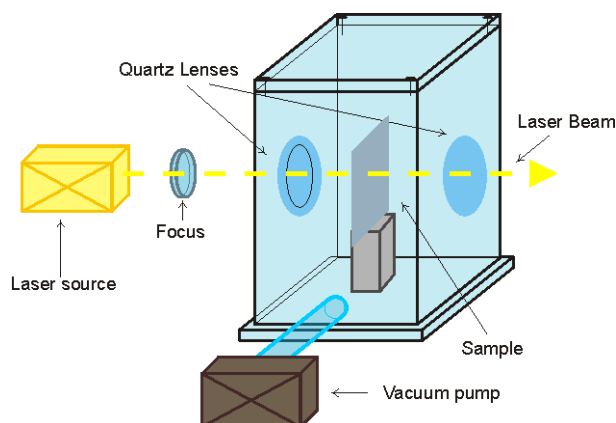The laser light source is a femtosecond titanium-sapphire laser[3.8](Clark MXR CPA 2001) emitting light with a wavelength of 775 nm (visible, red light), a pulse duration of 150 fs and a reiteration rate of 1 kHz. The value for the wave length is very similar to the one where the cluster compound has its absolute maximal absorption point and, therefore, it is expected that the cluster will absorb a large amount of energy.

With the help of a frequency doubler, the wave length can be set to 388.5 nm for further experiments. This value is also very similar to another point of maximal absorption and, as a consequence, large amounts of energy can be also transmitted to the cluster with this new set of experiment parameters. A mirror is used to separate the 775 nm and the 388.5 nm beams. Due to an incomplete doubling of the frequency, a loss of emission occurs. For that reason, only a maximal beam power of 40 mW can be achieved for this frequency. A focusing mirror is placed at last step before the sample, whose position with respect to the substrate can be also varied.

The starting mean power of the device is, in normal conditions, approximately 850 mW. This parameter can be changed with the help of a filter, which allows only a part of the emission to go through it. This makes a variation of the beam power from 220 mW to 5 mW possible for the experiments.
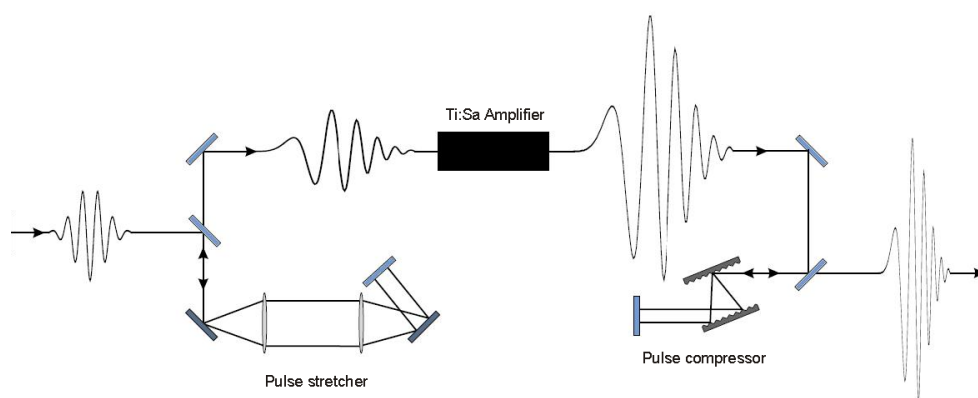


**Figure 3.53**: Scheme of the concept of the *chirped pulse amplification* (CPA). Extracted and adapted from [51].

This laser is based on the idea of the *chirped pulse amplification* (CPA, see scheme in Fig. 3.53). It consists of five main parts [51]:

- Diode laser, which serves as a pump laser for the system

- Erbium glass-fibre oscillator, which produces the beam for the amplifier

- Pulse stretcher, which dilates the seed pulses from the amplifier in order not to damage the elements of the system

---

[3.8]also known as Ti:sapphire laser, or Ti:$Al_2O_3$ laser.

- Double frequency Nd YAG[3.9]pump laser, which pumps the occupational inversion that amplifies the seed pulses

- Ti:Sa amplifier and pulse compressor, which amplify the seed pulses in a factor of $10^6$

### 3.4.2.1   Theoretical approximations

In order to investigate if the laser used is capable of decomposing the cluster molecules, the energy needed should be calculated and compared to the energy provided by the laser. However, no literature values exist for the formation enthalpy of the niobium cluster material $[Nb_6 Cl_{18}]^{4-}$ or any of its Na, K or Rb salts. This enthalpy can be roughly approximated by comparing it to the value of the $[Nb_6 Cl_{14}]$, which has been described in the literature [20]. Therefore, the proposed value for the enthalpy of $Rb_4[Nb_6 Cl_{18}]$ is 120 kcal $\cdot$ mol$^{-1}$ . With this value, a rough approximation for the total energy of a cluster molecule can be calculated by 5.20 . Taking into account that the cluster molecule has 42 bonds, the energy required to break each one of these bonds will lie well below 5.2 eV $\cdot$ molecule$^{-1}$. In parallel, the energy of a photon of the laser used can be calculated using Planck's law. For a wavelength of 775 nm, this value is 1.60 eV, which is considered sufficient to break the individual bonds within the cluster molecule.

Finally, considering that the laser beam has a diameter on the sample of 50 µm, that the cluster layer has approximately 0.5 µm of thickness and that the cluster molecule has a volume of approximately 0,52 nm$^3$ and assuming that the cluster coverage of this volume is of a 50 %, it can be calculated that $9.43 \cdot 10^{11}$ cluster molecules can be found inside the laser affected zone. With the value of the energy per cluster molecule obtained previously, it can be calculated that the energy needed to decompose all the cluster molecules in the beam zone is $1.51 \cdot 10^{12}$ eV ($2.42 \cdot 10^{-7}$ J). Using the fact that the laser used has a power of 220mW, the exposure time required to decompose all clusters within the exposed area is in the order of $1.10 \cdot 10^{-6}$ s. Therefore, the exposure times in the experiments performed can be considered to be largely sufficient to cause complete decomposition of the cluster, which is consistent with the observations made.

### 3.4.2.2   Experimental Results

Due to the reflection of metals at the used wave lengths, only glass substrates have been studied for the laser method. Some examples of the results for both wave lengths are shown in Fig. 3.54 and Fig. 3.55, where green refers to niobium and blue refers to chlorine. The results obtained are quite different depending on the parameters of the process, as will be exposed in the next sections.

As it can be observed in the results for the experiment at 775 nm (Fig. 3.54), the chemical mappings before and after the laser processing indicate that no traces of chlorine are found

---

[3.9]Also known as Nd:$Y_3 Al_5 O_{12}$
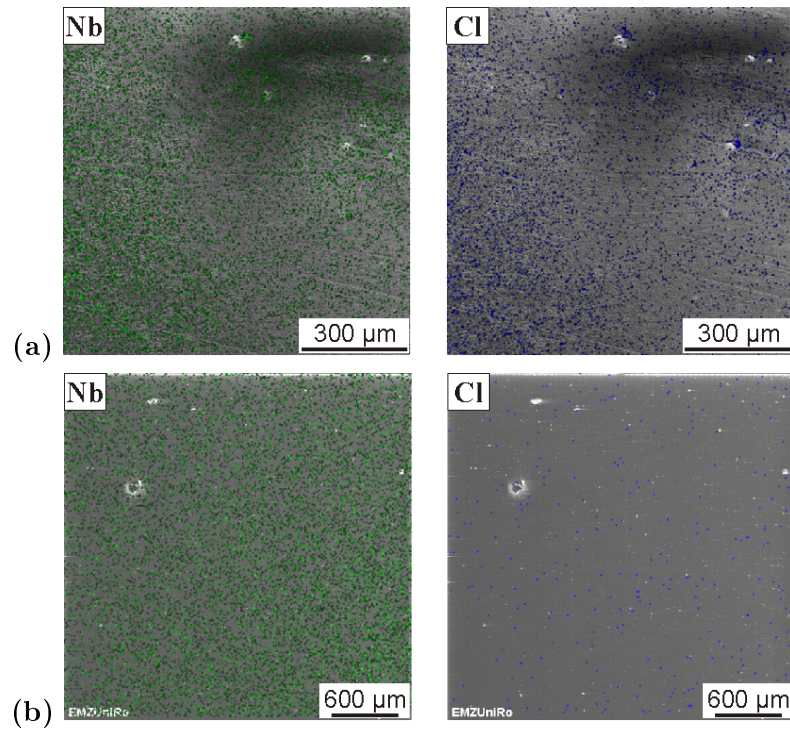
**Figure 3.54**: Decomposition process of the $Rb_4[Nb_6Cl_{18}]$ particles on a glass substrate. **(a)** $Rb_4[Nb_6Cl_{18}]$ particles deposited on glass before decomposition (deposited by SIT-6, 10 days). **(b)** Metallic Nb particles on glass after decomposition ($\lambda = 775\,nm$; $d_{focus} = 25\,cm$; $P = 20\,mW$).
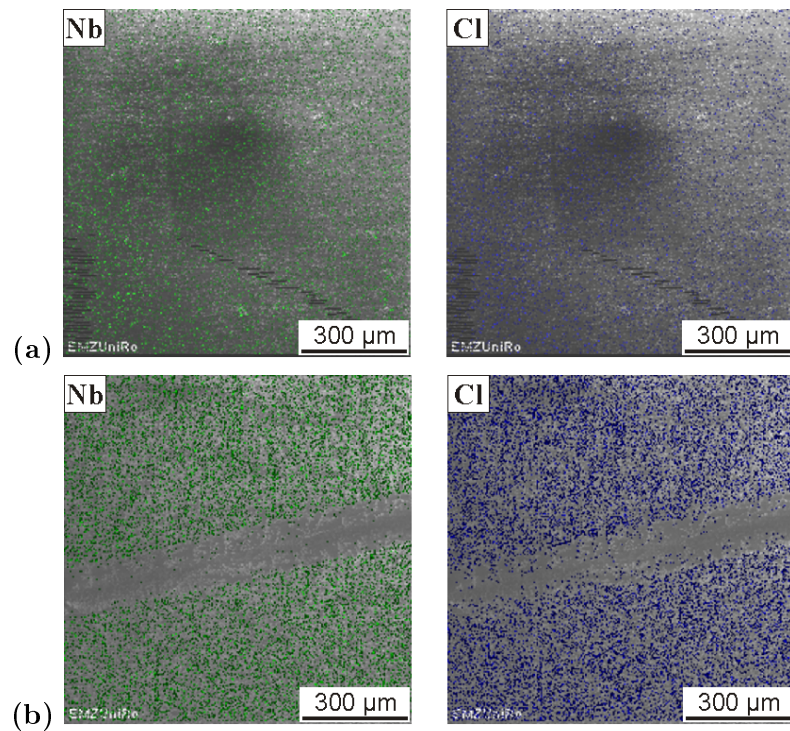


**Figure 3.55**: Decomposition process of the $Rb_4[Nb_6Cl_{18}]$ particles on a glass substrate. **(a)** $Rb_4[Nb_6Cl_{18}]$ particles deposited on glass before decomposition (deposited by SST-1). **(b)** $Rb_4[Nb_6Cl_{18}]$ particles on glass after decomposition ($\lambda = 388.5\,nm$; $d_{focus} = 25\,cm$; $P = 20\,mW$).

after the treatment[3.10]. Supposedly, a part of the energy from the laser beam is absorbed by the cluster molecules. These then decompose presumably following the reaction shown in section 3.4.1 (see reaction 3.4) leaving metallic niobium deposited on the surface. However, it has been observed that the efficacy of the decomposition process increases with the decreasing of the beam power. With regards to the results for the 388.5 nm experiment (Fig. 3.55), the only effect that has been observed is the complete removal of the cluster particles along the laser beam line.

**Dependence on the Precursor Deposition Method**  The laser decomposition experiments have been conducted using samples obtained with the two methods that showed the best deposition results when glass is used as a substrate (SST-1 and SIT-6). Some results for both deposition methods as well as for the uncoated glass are found in Fig. 3.56. It can be seen that the cluster particle sizes on the SST-1 sample are significantly larger than the sizes for the SIT-6 sample, as detailed in section 3.3.6.
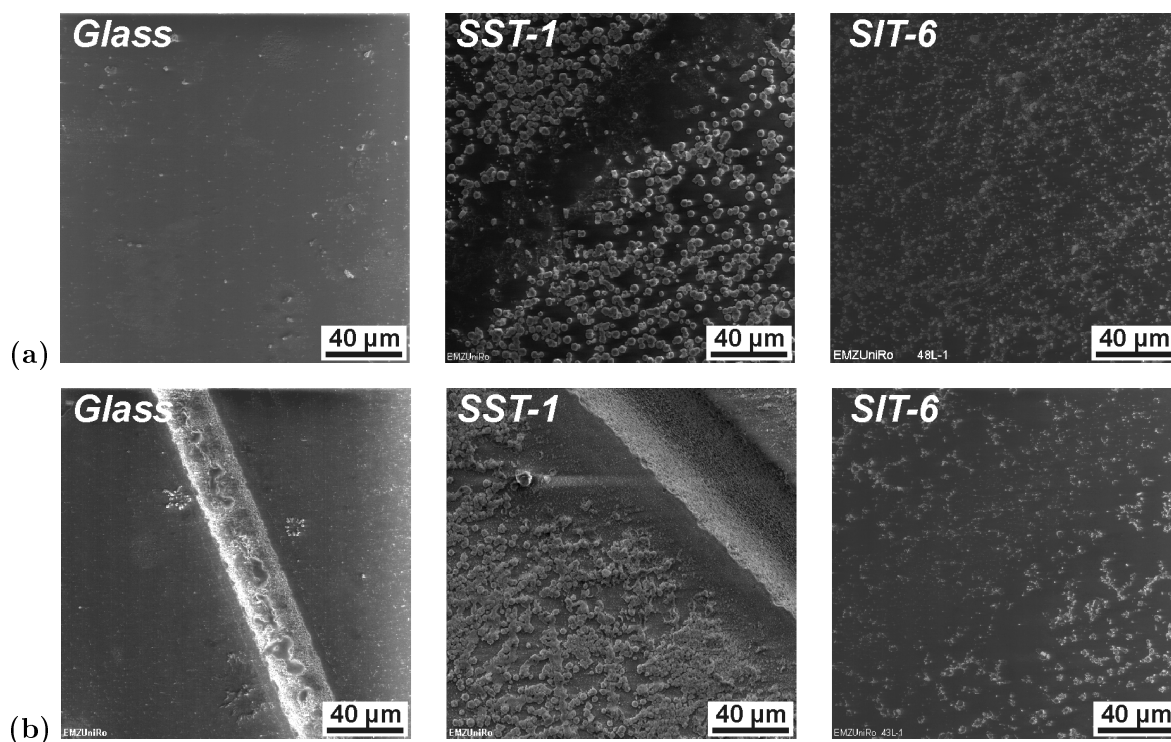


**Figure 3.56**: Dependence on the precursor deposition method. Decomposition of $Rb_4[Nb_6Cl_{18}]$ on a glass substrate using laser light. **(a)** $\lambda = 775\,\text{nm}$; $d_{\text{focus}} = 25\,\text{cm}$; $P = 10\,\text{mW}$. **(b)** $\lambda = 775\,\text{nm}$; $d_{\text{focus}} = 25\,\text{cm}$; $P = 200\,\text{mW}$.

With regards to the effect of the laser on the glass substrate, as shown in the same micrographs, whenever the SST-1 method is used, the glass substrate is damaged already by medium intensities of beam (from 80 mW onwards). On the contrary, with the use of the SIT-6 methods no

---

[3.10]Rb cannot be analysed for the case of glass substrates due to the overlap of its X-ray energy line with that of Si ($L\alpha_{Rb} = 1,69\,\text{keV}$ and $K\alpha_{Si} = 1,74\,\text{keV}$).

damaging of the substrate has been observed, even with beam intensities up to 220 mW.

With regards to the cluster coating, for the case of SST-1, the cluster particles can be removed even by small beam intensities, reaching a complete removal of the deposited cluster at 40 mW. However, with the use of the SIT-6, the particles are not removed at all by low intensities, and the damage or removal of the cluster particles only starts becoming measurable with a beam intensity of approximately 70 mW. Even at 200 mW some rests of the niobium cluster particles can be found on the surface. This is basically due to the higher adhesion of the SIT-6-deposited particles compared to those deposited by SST-1.

These results lead to the conclusion that the coating deposited by SIT-6 could be applied in the protection against laser irradiation or as optical coatings. However more research is needed in order to properly characterize the optical properties of the coating.

**Dependence on the Intensity of the Beam**    As stated in the previous section, the cluster decomposition as a function of the laser intensity applied has different results depending on the type of precursor deposition method that has been used. Some of the results for the dependence on the beam intensity is shown in Fig. 3.57.
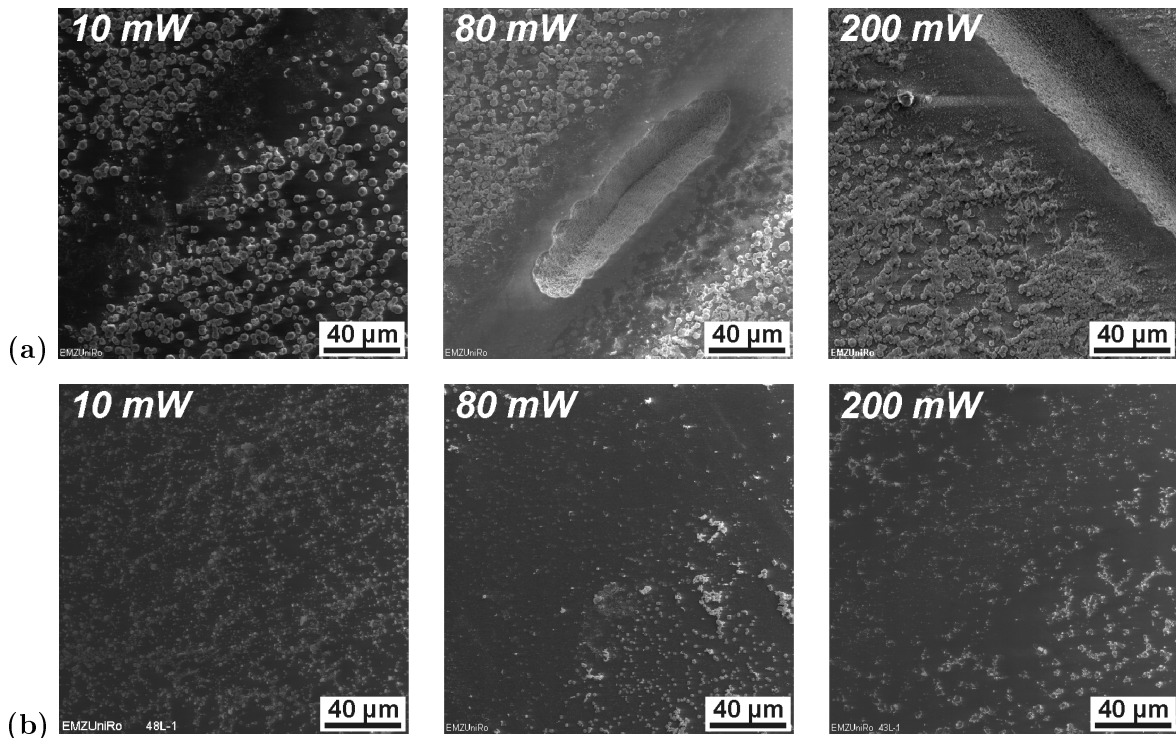


**Figure 3.57**: Dependence on the intensity of the beam. Decomposition of $Rb_4[Nb_6Cl_{18}]$ on a glass substrate using laser light ($\lambda = 775\,nm$; $d_{focus} = 25\,cm$) and cluster deposited by **(a)** SST-1 and **(b)** SIT-6 (10 days).

As expected, the damage on the substrate produced by the laser beam increases with increasing beam intensity. As a consequence of the energy of the beam, the samples experiment first a loss of cluster particles and then superficial destruction (partial or complete scratching). This

is the case of all samples, independently from the type of precursor deposition.

On one side, if the sample is submitted to low beam intensities (up to 70 mW), no damaging of the substrate can be observed on any of the pieces. However, when using the SST-1 method, the coating is almost completely removed by 40 mW, whereas for the case of SIT-6, all cluster particles remain on the surface.

On the other side, if the sample is submitted to high beam intensities (80 - 200 mW) extremely different results depending on the deposition method of the precursor are obtained. Using the SST-1 the substrates show partial damage by 80 mW and are completely scratched by 160 mW. For the SIT-6, no damaging can be observed at any beam intensity. For these last substrates, the clusters on the surface begin to be removed at approximately 80 mW.

**Dependence on the exposure time**   During the laser-decomposition process, the coated substrate is placed inside the vacuum chamber (see scheme in Fig. 3.52) and the chamber is moved perpendicularly to the laser beam at a constant speed. In this way, one displacement of the substrate under the laser is the minimum exposure that can be achieved with the available test set-up. Increased exposure can be achieved by repeating the procedure and the total energy deposited will be a multiple of the energy deposited in one single exposure. Therefore, the time on beam or exposure time can be measured in displacements. No differences between these methods and the static method[3.11] could be observed.

As shown in Fig. 3.58, no significant differences can be observed between the different exposure times. Therefore, it can be stated that the main change happens during the first exposure. No differences in the results between cluster deposition methods or intensities could be observed between the samples exposed one single time and the samples exposed multiple times.
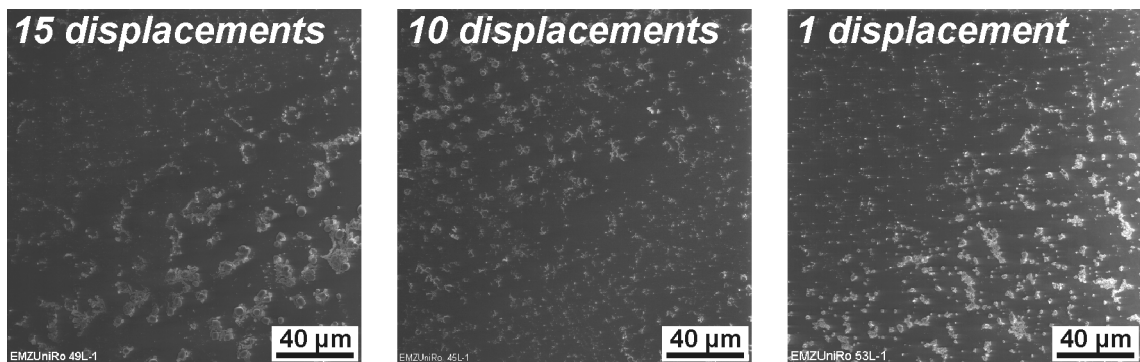


**Figure 3.58**: Dependence on the exposure time. Decomposition of $Rb_4[Nb_6Cl_{18}]$ on a glass substrate using laser light, $\lambda = 775\,nm$; $d_{focus} = 25\,cm$; $P = 160\,mW$; deposition using SIT-6 (10 days).

**Dependence on the Distance from the Focus**   Due to the lens arrangement, there is only one point in which the laser has its maximal energetic effect on the sample. This is the

---

[3.11]This method consists in leaving the chamber still during a certain amount of time while the laser beam acts on the sample.

so-called focus point. In the case of this project the sample is set at 25 cm from the focal point (in focus). Some results of the decomposition with the sample placed at several distances from the focus are shown in Fig. 3.59.

As seen in this figure, only 3 distances from the focus have shown some effects on the coating. Smaller and larger distances led to extremely weak beams with absolutely no effect on the sample. In this case, the results for the SST-1-treated substrates and the SIT-6-treated substrates are completely different.

Similar to the results described in sections 3.4.2.2 and 3.4.2.2, the substrate only is damaged with the use of the SST-1 precursor deposition and placing the sample in focus. With regards to the results outside from the focus, the substrate does not get damaged and only a part of the cluster particles are removed by the laser beam, as it might be expected.

The results for the substrates with SIT-6-deposited particles present no surprises. For the decomposition in focus, only a part of the cluster particles are removed by the laser beam. The results outside from the focus are similar to the results for the in-focus sample. This is probably due to a higher adhesion of the SIT-6-deposited cluster particles to the surface, which increases the resistance of the coating to the action of the laser.
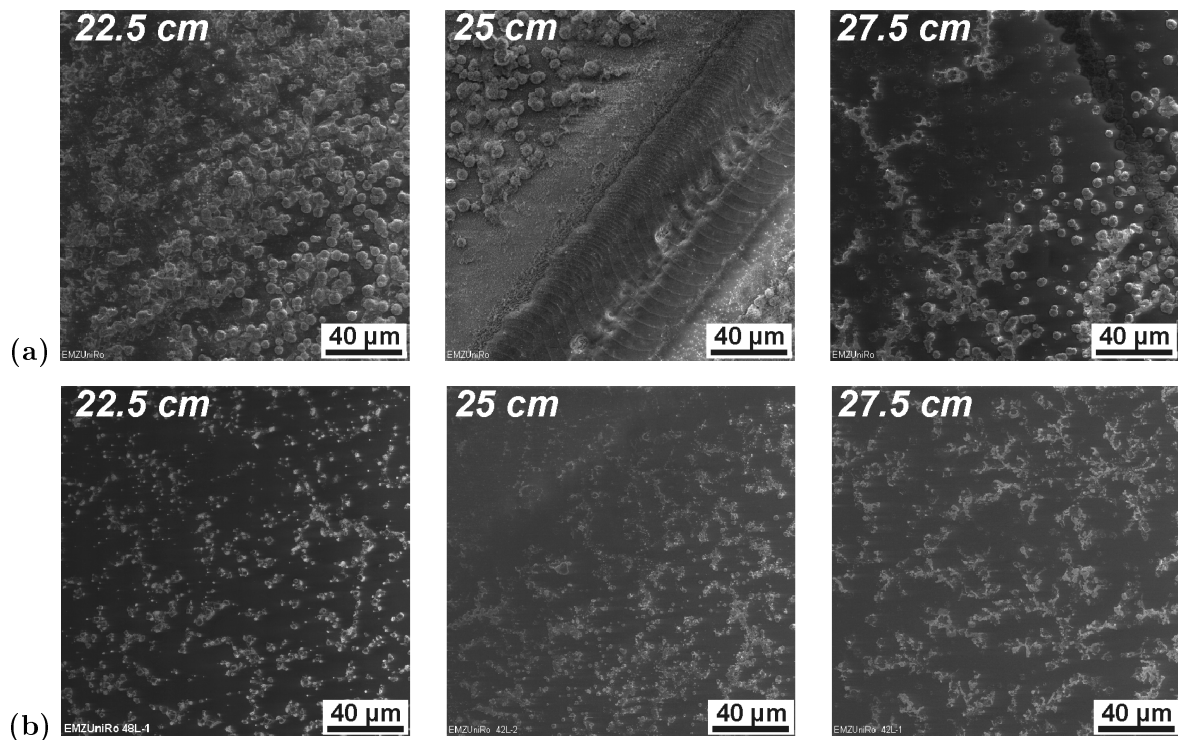


**Figure 3.59**: Dependence on the distance from focus. Decomposition of $Rb_4[Nb_6Cl_{18}]$ on a glass substrate using laser light ($\lambda = 775\,nm$; $P = 220\,mW$) and cluster deposition by **(a)** SST-1 and **(b)** SIT-6 (10 days).

**Dependence on the wave length**  Only two wave lengths can be tested with the available laser. The working value for the used laser is 775 nm, which belongs to the near infrared (NIR)

part of the electromagnetic spectrum. Some results using this wave length are found in Fig. 3.60a. As described in previous sections, the damage of the substrates and removal of the particles happen more frequently if the SST-1 is used. Other good examples of that are shown in Fig. 3.57.

The experimental test set-up used also allows doubling the frequency of the laser emission, resulting in a wave length of 388.5 nm, which belongs to the near ultraviolet (NUV) part of the spectrum. Due to limitations of the frequency doubler, only approximately 18 % of the whole 775 nm laser beam can be converted to a 388.5 nm beam (with a maximal intensity of 40 mW[3.12]).

Selected results for the reduced wave length tests are shown in Fig. 3.60b. These are significantly different from those obtained with the 775 nm wave length. In this case, the samples with particles deposited using both methods (SST-1 and SIT-6) experiment a removal of the particle coating, even with the use of low beam intensities. No damaging of the substrate could be seen, probably due to intensity limitations.



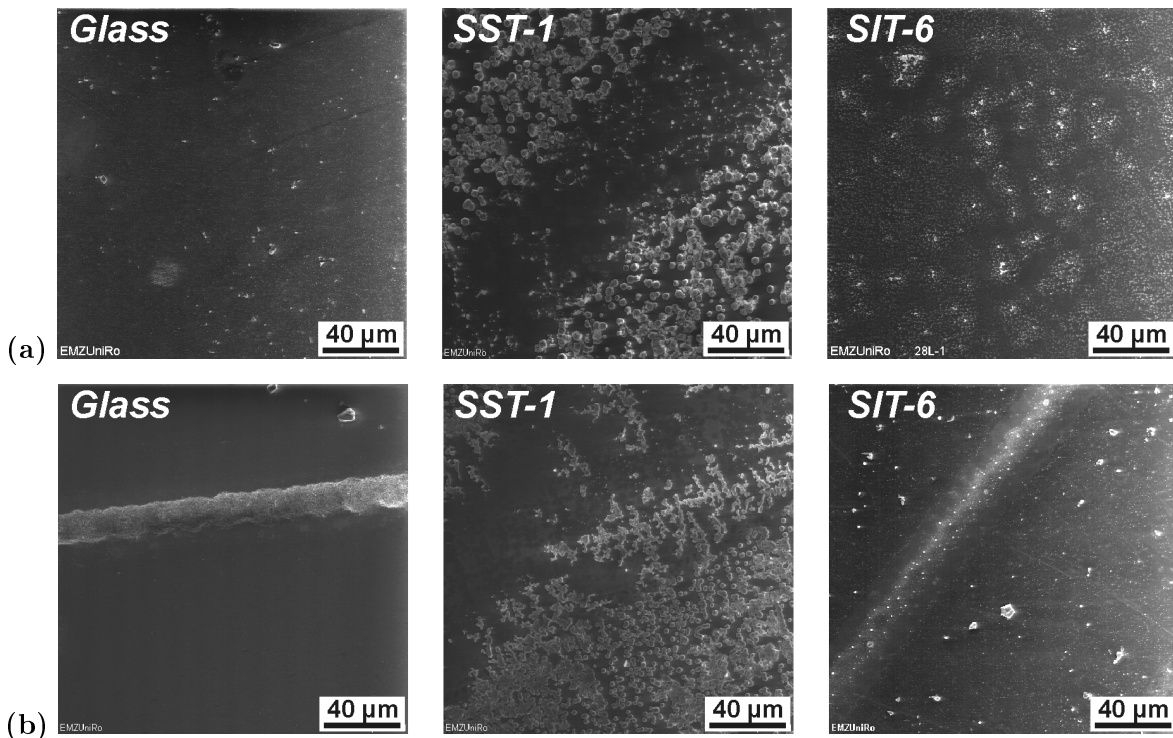**Figure 3.60**: Dependence on the wave length. Decomposition of $Rb_4[Nb_6Cl_{18}]$ on a glass substrate using laser light. **(a)** $\lambda = 775\,nm$; $d_{focus} = 25\,cm$; $P = 20\,mW$. **(b)** $\lambda = 388.5\,nm$; $d_{focus} = 25\,cm$; $P = 20\,mW$.

---

[3.12]The rest of the beam is reflected away, so that only the 388.5 nm light reaches the sample.

### 3.4.3 Evaluation of the decomposition methods

In the last sections it has been shown that it is possible to decompose the deposited cluster particle and obtain metallic niobium particles through an easy heating process. However this process can be only applied to substrates with a melting point above 650 °C.

On one side, the use of the heating process above 600 °C has produced successful results, as already commented, and it has been observed that the particle sizes before and after the decomposition vary only in small amount. It has also been shown that this heating temperature and the time at temperature have an influence on the morphology of the particles, obtaining more defined particles whenever higher temperatures and / or longer heating times are applied. The heating rate in which the particle is heated up to the chosen process temperature has been found to have no significant influence on the particle morphology.

On the other side, the laser treatment has apparently not been successful. Only a few experiments carried out using a very low intensity showed interesting results, in which the clusters have been supposedly decomposed. The success of this methods is however quite questionable, since all particles on the substrate have been transformed into metallic niobium and not only those where the laser light was applied. With the study of the effects of the process parameters on the particles, it has been found that whenever the particles are deposited using the SIT-6, these protect against laser irradiation (UV-Vis), avoiding damage of the substrate even at high intensities.

## 3.5 Deposition of other niobium precursors

In this section the most relevant results using niobium clusters ions $[\mathrm{Nb}_6\mathrm{Cl}_{18-z}\mathrm{X}_z]^{n-}$ with X different from Cl and z = 4 or 18 will be presented and the results of the deposition and growth behaviour of the Nb cluster and niobium coatings will be detailed. For this purpose the clusters $[\mathrm{K}(\mathrm{MeOH})_4]_2[\mathrm{Nb}_6(\mathrm{OMe})_{18}]$ and $[(\mathrm{Nb}_6\mathrm{Cl}_{12})\mathrm{Cl}_2(\mathrm{H}_2\mathrm{O})_4]\cdot 4\,\mathrm{H}_2\mathrm{O}$ have been used as niobium precursors.

As described in section 3.3.6, the solution spreading (SST-1, SST-2 and SST-3) and the substrate impregnation with reduced pressure and elevated temperature (SIT-8) work well on all substrates, obtaining homogeneous particle and element distributions and small particle sizes. In order to investigate whether similar or better results can be obtained with cluster compounds carrying ligands other than Cl, the deposition will be studied on aluminium and copper, since the deposition of the cluster chloride on these metals has produced good results.

### 3.5.1 Niobium methanolate cluster

As described in section 3.3.6, organic ligands tend to promote the attachment of the cluster particles on the surface. As a consequence, smaller cluster particles can be achieved, which

lead to smaller metal particles. This has been described several times in the literature, e.g. for the case of cyclopentadienyl ($[C_5H_5]^-$) or carbonyl (CO) as ligands [48, 49].

The niobium cluster compound with the chemical formula $[K(MeOH)_4]_2[Nb_6(OMe)_{18}]$ is used for this purpose, which is obtained by dissolving the niobium cluster chloride $K_4[Nb_6Cl_{18}]$ in a solution of potassium methanolate in methanol and by afterwards filtrating and removing the solvent. For exact experimental details see [52]. Due to the supposed instability of the compound in air, the experiments have to be carried out inside an argon-filled glove box or using Schlenk techniques.

This compound is an alcoholate-based cluster with an octahedral metal atom core surrounded by methanolate ligands (inner and outer), which is produced in our laboratory [52] (see the structure of this cluster in Fig. 3.61). In the last step of the synthesis a solution of the compound in methanol is obtained, which, after filtration, can be used directly as niobium precursor.
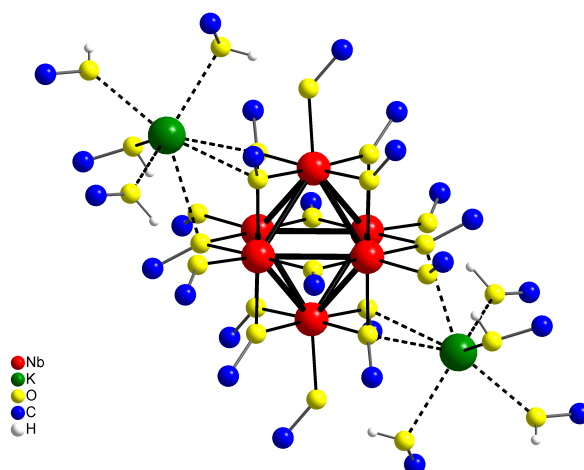


**Figure 3.61**: Structure of the $[K(MeOH)_4]_2[Nb_6(OMe)_{18}]$ (without methyl H atoms for clarity). Structure extracted from [52].

### 3.5.1.1   Cluster Particle deposition by SST

The deposition of the precursor is carried out following the procedures described for SST-1 (see section 3.3.1). Due to the supposed atmospheric instability of the compound, this has been conducted inside an argon glove box. Once completely dry, the samples are taken out of the protective argon atmosphere and are analysed by SEM and EDX techniques. Selected representative results for these experiments can be found in Fig. 3.62.

The results for both substrates are quite unexpected. Firstly, the particle sizes are in part very large and, secondly, the covering was almost complete and micro-cracks were formed during the drying due to an excess of matter in the coating and a very fast drying rate (especially for aluminium, 3.62b).

(a) (b)



**Figure 3.62**: SEM micrographs of $[K(MeOH)_4]_2[Nb_6(OMe)_{18}]$ particles on (a) copper and (b) aluminium (deposited by SST-1).

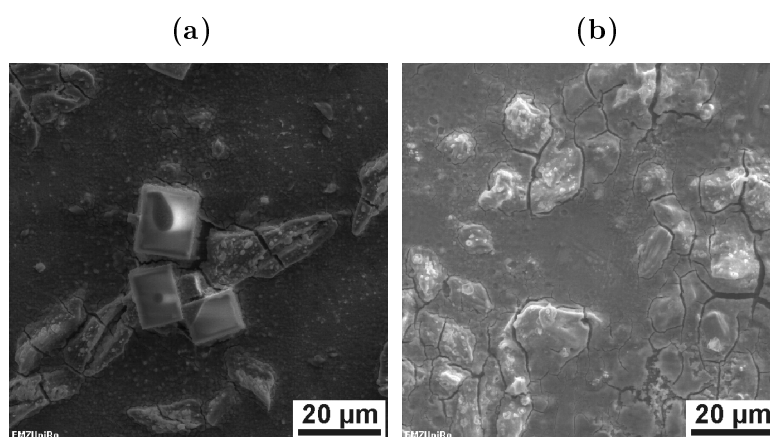In this case also the presence of potassium chloride could be detected by EDX and chemical mapping. This compound can be seen in the form of cubes in the micrograph in figure 3.62a. That is due to the fact that the chloride anions ($Cl^-$) coming from the ligand exchange in solution form KCl (together with the potassium cations in solution). With the evaporation of the solvent, these ions precipitate and crystallize in their typical cubic shape. This is caused by the direct use of the solution obtained in the last step of the cluster synthesis method.

### 3.5.1.2 Cluster Particle deposition by SIT

The deposition of the precursor is carried out using the procedures described for SIT-8 (see section 3.3.1). The SEM micrographs for the coated aluminium and copper substrates are shown in Fig. 3.63. Similar to the case of the chloride-based cluster, the use of the methanolate-based cluster and the SIT-8 has led to particles that are smaller than those obtained using SST-1 for this same precursor. However, these particle sizes are larger than the ones obtained with the cluster chloride.
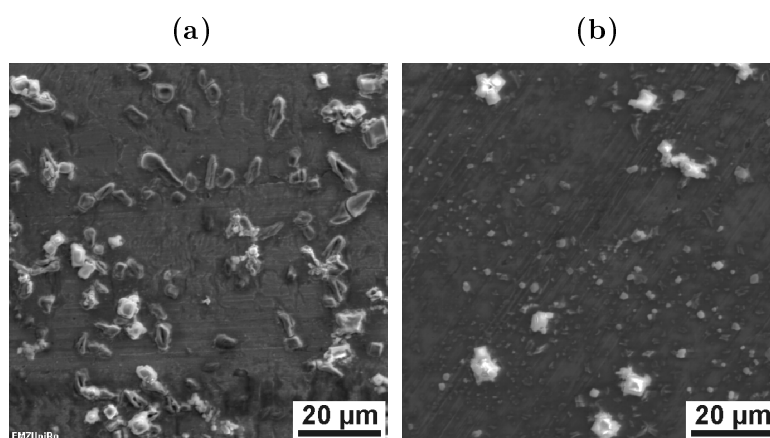
(a) (b)



**Figure 3.63**: SEM Micrographs of $[K(MeOH)_4]_2[Nb_6(OMe)_{18}]$ particles on (a)copper and (b) aluminium (deposited by SIT-8, 7 days).

The EDX graphs of these figures indicate that the amount of Nb, Cl, O and K is clearly less than using the SST-1 method, with approximately a 90 % less of material deposited. This behaviour is similar to that of the deposition of the cluster chloride and is merely a consequence of the deposition method.

As a result of the protective atmosphere inside the glove box, no oxidation or damaging of the substrates has been observed for any of these methods (SST-1 and SIT-8) or materials.

### 3.5.1.3   Decomposition of the cluster materials

Due to the fact that metals generally reflect the light with a wave length of 775 nm and 388.5 nm (used for the laser experiments) and the apparent lack of success of the laser decomposition method, only the cluster decomposition by direct heating has been studied for the methanolate cluster. This compound decomposes at approximately 350 °C, according to Differential Scanning Calorimetry measurements (DSC) [52], which offers the possibility to use this method with substrates with relatively low melting points (e.g. lead, zinc). However, only aluminium and copper have been studied.

For the deposition using SST-1, two different temperatures were studied for each compound:
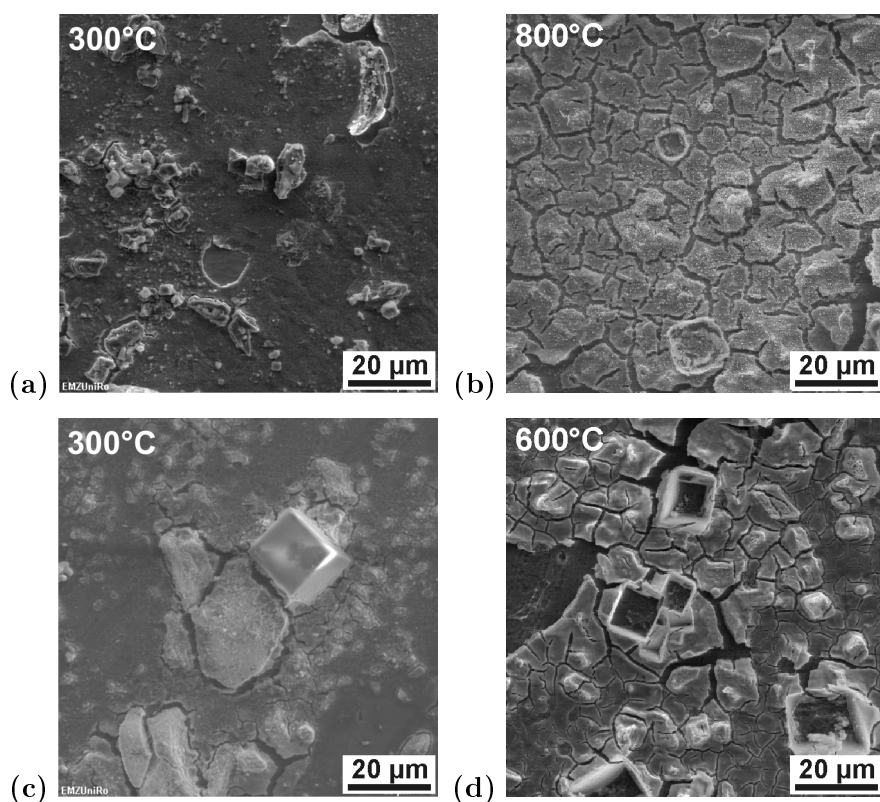


**Figure 3.64**: SEM micrographs of the decomposition of $[K(MeOH)_4]_2[Nb_6(OMe)_{18}]$ (SST-1). **(a)** Copper substrate, heating 1 hour at 300 °C and **(b)** 800 °C. **(c)** Aluminium substrate, heating 1 hour at 300 °C and **(d)** 600 °C.

300 °C, below the temperature where the decomposition of the cluster takes place, and a higher temperature, above that of the decomposition of the cluster (600 °C for aluminium and 800 °C for copper). For the method at low temperature and precursor deposition using SST-1 no differences can be observed between the pre- and post-decomposition states (see Fig. 3.62 and Fig. 3.64). Moreover, it has been analysed that the amounts of elements deposited in both cases are very similar, which leads to the conclusion that, as expected, no decomposition has taken place.

With regards to the high temperature method, it can be also seen in Fig. 3.64 that the results for both substrates are quite similar in appearance to the ones at lower temperature. The EDX graphs on these samples show large amounts of oxygen and potassium can still be found on the samples, despite a low amount of chlorine. It can be concluded from these results that the decomposition of the deposited KCl emerging from the ligand exchange has been indeed successful (also seen through the square-shaped holes in the coating in Fig. 3.64b and Fig. 3.64d), however the cluster decomposition process has not taken place at a higher temperature either.

It has been observed in the micrographs for the deposition of this new precursor using SST-1 that this compound tends to form a continuous, although slightly thin and irregular, coating. As shown in the micrographs of the samples after the deposition, some micro-cracks can appear on the layer through this treatment, caused most likely by the thermal shock and the different thermal expansion coefficients between the coating and the substrates. However, the fact that apparently almost no decomposition of the cluster has taken place after the one hour treatment indicates that this precursor is not adequate for the coating technology studied in this project.

For the decomposition of the cluster particles deposited with SIT-8, only the heating at 800 °C and 600 °C for copper and aluminium respectively has been studied since in both cases no decomposition could be observed at 300 °C. These results are shown in Fig. 3.65.



**(a)**                **(b)**

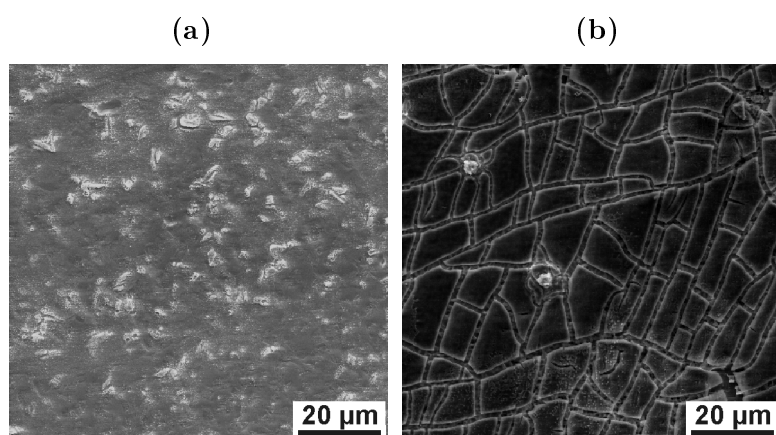**Figure 3.65**: SEM micrograph of the decomposition of $[K(MeOH)_4]_2[Nb_6(OMe)_{18}]$ on **(a)** copper (SIT-8, 7 days, heating 1 hour at 800 °C) and **(b)** aluminium (SIT-8, 7 days, heating 1 hour at 600 °C).

In this case the micrographs before and after the decomposition show some differences in

appearance, especially for the case of aluminium, where some micro-cracks have appeared on the samples. Since the amount of Nb is very low, it can be assumed that this layer is not formed by the cluster coating (as in the case of the SST-1). These observations lead to the conclusion that during the SIT-8 process, only KCl has been deposited and these particles are partly or completely removed from the surface through the heating process.

### 3.5.2   Niobium cluster compounds with water ligands

The dark green water solution of the niobium cluster $[(Nb_6Cl_{12})Cl_{12}(H_2O)_4]\cdot 4\,H_2O$[3.13] has served as niobium precursor. The synthesis of this compound is carried out according to the literature [22, 53]. Following this procedure, an aqueous solution is obtained as final step of the process, which is afterwards filtered in order to eliminate any non dissolved products and directly used as precursor solution. Since the cluster solution is stable in air, the deposition process can take place in the extraction hood. Using this cluster compound, the deposition behaviour and growth of the particles of neutral cluster molecules can be studied. As in the case of the cluster methanolate, only two methods (SST-1 and SIT-8) and two substrates (copper and aluminium) have been studied.

#### 3.5.2.1   Cluster Particle deposition by SST

The deposition has been carried out in the same manner as the deposition of the chloride cluster particles (see section 3.3.1). Some results obtained are shown in Fig. 3.66. The deposition worked rather well for the case of aluminium, with homogeneous distributions and particle sizes up to 5 µm in diameter. However, similar to the case of the methanolate cluster based deposition and due to the chloride anions in solution, alkali chloride particles were as well deposited (cubical particles in Fig. 3.66b).

<div align="center">(a)                                                   (b)</div>
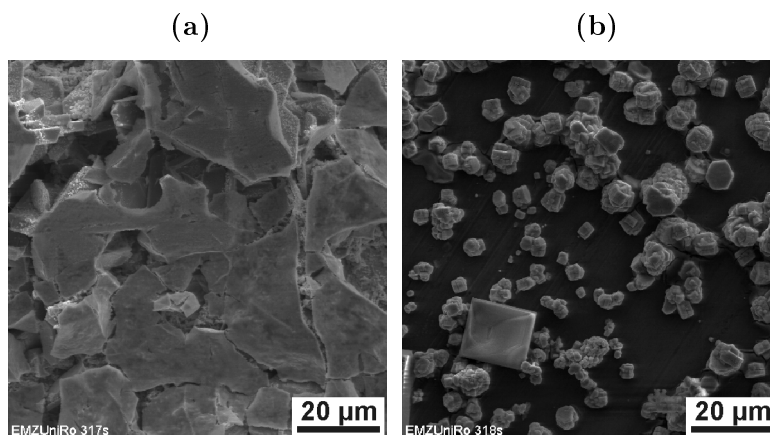


**Figure 3.66**: SEM Micrographs of $[Nb_6Cl_{14}(H_2O)_4]\cdot 4\,H_2O$ particles on **(a)** copper and **(b)** aluminium (deposited by SST-1).

---

[3.13]It can be also found as $Nb_6Cl_{14}\cdot 8\,H_2O$ in the literature.

During the deposition of the precursor on copper using SST-1, the substrate was strongly damaged (a green coloured compound, which was not further investigated, was formed on the surface of the substrate), most probably due to the contact with moist air. Therefore, the surface shown in Fig. 3.66a corresponds to this formed compound, which is presumably a copper chloride, although no clear statement can be made.

### 3.5.2.2 Cluster Particle deposition by SIT

The deposition of the precursor is carried out using the general procedures described for SIT-8 (see section 3.3.1). Some selected representative results for the deposition of $[Nb_6Cl_{14}(H_2O)_4] \cdot 4 H_2O$ using SIT-8 on copper and aluminium are found in Fig. 3.67. The results for the case of copper (Fig. 3.67a) are very similar to those obtained using the cluster chlorides, where particles sizes up to 1 µm and homogeneous distributions are achieved. For the case of aluminium (Fig. 3.67b) these results are not encouraging. The EDX graphs of the samples show that the amount of deposited cluster is relatively low (compared to the SST techniques). This can be also seen in the micrograph since only a few sporadic particles can be found on the surface.

**(a)** **(b)**
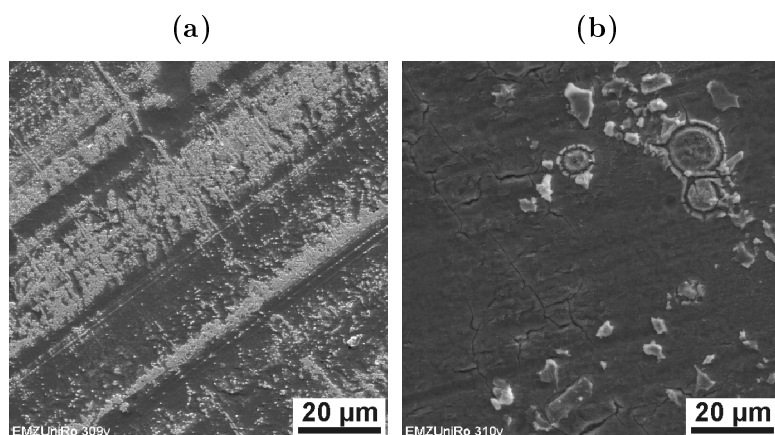


**Figure 3.67**: SEM micrographs of $[Nb_6Cl_{14}(H_2O)_4] \cdot 4 H_2O$ particles on **(a)** copper and **(b)** aluminium (deposited by SIT-8, 10 days).

Given these results, it appears that the adsorption of the aquo ligands on the substrate (probably through H-bridges to the oxides on the surface) is weaker than the adsorption of the chloride-based ions, which adsorbs to the substrates also trough the oxide passivation layer. This is in good accordance with the work of Prokopuk and Shriver [40].

### 3.5.2.3 Decomposition of the cluster materials

As commented in previous sections, due to the risk caused by the reflection of the laser light by metallic surfaces and the lack of success of the laser decomposition, this has not been used for these substrates. Therefore, only the decomposition using direct conventional heating has been studied.

**Figure 3.68**: SEM micrograph of the decomposition of $[Nb_6Cl_{14}(H_2O)_4] \cdot 4\,H_2O$ (SST-1) on Al, heating 1 hour at 600 °C.

An example of the decomposition on samples treated with SST-1 can be found in Fig. 3.68. Since the precursor deposition of the cluster on copper led to severe damaging of the metal surface, only the results for aluminium are shown. T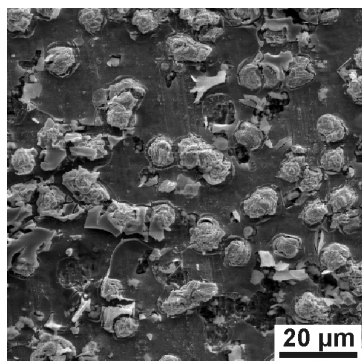he distribution and particle sizes are very similar to the ones before the decomposition (see Fig. 3.66b) concerning particle sizes and distribution. The EDX graphs indicate that the relative amount of chlorine has been reduced to a 10 % of the original value through the heating method, although this is mostly due to the decomposition of the alkali chloride particles. From these results it can be also concluded that the cluster has been partially decomposed, considering that the shapes of the particles have turned more irregular[3.14].

The results for the samples treated with SIT-8, which are shown in Fig. 3.69, also feature a similar appearance before and after the decompositions, compared to the samples in Fig. 3.67.



(a)                                                          (b)
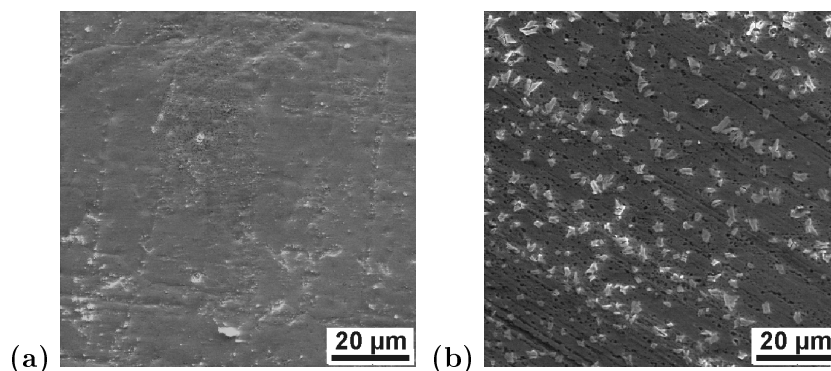
**Figure 3.69**: SEM micrographs of the decomposition of $[Nb_6Cl_{14}(H_2O)_4] \cdot 4\,H_2O$ on **(a)** copper (SIT-8, 10 days heating 1 hour at 800 °C) and **(b)** aluminium (SIT-8, 10 days, heating 1 hour at 600 °C).

With regards to the elements present on the sample, the EDX graphs show that the amount of niobium remains almost constant, whereas the amounts of chlorine and oxygen have been reduced through the heating process. This leads to the conclusion that, as in the case of the SST-1 deposited particles, the decomposition process works for these clusters, although only partially.

### 3.5.3   Evaluation of the process with other niobium precursors

It has been shown that the deposition using the niobium cluster compounds with methanolato and aquo ligands works well for the chosen substrates and techniques, although the results are

---

[3.14]The decomposition time for this samples has been the same than for the chloride-based precursors.

of worse quality than the ones obtained using the cluster chlorides. This is due to the higher adsorption efficiency of the halide ligands with respect to aqua or methanolate as described by Prokopuk and Shriver [40]. Moreover, the deposition of these cluster particles led in some occasions to inhomogeneously distributed particles with poor coverings. In some other cases a continuous coating (not in the form of single particles but as a layer) has been achieved, however its low amounts of niobium and chlorine make it of worse quality than the coating coming from the cluster chloride.

Due to the synthesis method based on ligand exchange, chloride anions are present in the solution used as precursor solution[3.15]. These chloride anions can then precipitate in the form of crystalline KCl (with the potassium coming from the cluster molecule). Even though these chloride particles can be eliminated through the cluster decomposition heating process, they are an irregularity that could affect the possible applications of the cluster coating.

With regards to the decomposition of the cluster particles, the results achieved showed mainly incomplete or absent decompositions even with long decomposition times (up to 1 hour), whereas the decomposition of the cluster chloride is complete after 5 minutes at high temperature. Furthermore, in all occasions where these already mentioned continuous material coatings have been produced, the use of the decomposition method by direct heating led to the formation of cracks in it. This process is most probably due to the different thermal expansion values that, in thermal shock conditions, provide different expansions of the coating and the substrate.

Considering these observations, it can be stated that the best results for the deposition and later decomposition of niobium clusters are achieved when using the cluster chloride, obtaining better particle distributions and smaller particle sizes than the rest of the tested methods.

## 3.6 Sample analysis methods

The appearance of the samples (particle sizes and distribution) is very important to the qualification of the samples. On a first step the samples are analysed using an optical Microscope (Zeiss Stemi 2000 with a light source KL 1500 LCD) up to an amplification of 50x. The pictures are taken using a digital reflex camera (Sony $\alpha$-200) with a maximal amplification of 12.5x. The edition of the pictures is performed with the picture edition software from Sony.

If promising results are obtained, the microscopic surface appearance and the composition (elements) are analysed using a scanning electron microscope and EDX. The analyses are performed using two different electron microscopes. These are a Zeiss DSM 960 A with a Quantum 2003 X-ray preamplifier (Kevex industries) in the group of Prof. Dr. Jonas in the Medical Faculty at the University of Rostock and a Zeiss DSM 960 with a SAMx X-ray

---

[3.15]The cluster is not crystallized, extracted, and re-dissolved. The solution obtained in the last step of the synthesis process is directly used as niobium precursor.

preamplifier (Noran Instruments) in the group of Prof. Dr. Gerber in the Institute of Physics at the University of Rostock.

For the SEM analyses, the microscope is set at a voltage of 10 kV and the electron detector at a distance of 6 mm from the sample. Pictures are taken mostly with a magnification of 1000x and 5000x. The picture edition is done with the program DIPS (Digital Image Processing Software).

For the EDX and chemical mapping analyses, the distance from the samples is set at 25 mm and the voltage used is also 10 kV. The X-ray signals are collected during approximately 100 s with a time to peak of 51.2 µs. For the mapping processes, the time to the peak is changed to 6.4 µs and the exposure time is set by 20 ms. The EDX-graph edition is done with the program WINEDS 4.0 (Quantum 2003) and IDfix (SAMx). The chemical mapping pictures are edited afterwards with the program DIPS. Some of the pictures are taken with a transmission electron microscope adapted with SEM accessories. These analyses are carried out with a Zeiss EM 912 with an X-ray detector Incax-act (Oxford Instruments).

In order to observe samples with a scanning electron microscope they must be electrically conductive, which is not the case for glass. Therefore the glass samples are sputtered with a gold micro-layer of a few nanometres in thickness (Baltec SCD 500 sputter coater) prior to the microscope analyses. The sample to be sputtered is placed in the device and vacuum is applied. The gold target is than bombarded with energetic ions. This process releases atoms from the surface of the metal that are then deposited on the sample. Due to the similarity of the X-ray emission line of gold with that of niobium ($M\alpha_{Au}$= 2.12 keV, $L\alpha_{Nb}$= 2.16 keV), the sputtering of the samples has only been used for the SEM imaging. In this way, it has been possible to obtain pure Nb peaks in the EDX diagrams.

# Chapter 4

# Properties and applications

It has been shown in the previous section that it is possible to homogeneously deposit niobium cluster particles on various substrates and decompose them to obtain metallic particles, which constitutes the main goal of this project. In this section some preliminary tests will be carried out in order to envisage potential applications for the new niobium coating.

## 4.1   Catalysis

Transition metals and their compounds (usually complexes) are known to be good catalysts, which is caused basically by their open electronic shell, their complex electronic structure and the fact that they have several stable states of oxidation [54]. This is the case of palladium or platinum, for example. In the case of niobium (and also tantalum) this statement is not completely true, since it rarely has catalytic effect in its elemental state [55]. However, some research has been carried out in the last years to study the use of niobium compounds in catalysis (mainly $Nb_2O_5$ and niobic acid, $Nb_2O_5 \cdot nH_2O$ ) [11].

The presence of hetero-atoms on a substrate can enhance its catalytic activity. This is due to the fact that chemical reactions proceed preferentially, or even exclusively, on specific active sites [56]. According to this, metallic niobium particles or compounds could be used, for example, as anchors in catalyzed reactions, enhancing the effect of the catalyst. An example of that is the case of ligand-free Nb and Nb-V clusters, which have been reported in the literature as catalysts [57].

### 4.1.1   Cluster materials in catalysis

Whereas the first studies on the synthesis and structure of transition metal cluster compounds date back to the early 60's [14–16], it was not until the early 80's that the first attempts to use them in catalysis were performed. In the work of Braunstein et al.  the use of a

palladium-molybdenum cluster as a catalyst in the carbonylation of nitrobenzene is described [31]. This constitutes the first use of heterometallic molecular clusters as precursors to catalytic nanoparticles.

Since then, numerous studies on the use of clusters as catalysts or catalyst enhancers, mostly supported on inert surfaces (e.g. silica or other oxides), have been conducted. For these investigations, either monometallic or heterometallic clusters can be used. In the first case, usually the whole molecule acts as catalyst (no decomposition of the cluster takes place) [58–60]. Moreover, some studies have demonstrated that the ligands surrounding the metal core can affect the activity and selectivity of the cluster [60]. In the second case, which constitutes the main application of cluster compounds in catalysis, heterometallic clusters are used as precursors to obtain bimetallic or trimetallic particles on inert surfaces. Carbonyl clusters are typically used for this purpose since these ligands can be easily eliminated by thermal activation [32, 48, 49, 61, 62].

### 4.1.2   Applications of niobium in heterogeneous catalysis

Niobium compounds can carry out various roles in catalysis, such as promoter or active phase, support, solid acid catalyst or oxidation catalyst. However, this metal is typically used in the form of niobium oxides or niobic acid instead of its pure metallic form.

Several reactions can be catalyzed by these compounds with interesting results. Some examples have been reported for the dehydration of alcohols using niobic acid [63, 64], the oxidative dehydrogenation of alkanes using heterometallic catalysts containing Nb [64, 65], the oxidation of methane to methanol using monolayers of $Nb_2O_5$ on other metallic and non-metallic oxides [63, 66] and the hydrogenation of CO and hydrocarbons using Pt or Pd particles supported on $Nb_2O_5$ [67, 68].

The catalytic activity of the niobium cluster materials has been also studied [69]. In this field, the results of Kamiguchi et al. are especially interesting. They have demonstrated that crystals of $[Nb_6Cl_{14}(H_2O)_4] \cdot 4\,H_2O$ (and also their Ta, Mo and W equivalents)[4.1] are able to efficiently catalyze various reactions such as the synthesis of some organic compounds [70], the hydrogenation and dehydrogenation of alkenes [71, 72], or the dehydrogenation of amines [73].

### 4.1.3   Evaluation of the catalytic activity of $Rb_4[Nb_6Cl_{18}]$ in hydrogenation

In general, no reaction occurs between $H_2$ and organic compounds at temperatures below 480 °C and atmospheric pressure. However the use of the suitable catalyst enables the reaction at lower temperature and lower $H_2$ pressure. Usually platinum group metals (platinum, palladium and nickel), rhodium, and ruthenium are used as highly active and selective catalysts [74].

---

[4.1] $[Ta_6Cl_{14}(H_2O)_4] \cdot 4\,H_2O$, $(H_3O)_2[(Mo_6Cl_8)Cl_6] \cdot 6\,H_2O$, and $(H_3O)_2[(W_6Cl_8)Cl_6] \cdot 6\,H_2O$.

Taking into account what has been described in the previous sections, it is possible to envisage that the studied chloride-based cluster could be used as catalyst material, either as catalyst on inert surfaces or as improvement for other catalyst materials.

In order to test the catalytic activity of the new niobium cluster supported catalyst, the hydrogenation reaction of 1-hexene to obtain n-hexane has been the chosen reaction, which is represented by the reaction in Fig. 4.1. The experiments and analysis of the catalytic activity have been carried out in the laboratories of Prof. Dr. Kragl in the Leibniz Institute for Catalysis at the University of Rostock.
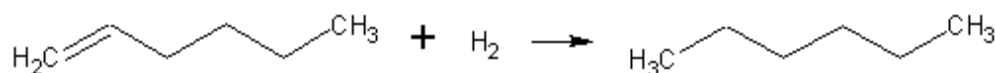


**Figure 4.1**: Hydrogenation reaction of 1-hexene to n-hexane.

For these reactions, 20 ml of the reactant are charged in an autoclave with a 50 ml vessel equipped with a stirrer (Parr Autoclave). Typically, four pieces (cluster coated glass, metallic copper and cluster coated copper depending on the experiment, all with the same size and the same amount of coating) are also placed at the bottom of the vessel (approximately 1 x 1 cm each piece). Prior to the reaction, the vessel is purged using Schlenk techniques (alternating vacuum and argon, three to five times). The pressure of the hydrogen is approximately 40 bar at a temperature of 100 °C. The reaction time is two hours (once the reaction temperature is reached) and the stirrer turns at a speed of approximately 400 rpm. After this time, the device is cooled down to room temperature. A scheme of the process is shown in Fig. 4.2. The products are analysed by gas chromatography (GC) in toluene solution.
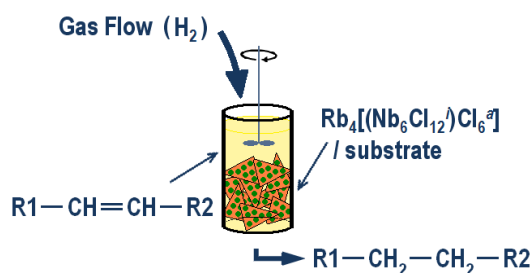


**Figure 4.2**: Scheme of the catalysis process.

### 4.1.3.1 Catalytic activity of cluster coated glass

The adhesion of cluster molecules to the glass substrate has been found to be good. Moreover, it has been shown that the washing of the substrates in water or methanol has no significant effect on the coating (see section 3.3.3). Therefore, the first preliminary tests on the catalytic

behaviour of cluster particles have been conducted using niobium cluster particles on a glass substrate.

The catalytic reaction has been monitored by gas chromatography (GC) (see Fig. 4.3)[4.2]. The products of the reactions show almost no transformation of the 1-hexene (the conversion of the alkene into alkane is approximately 2 %) at the chosen conditions, which reveals that the cluster particles on glass have a negligible catalytic activity.
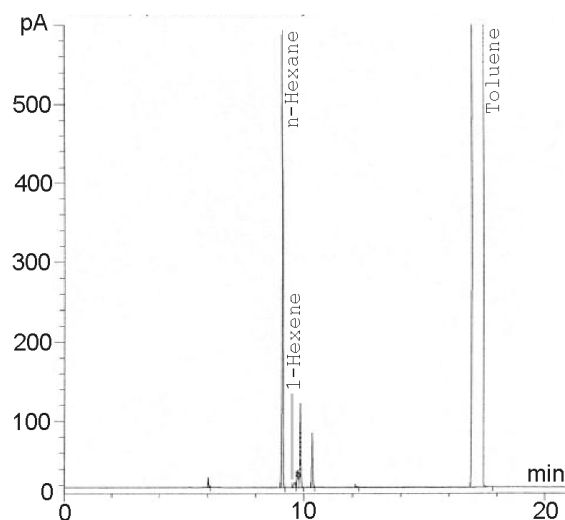


**Figure 4.3**: Gas chromatography of the products of the 1-hexene hydrogenation reaction catalyzed by glass-supported $Rb_4[Nb_6Cl_{18}]$.
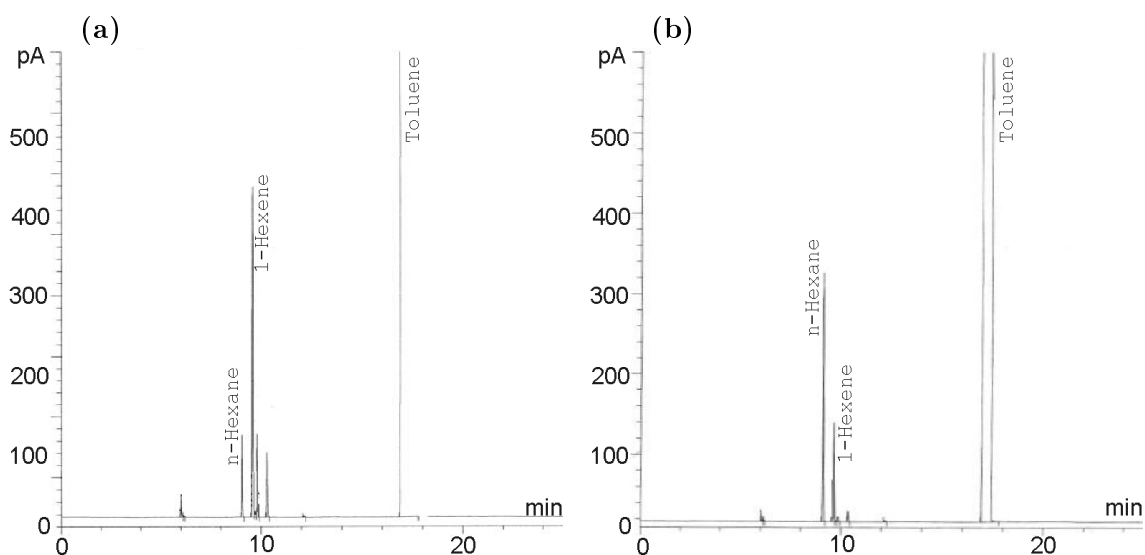


**Figure 4.4**: Gas Chromatography of the products of the 1-hexene hydrogenation reaction catalyzed by **(a)** copper and **(b)** copper-supported $Rb_4[Nb_6Cl_{18}]$.

---

[4.2] The most important peaks are shown in the graph. All other peaks correspond to impurities in toluene.

### 4.1.3.2   Catalytic activity of cluster coated copper

Since it has been shown in the previous paragraphs that the cluster molecule itself does not have any catalytic effect on the chosen reaction, the effect of the cluster on an active substrate (i.e. copper) will also be studied. Copper is known to constitute a rather good catalyst, even as a bulk material, but is not as good as some other transition metals such as palladium or platinum. Due to the non perfect catalytic effect provided by this metal, the enhancement or encapsulation of the catalyst can be studied. The results for the use as catalyst of both metallic copper and the Cu-supported cluster particles are shown in Fig. 4.4[4.2].

For the reaction catalyzed by elemental copper (without cluster coating) the conversion reached a value of approximately 80 % of 1-hexene converted into n-hexane, as shown in Fig. 4.4a. This is consistent with the catalytic effect of copper described above. The fact that the metal is not shaped as nanoparticles causes a reduction in the active surface what is translated in a reduction of its activity to approximately 80 %.

In contrast, if the hydrogenation reaction is carried out using the supported cluster particles, the conversion is reduced to approximately 30 % (conversion of 1-hexene to n-hexane, see Fig. 4.4b). Therefore, it can be stated that the cluster particles reduce the catalytic effect of the copper substrate. Parallel to what has been observed for the cluster coated glass samples, the niobium cluster particles do not have any catalytic effect on the chosen reaction. On the contrary, the fact that part of the copper surface is covered by the cluster particles reduces the number of catalytic sites on which the reaction can take place and, as a consequence, the conversion is reduced to less than half of its original value.

To sum up it can be stated that the studied chloride cluster has no noticeable catalytic effect for the chosen reaction, neither as particles supported on an inert surface (glass) nor as particles supported on an active substrate (copper).

## 4.2   Hardening of surfaces

Numerous methods for surface hardening are available on the market, such as the infusion of heteroatoms in a material (case hardening), the change of the crystalline grain size (grain boundary strengthening) or the heating and rapid cooling of the material (quenching). These methods enhance the hardness of the materials by affecting their internal structure.

The hard material coatings constitute a second group of hardening methods that do not change the structure of the substrate on which they are applied. To date, the hardening coating science has used hard compounds (e.g. metallic and non metallic carbides, nitrides or borides) to coat softer materials in order to enhance its superficial hardness [75].

As already introduced in section 1.2.1, pure metallic niobium has a hardness of 1.32 GPa (Vickers Hardness of the bulk metal, extracted from [76, 77]). This value classifies it as one of

the hardest elements. For this reason, the hardening of surfaces could be a possible application of the new niobium coatings, which would constitute a whole new type of hardening coatings.

### 4.2.1   Hardness tests

Hardness is a very important feature for the characterization of a material. However, it is at the same time a very imprecise term [78]. In its wider meaning, hardness defines the rigidity of the material, and it is calculated as the resistance to deformation caused by an externally applied force. These hardness values depend on all the parameters applied during the test, such as the magnitude of the force applied and the rate at which this force is applied. Some of the most common hardness tests and their measuring parameters are found in Fig. 4.5.
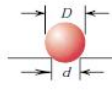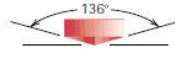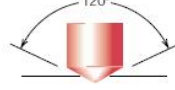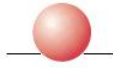


| Test | Indenter | Shape of Indentation | | Load | Formula for Hardness Number[a] |
| | | Side View | Top View | | |
| --- | --- | --- | --- | --- | --- |
| Brinell | 10-mm sphere of steel or tungsten carbide | $D$, $d$ | $d$ | $P$ | $HB = \dfrac{2P}{\pi D[D - \sqrt{D^2 - d^2}]}$ |
| Vickers microhardness | Diamond pyramid | 136° | $d_1$, $d_1$ | $P$ | $HV = 1.854 P/d_1^2$ |
| Knoop microhardness | Diamond pyramid | $t$, $l/b = 7.11$, $b/t = 4.00$ | $b$, $l$ | $P$ | $HK = 14.2 P/l^2$ |
| Rockwell and Superficial Rockwell | Diamond cone, $\frac{1}{16}$, $\frac{1}{8}$, $\frac{1}{4}$, $\frac{1}{2}$ in. diameter steel spheres | 120° | | 60 kg, 100 kg, 150 kg } Rockwell, 15 kg, 30 kg, 45 kg } Superficial Rockwell | |

**Figure 4.5**: Hardness tests parameters. Extracted from [1].

These tests are normalized and performed very frequently, more than any other mechanical tests. This is thanks to the simplicity of the test preparation and procedure and due to the relatively low destruction grade on the sample after the test. The fact that other mechanical properties can be also estimated from the hardness value, such as the tensile strength, enhances the popularity of these tests.

The most appropriate tests to measure the hardness of thin samples and coatings are the Knoop hardness test (HK) or the Vickers hardness test (HV)[4.3] . In both cases a small diamond pyramid is forced into the surface of a material with an applied load and the deformation of the samples is measured. The loads required are small (from 0.01 N to 10 N) and therefore they are often referred to as micro-hardness tests. The hardness scales for both methods are approximately equivalent, although Knoop is more suitable for brittle materials such as ceramics and Vickers is typically used for soft metals.

---

[4.3]For the case of hard materials, macro-indentation is carried out. For this test, several procedures are available. The Rockwell hardness tests (HR) and the Brinell hardness tests (HB) are the most common.

### 4.2.2 Evaluation of the samples

Due to the low thickness of the available samples (between 0.1 mm and 0.3 mm) and of the coating (approximately up to 5 µm), the hardness is tested with the Vickers method (micro-hardness) using a Shimadzu HMV - 2 indenter. A diamond pyramid is used as indenter. The parameters for the Vickers hardness measure are shown in Fig. 4.5. The load used for each substrate material (aluminium, copper and zirconium) is the smallest one for which a certain pre-defined neat indentation is obtained (an example is shown in Fig. 4.6). These are 0.05 N for aluminium, 0.2 N for copper and 0.5 N for zirconium. The effect of the indenter is



**Figure 4.6**: Neat indentation on a steel surface (Vickers hardness, 1 N applied load).

calculated with the software MPT Hard test. Three tests are carried out on each sample and a mean value is extracted from them. In order to analyse the effect of the coating, both sides of a sample are tested (coated and uncoated side). The analyses have been performed in the laboratories of Prof. Dr. Keßler in the Institute of Engineering at the University of Rostock. The results of the hardness tests are shown in table 4.1.
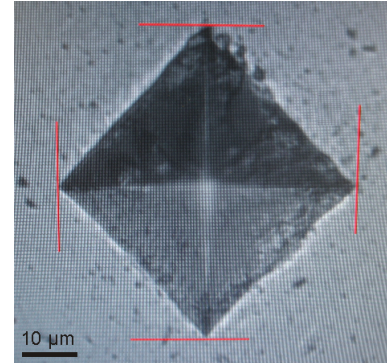
| Sample | Substrate | Precursor deposition method | Heating T | Heating time | Pre-heating | Vickers Load | Hardness substrate (GPa) | Hardness coating (GPa) |
|---|---|---|---|---|---|---|---|---|
| 1 | Al | SST-1 | 600 °C | 10 min | 5 °C · min$^{-1}$ | 0.05 N | 0.21 | 0.27 |
| 2 | Cu | SST-1 | 800 °C | 10 min | 5 °C · min$^{-1}$ | 0.2 N | 0.52 | 0.70 |
| 3 | Zr | SST-1 | 1000 °C | 10 min | 5 °C · min$^{-1}$ | 0.5 N | 2.20 | 3.13 |
| 4 | Cu | SST-1 | 900 °C | 10 min | 5 °C · min$^{-1}$ | 0.2 N | 0.42 | 0.48 |
| 5 | Cu | SST-1 | 900 °C | 4 h | 5 °C · min$^{-1}$ | 0.2 N | 0.52 | 0.61 |

**Table 4.1**: Hardness values.

In the case of aluminium (see sample **1** in table 4.1) the primary hardness of the uncoated sample has been found to be 0.21 GPa whereas the one for the coated sample is 0.27 GPa. The difference between these values can, however, not be considered significant. The fact that the thickness of the samples is very small added to the very low hardness of aluminium makes the testing of aluminium very difficult since the metal easily bends during the test. For these reasons, the difference has not been taken into consideration and it cannot be confirmed that the coating hardens the metal in this case.

For the case of copper (see sample **2** in table 4.1), the value of the hardness for the uncoated sample has been found to be 0.52 GPa whereas that of the coated sample has been found to be 0.70 GPa. Due to the larger hardness value of Cu with respect to Al, the difference in this case is significant and it can be said that the coating hardens the copper surface.

With regards to zirconium (see sample **3** in table 4.1), the hardness has been calculated by 2.20 GPa for the uncoated side and by 3.13 GPa for the coated side. The difference between both values is even larger in this case, which also leads to the conclusion that the coating hardens the substrate.

In a further set of experiments it has been observed that the induced hardness also depends on the heating temperature and time. As shown in table 4.1, the increase of the decomposition temperature seems to decrease the hardness of the whole sample. This is shown by sample **4**, where the hardness of the uncoated substrate is lower than that of the uncoated substrate heated at 800 °C (sample **2**). This behaviour is expected, since the cluster decomposition process constitutes an annealing step for the substrate, which reduces its hardness. The efficacy of the annealing process increases with temperature. The hardness of the substrate can be later increased again through quenching or quenching and tempering processes (see sample **5** in table 4.1).

On overall, a general tendency of the coating to increase the hardness of the sample can be observed. However, the values available in this section are not sufficient to support a clear statement and to quantify the hardness increase provided. This is mostly due to the low thickness of the samples, which is translated in a difficult testing of the samples. Further tests need to be conducted in order to better characterize the hardness increase provided by the niobium particles on the substrates.

## 4.3   Wear and abrasion resistance

An adequate adhesion to the underlying substrate is an extremely important factor for any intended function or application of a film or a coating, since they can be used for a variety of purposes (e.g. decorative, protective, functional).

Another important property of the refractory metals is their low friction coefficient (0.46 for the case of niobium[4.4]). This factor, together with the high hardness of these materials, makes them good candidates to avoid wear and abrasion. As a consequence, if a sufficient adhesion between coating and substrate is achieved, an important potential application for refractory metals could be their use as wear and abrasion resistant coatings.

In order to investigate this potential application it is necessary to test the adhesion of the coatings on the substrate and its overall resistance to wear.

### 4.3.1   Wear and abrasion resistant coatings

Wear is one of the main causes of the damage in engineering components and can often lead to the failure of machines or devices. For that reason, its reduction through right material

---

[4.4]Friction coefficient of a fixed Nb surface and moving block of the same element [76, 77].

selection, heat treatments, coatings and design or lubrication has a very relevant economic and technical importance.

The most common wear resistance method is the lubrication of the surfaces, mainly with the use of greases or oils. These substances, called lubricants, are mostly liquids introduced between two moving surfaces that reduce the friction between them. They typically contain up to 90 % of base oil (mainly petroleum fractions) and 10 % additives, which can increase the viscosity, resistance to corrosion and reduce oxidation, ageing or contamination.

Also hard matter coatings can be used in order to avoid abrasion and wear. Several commercial wear resistance coatings are available nowadays. Among them, two examples are the thin dense chromium coating (e.g. Armoloy® TDC Coating [79]) or the tungsten carbide-based coatings (e.g. Hardide Coatings® [80]).

For that purpose, also the niobium coating represents an alternative to be considered. An increase on abrasion resistance can be achieved by increasing the surface hardness and/or by reducing the friction coefficient of the surface. It has been shown that the niobium coating studied in this project is able to harden substrates (see section 4.2). However, in order for it to be used as wear and abrasion resistant coatings, also the adhesion of the coatings has to be tested.

### 4.3.2 Adhesion tests

The adhesion tests have been performed in our laboratories using an adapted scratch test. The abrasion resistance of a coated material can be defined as its ability to withstand external mechanical forces that tend to remove material from its surface. A simple means of measuring the abrasion resistance of a certain material is by applying a known friction load tangential to it and measuring the effects on its surface.

A possible test set-up to conduct this experiment consists of a body with a certain mass that can be moved over a flat surface where the coating of interest has been applied. If the test set-up ensures that the force applied to the body is parallel to the coated surface, then the friction load only depends on the mass of the body and the friction coefficient between the body and the surface[4.5]. The friction load is independent from all other parameters like, for example, the speed at which the surface to be tested is moved.

Therefore, in order to test the adhesion of the niobium coating (after decomposition of the cluster) to the substrate, the procedure depicted in the scheme in Fig. 4.7 is applied to the samples. Sand paper with a grit of 180 and 320 (CAMI and ISO/FEPA designation) with average particle diameter sizes of 82 μm and 41 μm respectively is used for the experiments.

---

[4.5]The friction force can be easily calculated as $F_\mu = \mu \cdot M \cdot g$, and the friction load as $\sigma_\mu = \frac{F_\mu}{S} = \frac{\mu \cdot M \cdot g}{S}$. Therefore it can be stated that the friction load depends only on the mass of the body, the friction coefficient between the test body and the test surface and the contact surface between them and is independent of the velocity at which the sample is moved.

The used weights vary from 50 g to 250 g. The results are analysed immediately after the scratch using an optical microscope (Zeiss Stemi 2000. with a light source KL 1500 LCD) and the pictures are taken using a digital reflex camera (Sony $\alpha$-200) and edited with the Sony Picture Edition Software.
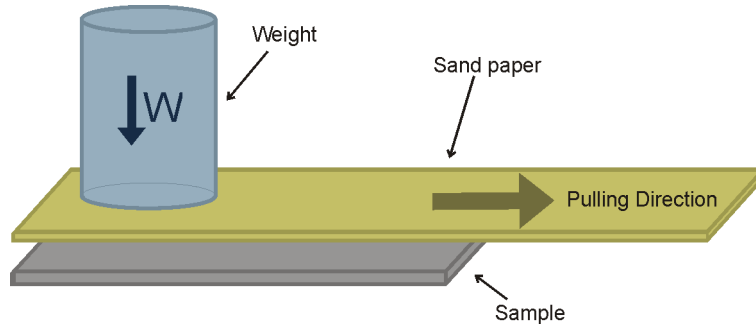


**Figure** 4.7: Scheme of the adhesion test procedure.

### 4.3.2.1    Adhesion on metals

The results obtained for coated metals indicate that the particle coating does provide some degree of additional abrasion resistance. The results of the scratch test using a sand paper with a grit of 180 (CAMI and ISO / FEPA designation, average particle size of 82 µm) and load 150 g are shown in Fig. 4.8 and 4.9. It can be seen there that the coated samples get generally less scratched than the uncoated ones. This behaviour can be explained by the increase in hardness (which has been showed in section 4.2) and the decrease on friction coefficient provided by the coating.
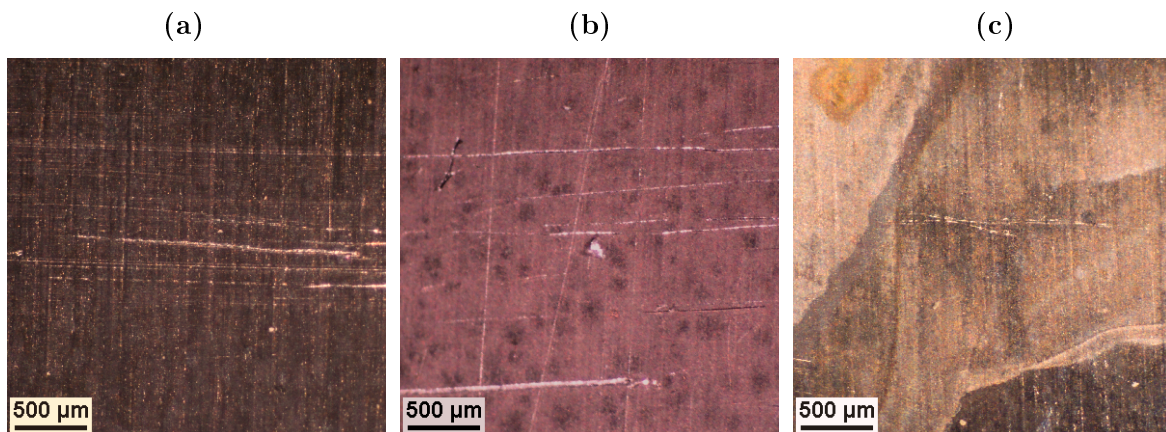


**Figure** 4.8: Scratch tests on (a) a copper metallic surface, (b) $Rb_4[Nb_6Cl_{18}]$ particles on Cu (SST-1 and decomposition during 1 h at 800 °C), and (c) $Rb_4[Nb_6Cl_{18}]$ particles on Cu (SIT-8, 10 days and decomposition during 1 h at 800 °C).

In addition to these measurements, for the case of metals, it has also been observed that the adhesion of the coating is independent of the type of substrate on which it is applied since it is similar on all cases (comparing for example 4.8a to 4.9a and 4.8b to 4.9b).

With regards to the adhesion of the coating depending on the precursor deposition method, SIT-8-deposited precursor particles seem to show a stronger adhesion than those deposited by other methods. This is consistent with the idea introduced in chapter 3.3 that the particles deposited by SIT methods are better attached to the surface, due mostly to the purely chemical bonds provided by the method.

In conclusion, it has been shown that a good adhesion exists between the coating and the substrate for the case of metals. However, for possible applications, further tests are needed.

**(a)**                    **(b)**                  **(c)**



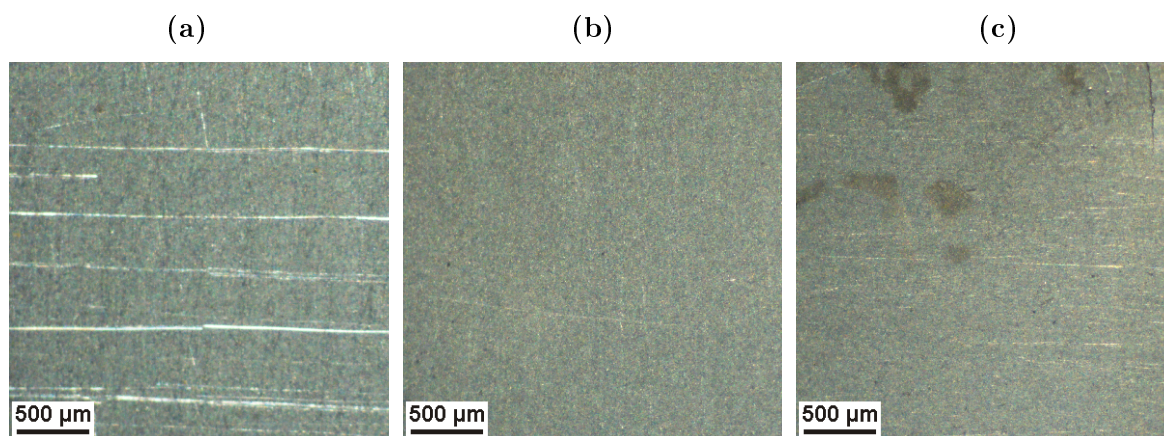**Figure 4.9**: Scratch tests on **(a)** zirconium metallic surface, **(b)** $Rb_4[Nb_6Cl_{18}]$ particles on Zr (SST-1 and decomposition during 1 h at 900 °C), and **(c)** $Rb_4[Nb_6Cl_{18}]$ particles on Zr (SIT-8, 10 days and decomposition during 1 h at 900 °C).

#### 4.3.2.2  Adhesion on glass

It has already been exposed that the adhesion of the particles on glass using SIT-6 is very strong (see section 3.3.3). In this section this will be investigated in more detail and compared to the adhesion of the SST-1 deposited particles. The results obtained for the adapted scratch test with a sand paper with a grit of 180 (CAMI and ISO / FEPA designation, average particle size of 82 µm) and load of 250 g are shown in Fig. 4.10.

The scratch test for the SST-1-deposited particles shows that the adhesion is rather poor, since the coating can be scratched out very easily. This behaviour may be explained by the very rapid evaporation of the solvent, which does not allow all particles in solution enough time for a proper adsorption to the surface.

For the case of the SIT-6-deposited particles, it has been found that the adhesion to the glass substrate is extremely strong since the adapted scratch test has almost no effect on the coating. This adherence of the particles to the surface is probably caused by strong chemical bonds between the cluster particles and the glass substrate and, therefore, the adherence is very strong, as already commented in the beginning of this chapter.

Considering these results and the ones from the laser decomposition on glass, it can be stated

that the cluster layer deposited by SIT-6 could be used as a protective coating for glass substrates. However, more research is needed in this project part.
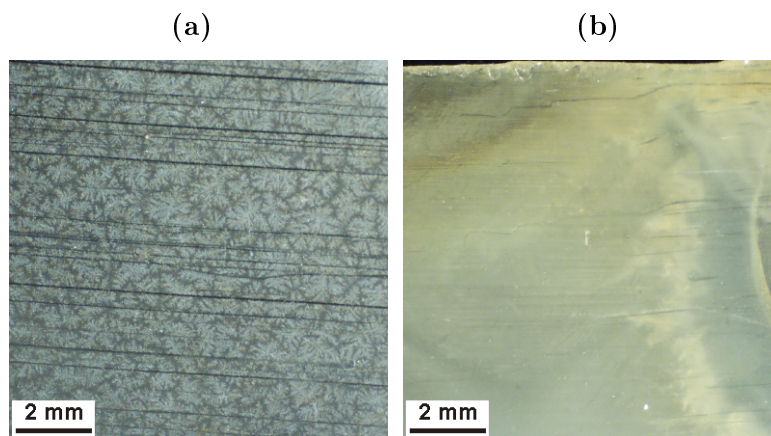
**(a)**                                    **(b)**



**Figure 4.10**: Scratch tests. $Rb_4[Nb_6Cl_{18}]$ particles on glass. **(a)** Particles deposited by SST-1. **(b)** Particles deposited by SIT-6.

# Chapter 5

# Conclusions

The main goal of this work has been to investigate the use of metal-rich niobium halide cluster compounds with the formula $M_4^I[Nb_6Cl_{18}]$ ($M^I$ = Na, K or Rb) as precursor to achieve the deposition of pure metallic niobium particles on the surface of a variety of metallic and non-metallic substrates. The results obtained have confirmed that it is possible to deposit metal-rich niobium halide clusters on various surfaces and that these particles can be decomposed using a thermal treatment, thereby obtaining metallic niobium particles on the surface. The observed change in material properties indicates that the investigated coatings could find applications as surface hardening processes or as abrasion resistant coatings.

In terms of particle distribution, the results obtained indicate that small cluster particles can be deposited on the surfaces of metallic substrates as well as on glass. It has also been shown that it is possible to achieve a homogeneous particle deposition pattern, both in the physical distribution of the niobium particles over the substrate as well as in its size. In particular, it has been demonstrated that particle diameters in the lower micrometer range (from 200 nm to 5 µm) can be consistently obtained.

In this respect, several process parameters have been systematically varied in order to investigate their influence on the particle size and morphology. The available evidence indicates that the size of the particles mainly depends on the deposition method and the type of substrate. It has been shown that the smallest particles can be achieved with the use of the SST-3 and SIT-8 deposition methods. With regards to the substrates, it has been found that the particles deposited on tin are always smaller than those deposited on other metals. The cation in the cluster compound $M_4^I[Nb_6Cl_{18}]$ used as precursor ($M^I$ = Na, Rb, or K) has also been found to play an important role in the size and distribution of the particles, obtaining outstanding results with the deposition of $Rb_4[Nb_6Cl_{18}]$.

The shape of the obtained particles has also been found to be dependent on the precursor deposition method. The solution spreading technique without external drying influence (SST-1) has been found to originate predominantly cylindrically shaped particles. This phenomenon

is thought to be mostly due to the slow drying rate of the solvent. It has been also observed that if this drying rate is increased (SST-2 and SST-3) the particles obtained are spherical instead of cylindrical.

The deposition of the cluster precursor using SIT techniques has been found to lead mainly to spherically shaped particles. Cylindrical particles have only been observed in some SIT-4 and SIT-5 samples, although this is not the usual behaviour with these cases. This is consistent with the observation on SST methods that slow solvent drying rates are a significant factor for the obtention of cylindrical particles.

It has been also demonstrated that the cluster compounds deposited on the substrates can be thermally decomposed if they are treated at a temperature above 600 °C thereby obtaining small metallic niobium particles. Similarly to the deposition of the cluster particles, the size range of these niobium particles has also been found to depend on the deposition method and on the substrate. As expected, the size of the resulting niobium particles has been observed to be smaller than the originating precursor particles.

The results for the laser decomposition process have been significantly different to those achieved with thermal treatment in an oven. No clear decomposition of the precursor particles could be achieved in any of the laser-treated samples. A significant result, however, is that SIT-6 coatings on glass have been found protect the glass substrate against radiation. The fact that the coating does not get damaged by low beam intensities suggests that the beam is reflected away by the cluster particles. In regards to this, a possible application for this coating could be as a radiation protective layer.

The behaviour of the cluster deposition and decomposition depending on the ligands in the cluster ion has been also investigated. In order to do that, clusters based on the same cluster core as $[Nb_6Cl_{18}]^{4-}$ but with different ligands have been used.

The results indicate that these cluster types $[Nb_6Cl_{18-z}X_z]^{n-}$ with X different from Cl and z = 4, 18 can be deposited using the same methods used for the chlorine-based cluster. However, the deposition of the methanolate-based and the water-based cluster lead in most of the cases to larger particles than the deposition of the chloride-based cluster. For the case of the methanolate-based cluster, this is due to the significantly larger ligands surrounding the niobium core, and for the case of the water-based cluster, this is due to the water molecules surrounding the cluster. Another disadvantage of the deposition with these clusters is the alkali chloride particles that have also been observed to precipitate during the precursor deposition process. This is a result of the chloride ions in excess in the solution, which originate from the ligand exchange process during the preparation of the cluster solution for the deposition.

With regards to the decomposition of the water- or methanolate-based cluster particles, this has been studied following the general methodologies described in the experimental section. The results indicate that the decomposition has been mostly incomplete or inexistent. Therefore, it can be stated that the best results in terms of particle deposition and later decomposition

are achieved with the use of $M_4^I[Nb_6Cl_{18}]$ ($M^I$ = Na, K, Rb) as niobium precursor.

Some preliminary studies on possible properties and applications for these new niobium coatings have also been conducted. Their application in catalysis has been studied, which has shown that the cluster on inert surfaces does not have catalytic activity for the hydrogenation of alkenes (the chosen reaction). Moreover, the possible enhancement of the catalytic properties of other metals has also been studied, leading to the conclusion that the catalytic activity diminishes with the increase in cluster covering. This is due to the fact that the catalytic sites are mostly covered by the non-reactive cluster particles.

The hardening of surfaces has been also studied for some selected niobium-coated samples. These experiments lead to the conclusion that the niobium metal particles do enhance the superficial hardness of the treated substrates. However, the results are not conclusive in all the tested cases. Further work is required to properly characterize the hardening effect on the studied surfaces.

The last application that has been studied is the potential use of the niobium coatings as abrasion or wear resistant coatings. For this purpose, the adhesion of the coating to the substrates has been tested. The results indicate that the coated samples experience an increase in abrasion resistance with respect to the uncoated material.

# Chapter 6

# Outlook

The scope for further research in this subject can be divided in two different lines of work: 1) the obtention of smaller niobium particles to improve the covering of the surface and 2) the better characterization of the coating properties to facilitate its use as surface treatment for engineering applications.

With regards to the deposition of the cluster particles, a major covering of the substrate can be achieved if smaller particles are obtained. So far, the mean size of the deposited particles range from 200 nm to 5 µm. It is thought, however, that these sizes can be diminished to a few nanometres by increasing the drying rate of the solvent and / or by increasing the temperature during the deposition process and / or by decreasing the cluster concentration in the precursor solution. However, the use of this last process would also reduce the amount of cluster deposited on the substrate and therefore the coating would also be reduced. This procedures should be further investigated.

With regards to the potential applications, it has already been shown that the niobium cluster coated samples have no effect in the catalysed hydrogenation of alkenes. However the hydrogenation of other compounds or the effect on other reactions should be investigated. The catalytic activity of the metallic niobium coated substrates should also be tested.

Currently, the most promising envisaged application is as surface protection in the form of hardening coating and / or as wear and abrasion protection coating. On one side, the first experiments on the hardness of the pieces showed interesting results, although they are not conclusive enough and it should be further investigated (see section 4.2). An increased number of tests on the complete range of substrates and deposition methods used would provide a better characterization of the improvement achieved by the coating. Its application as wear and abrasion resistant coating should also be further investigated. The use of standardized scratch tests on the available substrate-coating combinations would also provide a better characterization of the improvement achieved.

On the other side, other different applications for the niobium coating can be envisaged. As

described in section 1.2.1, niobium can be used as an additive in steel in order to avoid corrosion. For this reason, once an improved covering of the substrate is achieved, a niobium coating could also be used as a corrosion resistant coating. It is also well known that niobium has a high melting point and a relatively low thermal conductivity. Consequently, it may be considered as a candidate for thermal barrier coatings.

# Chapter 7

# Summary

Numerous methods for surface treatment are currently very important industrial processes of widespread use in a variety of engineering applications. The surface modification of various materials with particles of sizes down to the nano scale constitutes a good example of a new kind of treatments that is currently quickly becoming technologically important. A new, promising line of investigation in this area is the use of transition metal cluster compounds to modify surfaces. The main goal of this work is to investigate the use of metal-rich niobium halide cluster compounds with the formula $M_4^I[Nb_6Cl_{18}]$ ($M^I$ = Na, K or Rb) as precursors to achieve the deposition of pure metallic niobium particles on the surface of a variety of metallic and non-metallic substrates.

The deposition of the metal on the surface is conducted in four steps: cluster synthesis and precursor solution preparation, substrate preparation, cluster deposition and cluster decomposition.

The cluster preparation phase consists of two parts: the synthesis of the cluster compound and the production of the precursor solution. The cluster compound used is the already mentioned niobium cluster halide, which is prepared in the form of a dark green powder. The starting materials are elemental niobium powder, $NbCl_5$ and carefully dried $M^ICl$. The chemical reaction is carried out following a high temperature solid state chemistry procedure summarized in the reaction shown in 7.1 [23]. For the preparation of the final cluster solution, several solvents have been tested (e.g. acetone, methanol, or water), and methanol is the one that has provided the best results with regards particle sizes and coating homogeneity.

$$20 \, M^ICl + 14 \, NbCl_5 + 16 \, Nb \xrightarrow{\Delta} 5 \, M_4^I[Nb_6Cl_{18}] \qquad (M^I = Na, K, Rb) \qquad (7.1)$$

With regards to the substrate preparation, two aspects have been investigated. On one side, the effect of cleaning the surface of the substrate: the substrate is cleaned with acetone in order to remove any traces of grease or other contaminants that would difficult the deposition of the niobium precursor. It has been shown that this cleaning improves indeed the deposition of the

cluster particles, achieving smaller particle sizes and more homogeneous distributions on the cleaned substrates. On the other side, concerning the effect of the passivation layer present on the surface of some metallic substrates, it has been observed that the removal of this layer affects negatively the deposition of the cluster. The results indicate that whenever this layer is removed, the distribution of the cluster particles becomes less homogeneous.

In the third step, the cluster deposition, the cluster material from the prepared solution is deposited on the substrates. In order to obtain uniformly distributed cluster particles on the substrate surfaces, two different groups of techniques have been tested, the solution spreading technique (SST) and the substrate impregnation technique (SIT). In the SST method the cluster solution is evenly distributed on the cleaned surface and the solvent is slowly evaporated at room temperature (SST-1). Some variations have been applied to this method, for example the use of an ultra-sound bath during the drying of the samples (SST-2) or the use of external drying (dryer, SST-3). In the SIT method the previously cleaned substrate is placed in the cluster solution and left there up to 15 days without evaporation of the solvent (SIT-6). As in the case of the SST, also some variation have been applied to the methods as, for example, the drying of the solution at room temperature or using external heat (SIT-4 and SIT-5 respectively), or the reduction of the pressure in the reaction tube, also at room temperature or using external heat (SIT-7 and SIT-8 respectively).
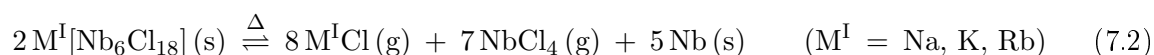
The particle size has been found to be highly dependent on the deposition method and the substrate. The results indicate that the SST methods (with and without externally-influenced drying, SST-1, SST-2 and SST-3) produce highly homogeneous particle distributions on metallic and non-metallic surfaces. Particles from 300 nm to 10 µm in diameter can be obtained with the use of these methods, with SST-3 being the technique that has produced the smallest particles among the solution spreading techniques.

The investigated SIT methods have again confirmed that the particle size and distribution is highly dependent on the deposition method and the substrate. In particular, it has been possible to obtain smaller particle sizes than with SST methods. The best results have been achieved with the methods without solution drying (SIT-6 for glass substrates and SIT-7 and SIT-8 for all substrates). The first one of these methods, the SIT without evaporation of the solution and without reduced pressure (SIT-6), works very well on glass substrates, achieving small particle sizes with a maximal diameter size of 1 µm. However, these good results could not be repeated on metallic substrates. With regards to the methods with reduced pressure (SIT-7 and SIT-8), the results for the metals have been very good. The particles have achieved sizes down to 200 nm with rather homogeneous distributions.

The use of these methods (SST and SIT) on substrates with different shapes (e.g. foils, chunks or grains) has shown that it is possible to obtain microscopic homogeneous cluster particle distributions on foils as well as on substrates with irregular shapes. However, the macroscopic distribution of these last substrate types is mostly not homogeneous.

Finally, the fourth step of the process consists on the decomposition of the deposited cluster

particles in order to obtain metallic niobium on the surface of the substrate. In order to achieve this decomposition, energy must be applied to the cluster particles. Two kinds of decomposition methods have been studied. The first one is the decomposition by direct heating. This decomposition follows the reaction shown in 7.2, which was studied in the late 60's [39].

$$2\,\mathrm{M^I[Nb_6Cl_{18}]\,(s)} \;\overset{\Delta}{\rightleftharpoons}\; 8\,\mathrm{M^I Cl\,(g)} \,+\, 7\,\mathrm{NbCl_4\,(g)} \,+\, 5\,\mathrm{Nb\,(s)} \qquad (\mathrm{M^I = Na,\ K,\ Rb}) \qquad (7.2)$$

It has been demonstrated that even after short heating periods (e.g. 5 min) the chloride and alkali ions can be removed from the surface of the substrate (in the form of volatile $NbCl_4$ and $M^I Cl$) and only niobium particles remain as metallic coating. These gaseous compounds can be eliminated with the use of a vacuum pump. The size of the resulting niobium particles has been found to be only slightly smaller than that of the precursor particles.

The second decomposition method tested is based on the use of laser. Due to the risk of reflected beams with the use of metallic substrates, only cluster coated glass has been used for these experiments. The analysis of the results indicate that the cluster particles could not be decomposed with the variations of the process parameters that have been studied (beam intensity, distance from focus, wave length and exposure time). However, some interesting behaviours have been observed during the test of the SIT-6-coated glass samples that indicate that the cluster coating could be used as optical coating or as radiation protection. More research is needed in this area.

Some studies on the influence of the ligands on the particle distribution and sizes of the niobium clusters have also been carried out. To that effect, cluster compounds with the chemical formula $[Nb_6Cl_{18-z}X_z]^{n-}$ (with X different from Cl and z = 4, 18) have been used as niobium precursors. The results have shown that it is possible to homogeneously deposit these niobium cluster types, with particle sizes similar to those of the chloride cluster. However, the decomposition of these cluster particles has been less successful, since it has been in most of the cases inexistent or incomplete using the same parameters as for the decomposition of the chloride cluster. Moreover, alkali chloride particles have been also deposited in most of the cases, coming from the synthesis process of the cluster compound, which is performed through ligand exchange.

In the final part of the project, some possible applications of the cluster and the obtained niobium coatings have been studied. On one side, the possible application of the niobium cluster coating as supported catalyst for heterogeneous catalysis has been tested. However, the results of the reaction of the cluster particles on inert surfaces showed no catalytic effect for the hydrogenation of 1-hexene and the use of the cluster on catalytic surfaces for the mentioned reaction showed encapsulation of the catalytic sites, and, consequently, a reduction of the conversion rate.

On the other side, the possible applications of the metallic niobium coating as a mechanical coating have also been studied. In particular, the hardness increase and the abrasion resistance

of the resulting new coating composed of small niobium particles have been tested.  The results
of these tests have been favourable, resulting in an increased hardness of the coated samples
compared to the uncoated substrates and an increase of the abrasion resistance of the coated
samples.  These results indicate that these new coatings could have potential applications as
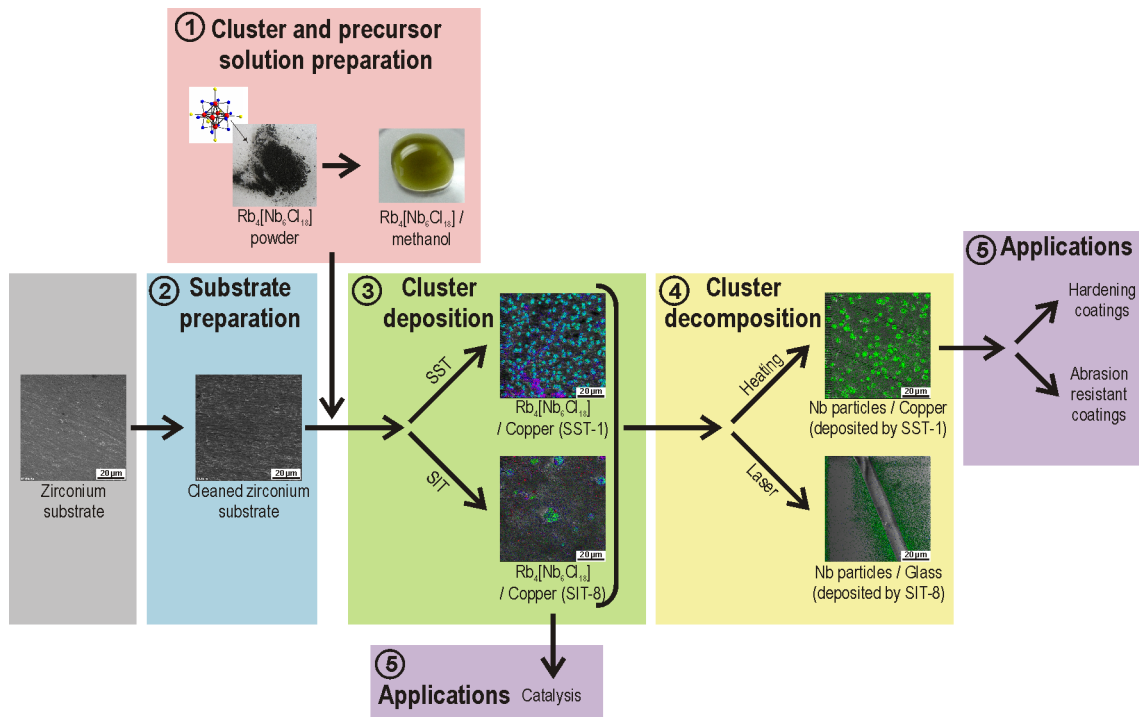hardening coatings or abrasion resistant coatings.



**Figure 7.1**: Summary of the main parts and achivements of the project.

# Bibliography

[1] H. D. Callister. *Fundamentals of Materials Science and Engineering*, chapter 1. John Wiley & Sons, New York, USA, 2001.

[2] R. A. Haefer. *Oberflächen- und Dünnschichttechnologie*, volume 1, chapter 1. Springer, Berlin, Germany, 1987.

[3] W. Tillmann and E. Vogli. *Modern Surface Technology*, chapter 1. Willey-VCH, Weinheim, Germany, 2004.

[4] M. Oles, E. Nun, G. Dombacher, and B. Schleich. In $1^{st}$ *Annual International IEEE-EMBS Special Topic Conference on Microtechnologies in Medicine & Biology*, pages 331–333, Lion, France, 2000.

[5] Z. Cerman, A. K. Stosch, and W. Barthlott. *Biol. Unserer Zeit*, 34:290–296, 2004.

[6] M. Fröba, W. Scheld, C. Gath, and F. Hoffmann. *Chem. Unserer Zeit*, 38:162–171, 2004.

[7] G. Liang, J. Huot, S. Boily, A. Van Neste, and R. Schulz. *J. All. Comp.*, 292:247–252, 1999.

[8] M. Breysse, G. Djega-Mariadassou, S. Pessayre, C. Geantet, M. Vrinat, G. Perot, and M. Lemaire. *Catal. Today*, 84:129–138, 2003.

[9] I. P. Gibson. *Thin Solid Films*, 83:27–36, 1981.

[10] N. P. Padture, M. Gell, and E.H. Jordan. *Science*, 296:280–284, 2002.

[11] I. Nowak and M. Ziolek. *Chem. Rev.*, 99:3606–3624, 1999.

[12] H. Briehl. *Chemie der Werkstoffe*, chapter 3. B. G. Teubner Verlag / GWV Fachverlage GmbH, Wiesbaden, Germany, 2008.

[13] Values extracted from Companhia Brasileira de Metalurgia e Mineração (Brasilian Company of Metallurgy and Minery, Araxá, Brasil.

[14] F. A. Cotton. *Inorg. Chem.*, 2:1166–1171, 1963.

[15] F. A. Cotton. *Inorg. Chem.*, 3:1217–1220, 1964.

[16] F. A. Cotton. *Metal Clusters in Chemistry*, volume 1, chapter 1. Wiley-VCH, Weinheim, Germany, 1999.

[17] W. A. de Heer. *Metal Clusters at surfaces*, chapter 1. Springer, Berlin-Heidelberg, Germany, 2000.

[18] M. Abe, T. Michi, A. Sato, T. Kondo, W. Zhou, S. Ye, K. Uosaki, and Y. Sasaki. *Angew. Chem.*, 115:3018–3021, 2003.

[19] C. Perrin, S. Cordier, S. Ihmaine, and M. Sergent. *J. All. Comp.*, 229:123–133, 1995.

[20] H. Schäfer and H. G. von Schnering. *Angew. Chem.*, 76:833–849, 1964.

[21] P. J. Kuhn and R. E. McCarley. *Inorg. Chem.*, 4:1482–1486, 1965.

[22] A. Simon, H. G. von Schnering, H. Wöhrle, and H. Schäfer. *Z. Anorg. Allg. Chem.*, 339:155–170, 1965.

[23] P. B. Fleming, L. A. Müller, and R. E. McCarley. *Inorg. Chem.*, 6:1–4, 1967.

[24] A. Simon. *Angew. Chem. Int. Ed. Engl.*, 27:159–183, 1988.

[25] C. Perrin and M. Sergent. *Eur. J. Solid State Inorg. Chem.*, 28:933–948, 1991.

[26] T. Hughbanks. *J. All. Comp.*, 229:40–53, 1995.

[27] J. D. Corbett. *J. Chem. Soc., Dalton Trans.*, 5:575–587, 1996.

[28] G. Meyer. *Chem. Rev.*, 88:93–107, 1998.

[29] N. Prokopuk and D. F. Shriver. *Adv. in Inorg. Chem.*, 46:1–49, 1999.

[30] J. D. Corbett. *J. Chem. Soc., Dalton Trans.*, 13:1961–1968, 2000.

[31] P. Braunstein and R. Bender. *Organometallics*, 1:1236–1238, 1982.

[32] D. S. Shephard, T. Maschmeyer, G. Sankar, J. M. Thomas, D. Ozkaya, B. F. G. Johnson, R. Raja, R. D. Oldroyd, and R. G. Bell. *Chem. Eur. J.*, 4:1214–1224, 1998.

[33] R. J. Phuddephatt. *Metal Clusters in Chemistry*, volume 2, chapter 2.1. Wiley-VCH, Weinheim, Germany, 1999.

[34] F. Grasset, S. Cordier, F. Dorson, Y. Molard, C. Perrin, H. Haneda, and M. Mortier. contribution in the International Workshop on Transition Metal Clusters, Rennes, France, 2008.

[35] M. Remskar, M. Virsek, A. Mrzel, and A. Jesihr. contribution in the International Workshop on Transition Metal Clusters, Rennes, France, 2008.

[36] G. Gille. contribution in the Materials' Days, Functional Materials and Nanotechnology, Rostock, Germany, 2008.

[37] P. Braunstein and J. Rosé. *Metal Clusters in Chemistry*, volume 2, chapter 2.2. Wiley-VCH, Weinheim, Germany, 1999.

[38] F. Lefebvre, J.-P. Candy, and J. M. Basset. *Metal Clusters in Chemistry*, volume 2, chapter 2.7. Wiley-VCH, Weinheim, Germany, 1999.

[39] A. Simon, H.-G. von Schnering, and H. Schäfer. *Z. Anorg. Allg. Chem.*, 361:235–248, 1968.

[40] N. Prokopuk and D. F. Shriver. *Chem. Mater.*, 10:10–12, 1998.

[41] R. A. Mackay and R. F. Schneider. *Inorg. Chem.*, 6:549–552, 1967.

[42] L. F. Piedra-Garza and M. Köckerling. *Inorg. Chem.*, 45:8829–8831, 2006.

[43] Information from the German Association of Glass Industries (Bundesverband Glasindustrie e.V.).

[44] T. P. Seward III and T. Vascott. *High temperature glass melt property database for process modeling*. The American Ceramic Society, Westerville, Ohio, USA, 2005.

[45] B. H. W. S. de Jong. *Ullmann's Encyclopedia of Industrial Chemistry*, volume 15. Wiley-VCH, Weinheim, Germany, 2000.

[46] M. Zinke-Allmang, L.C. Feldman, and M.H. Grabow. *Surf. Sci. Rep.*, 16:377–463, 1992.

[47] H. Brune. *Metal Clusters at Surfaces*, chapter 3. Springer, Berlin-Heidelberg, Germany, 2000.

[48] F. Schweyer-Tihay, C. Estournès, P. Braunstein, J. Guille, J.-L. Paillaud, M. Richard-Plouet, and J. Rosé.

[49] S. Grosshans-Vielès, P. Croizat, J.-L. Paillaud, P. Braunstein, O. Ersen, J. Rosé, B. Lebeau, P. Rabu, and C. Estournés. *J. Clus. Sci.*, 19:73–88, 2008.

[50] B. Spreckelmeyer. *Z. Anorg. Allg. Chem.*, 365:225–241, 1969.

[51] T. Pancur. *Untersuchung der Isomerisierungsdynamik von Azobenzolen und der strahlungslosen Desaktivierung von Nukleobasen mit Hilfe der Femtosekunden-Fluoreszenzspektroskopie.* PhD thesis, University of Kiel, Germany, 2004.

[52] A. Flemming and M. Köckerling. *Angew. Chem. Int. Ed.*, 48:2605–2608, 2009.

[53] J. A. Parsons, A. Vongvusharintra, and F. W. Koknat. *Inorg. Nucl. Chem. Letters*, 8:281–286, 1972.

[54] S. T. Oyama. *Handbook of Heterogeneous Catalysis*, volume 1. Wiley-VCH, Weinheim, Germany, 1997.

[55] D. E. Wigley. *Encyclopedia of Inorganic Chemistry*, volume 5. John Wiley & Sons, Chichester, England, 1994.

[56] G. A. Somorjai. *Introduction to Surface Chemistry and Catalysis*, chapter 1. John Wiley, New York, USA, 1994.

[57] C. Berg, T. Schindler, M. Kantlehner, G. Niedner-Schatteburg, and V. E. Bondybey. *Chemical Physics*, 262:143–148, 2000.

[58] M. Castiglioni, R. Giordano, and E. Sappa. *J. Organomet. Chem.*, 258:217–234, 1983.

[59] P. Michelin-Lausarot, G. A. Vaglio, and M. Valle. *J. Organomet. Chem.*, 275:233–237, 1984.

[60] P. J. Dyson, D. J. Ellis, and G. Laurenczy. *Adv. Synth. Catal.*, 345:211–215, 2003.

[61] T. Yamamoto, T. Shido, S. Inagaki, Y. Fukushima, and M. Ichikawa. *J. Am. Chem. Soc.*, 118:5810–5811, 1996.

[62] R. Raja, T. Khimyak, J. M. Thomas, S. Hermans, and B. F. G. Johnson. *Angew. Chem. Int. Ed.*, 40:4638–4662, 2001.

[63] T. Iizuka, K. Ogasawara, and K. Tanabe. *Bull. Chem. Soc. Jpn.*, 56:2927–2931, 1983.

[64] K. Tanabe and S. Okazaki. *Appl. Catal. A*, 133:191–218, 1995.

[65] R. Burch and R. Swarnakar. *Appl. Catal.*, 70:129–148, 1991.

[66] J.-M. Jehng and I. E. Wachs. *Catal. Today*, 16:417–426, 1993.

[67] T. Iizuka, Y. Tanaka, and K. Tanabe. *J. Molec. Catal.*, 17:381–389, 1982.

[68] M. D. Phadke and E. I. Ko. *J. Catal.*, 100:503–506, 1986.

[69] G. Miller. *J. All. Comp.*, 229:93–106, 1995.

[70] S. Kamiguchi, I. Takahashi, H. Kurokawa, H. Miura, and T. Chihara. *Appl. Catal. A*, 309:70–75, 2006.

[71] S. Kamiguchi, S. Iketani, M. Kodomari, and T. Chihara. *J. Clus. Sci.*, 15:19–31, 2004.

[72] S. Kamiguchi, S. Takaku, M. Kodomari, and T. Chihara. *J. Molec. Catal. A*, 260:43–48, 2006.

[73] S. Kamiguchi, A. Nakamura, A. Suzuki, M. Kodomari, M. Nomura, Y. Iwasawa, and T. Chihara. *J. Catal.*, 230:204–213, 2005.

[74] H. Arnold, F. Döbert, and J. Gaube. *Handbook of Heterogeneous Catalysis*, volume 7. Wiley-VCH, Weinheim, Germany, 1997.

[75] R. Elsing. *Beschichten mit Hartstoffen*, chapter 1. VDI-Verlagg, Düsseldorf, Germany, 1992.

[76] UK WebElements Ltd. Extracted from the website www.webelements.com.

[77] Extracted from the website of the Magnetic Materials Group in the University of Birmingham, UK.

[78] K. Sato. *Prog. Org. Coatings*, 8:1–18, 1980.

[79] Extracted from Armoloy of PHILADELPHIA, INC., www.armoloycompany.com.

[80] Extracted from Hardide Coatings Limited, www.hardide.com.

# Appendix A

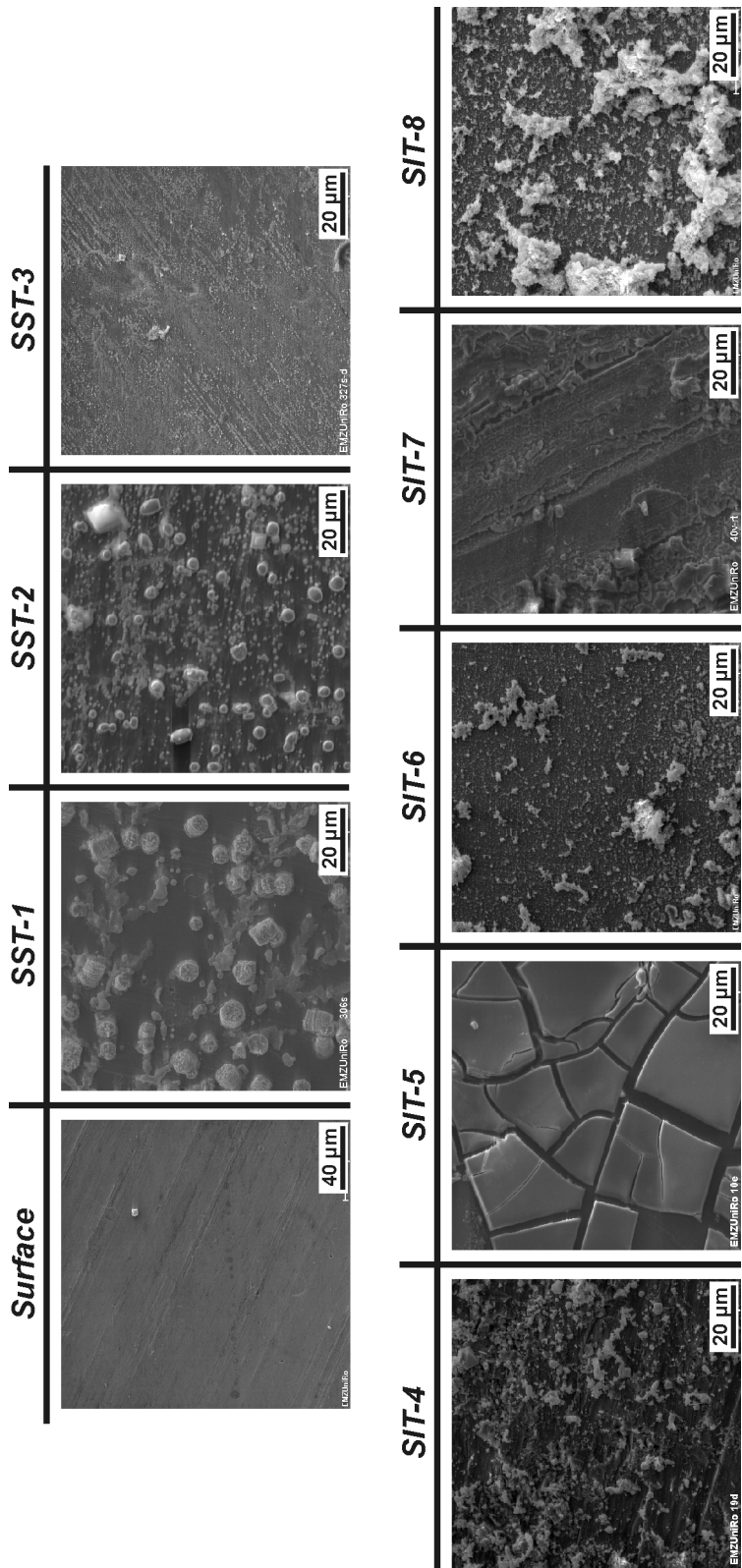# Deposition methods. SEM Micrographs

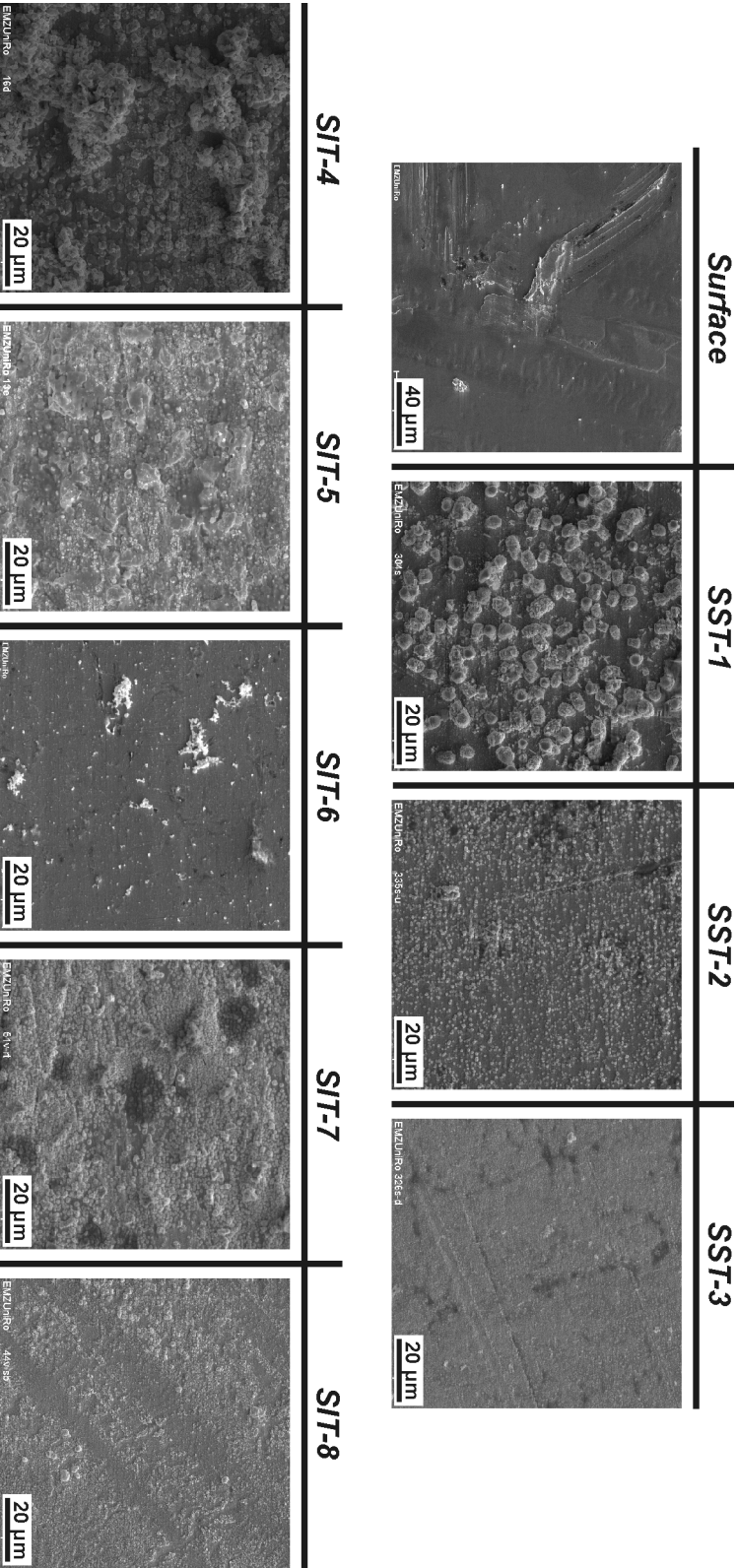**Figure A.1:** Metallic surface and cluster deposition on aluminium.

**Figure A.2:** Metallic surface and cluster deposition on copper.
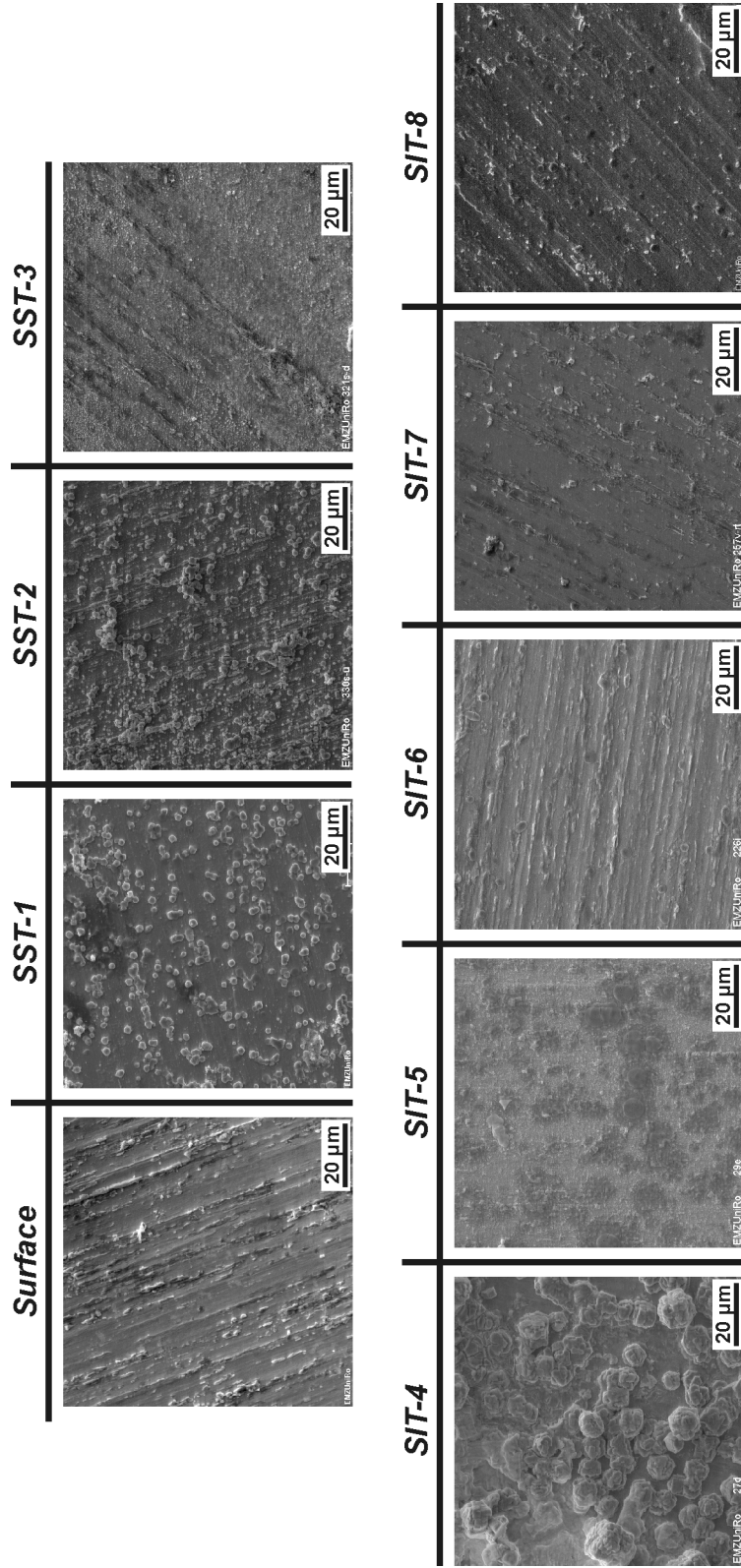
97



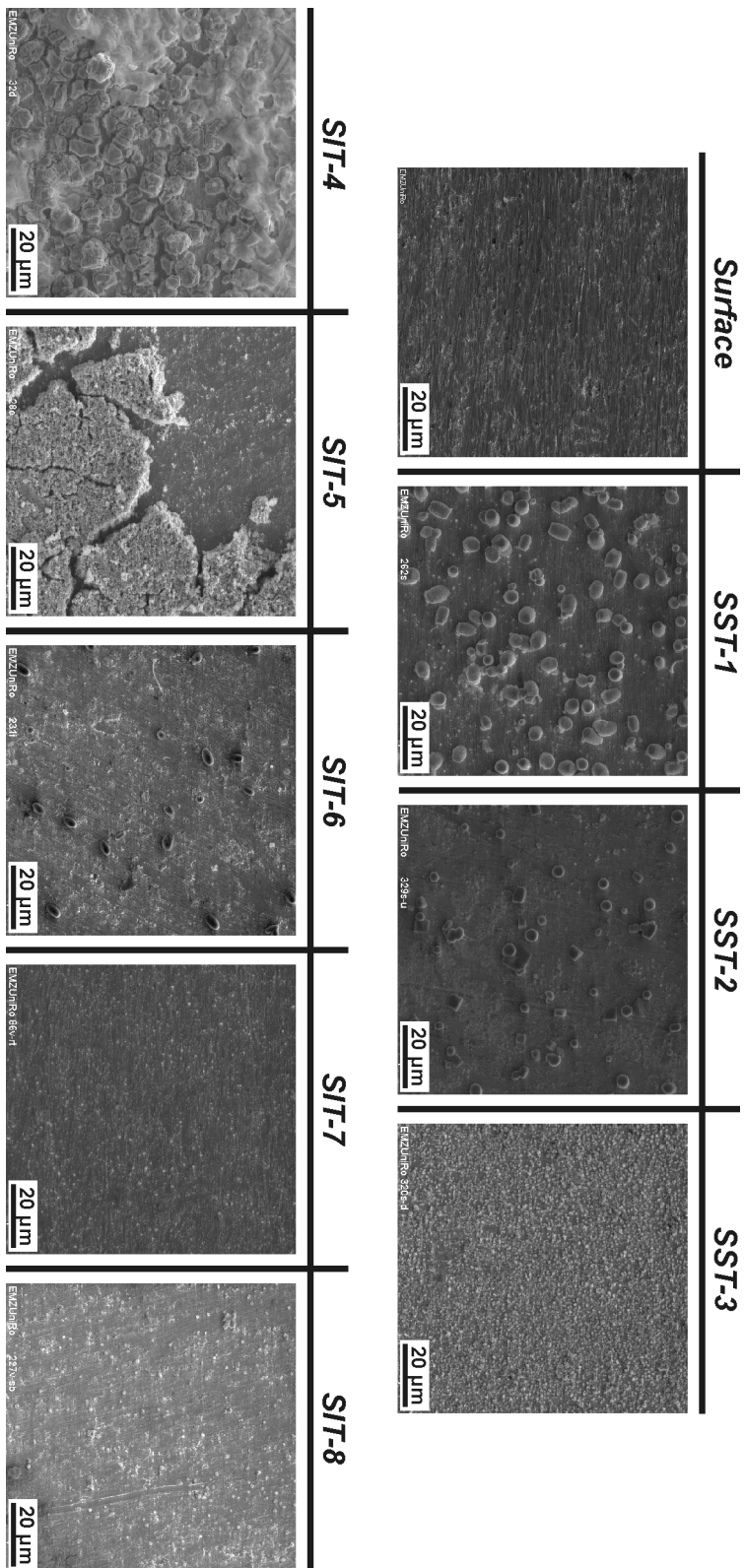**Figure A.3:** Metallic surface and cluster deposition on molybdenum.

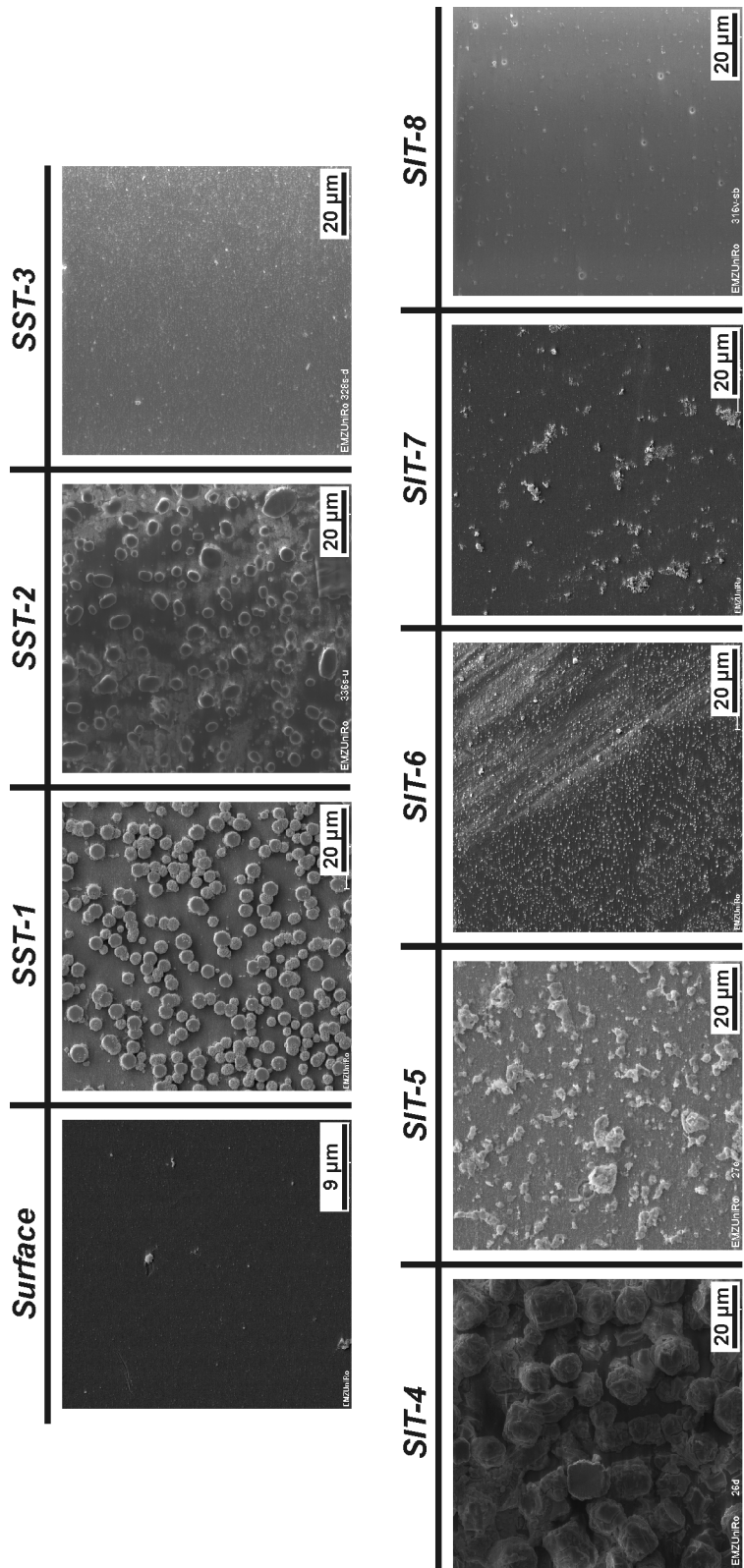**Figure A.4:** Metallic surface and cluster deposition on zirconium.

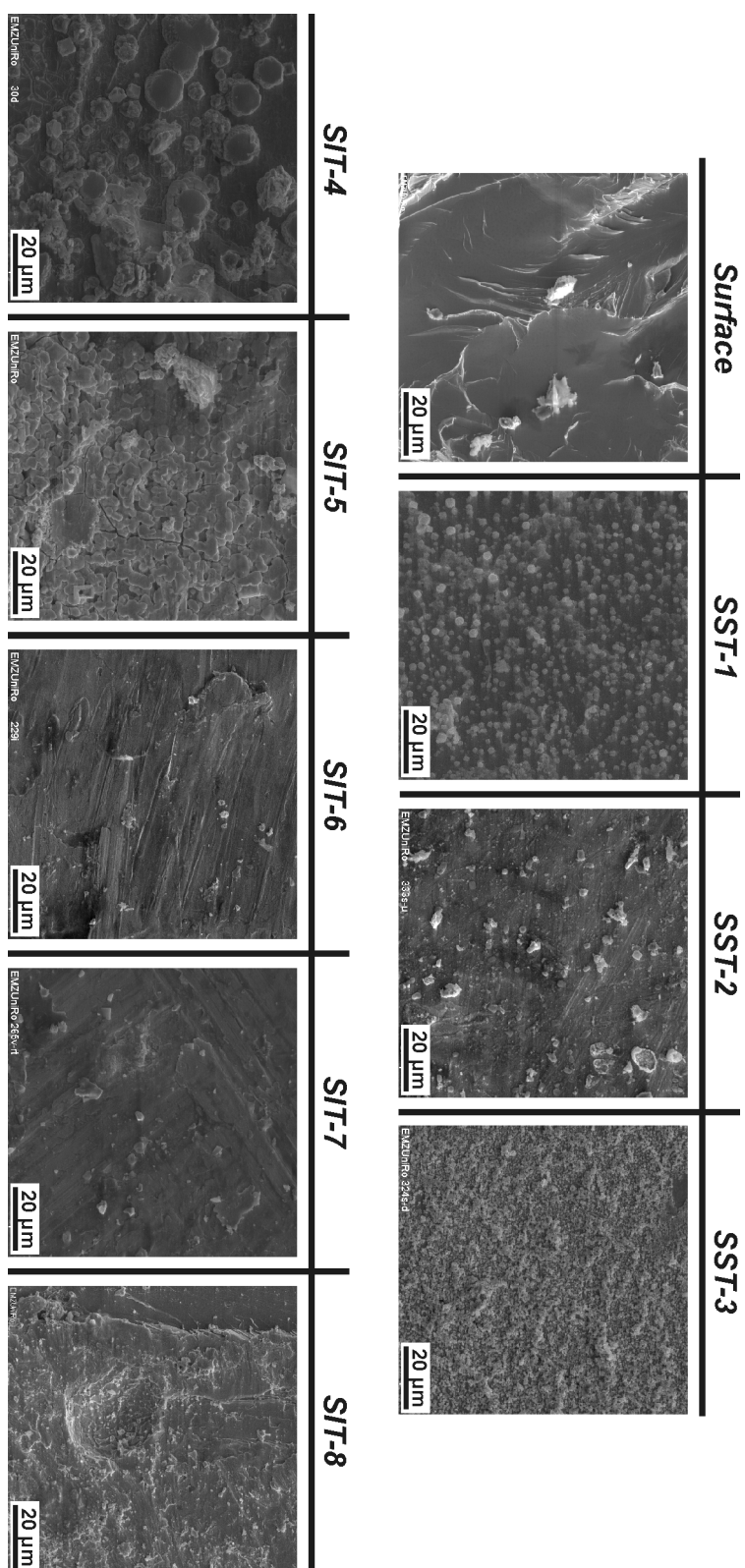**Figure A.5:** Glass surface and cluster deposition on glass.

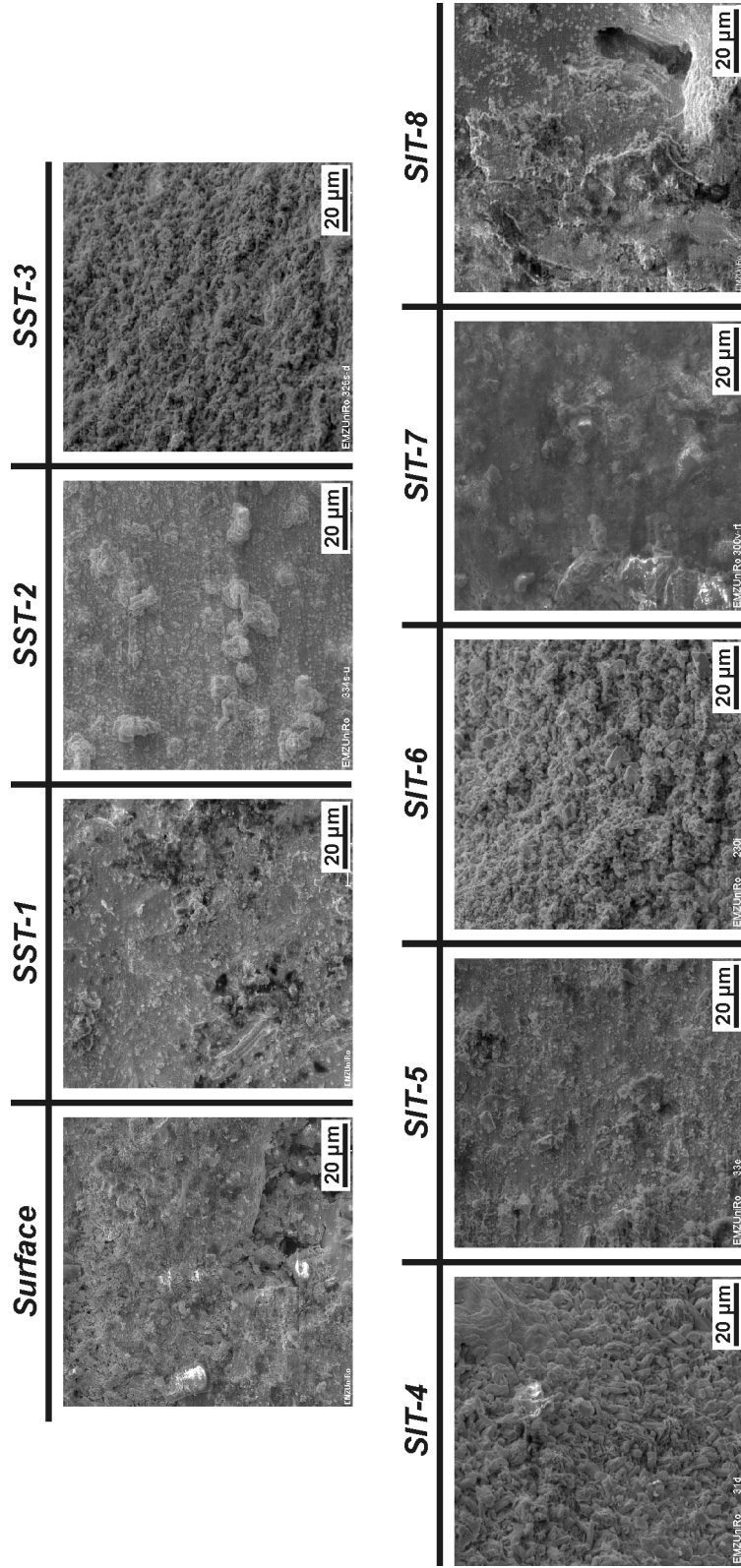**Figure A.6:** Metallic surface and cluster deposition on chromium.

**Figure A.7**: Metallic surface and cluster deposition on lead.
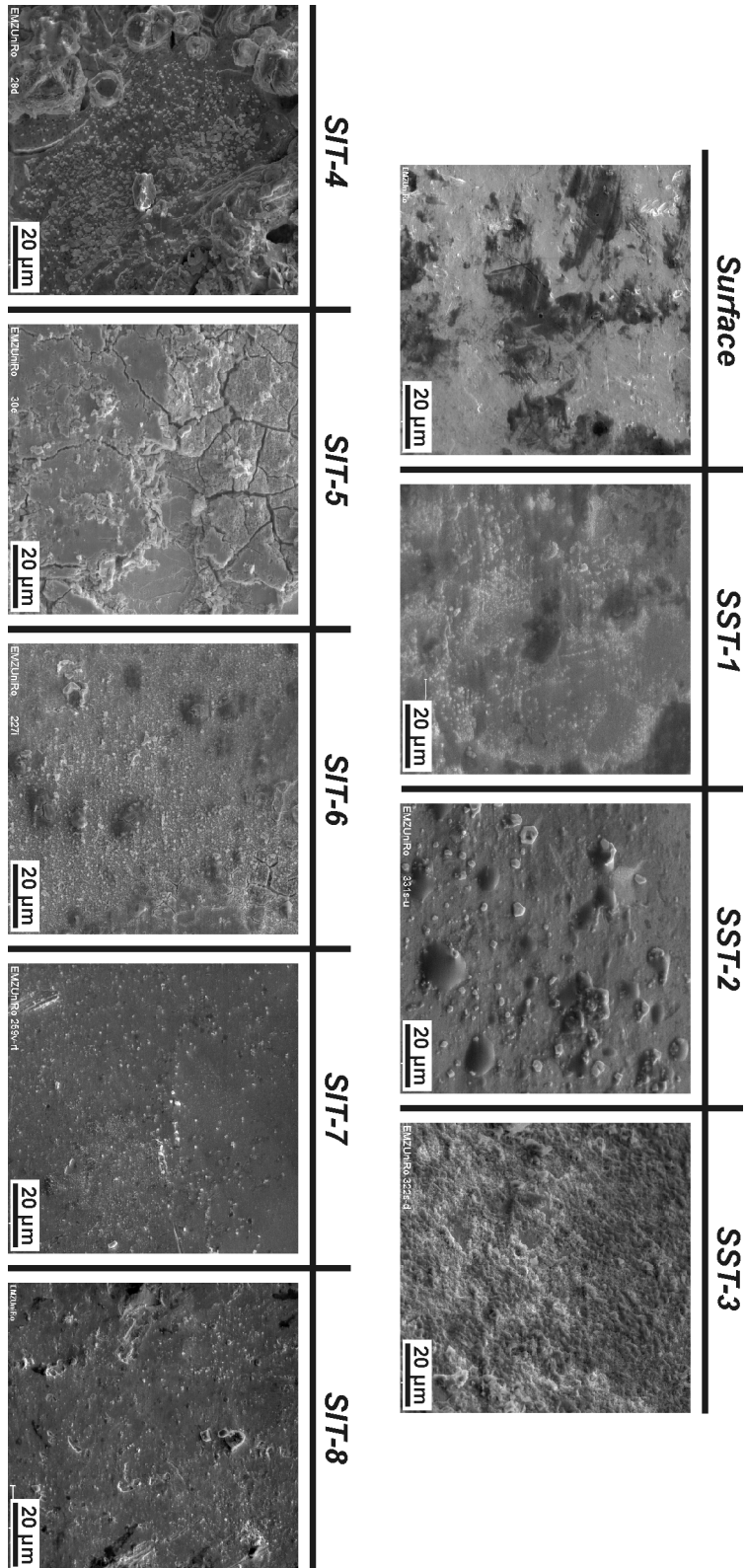
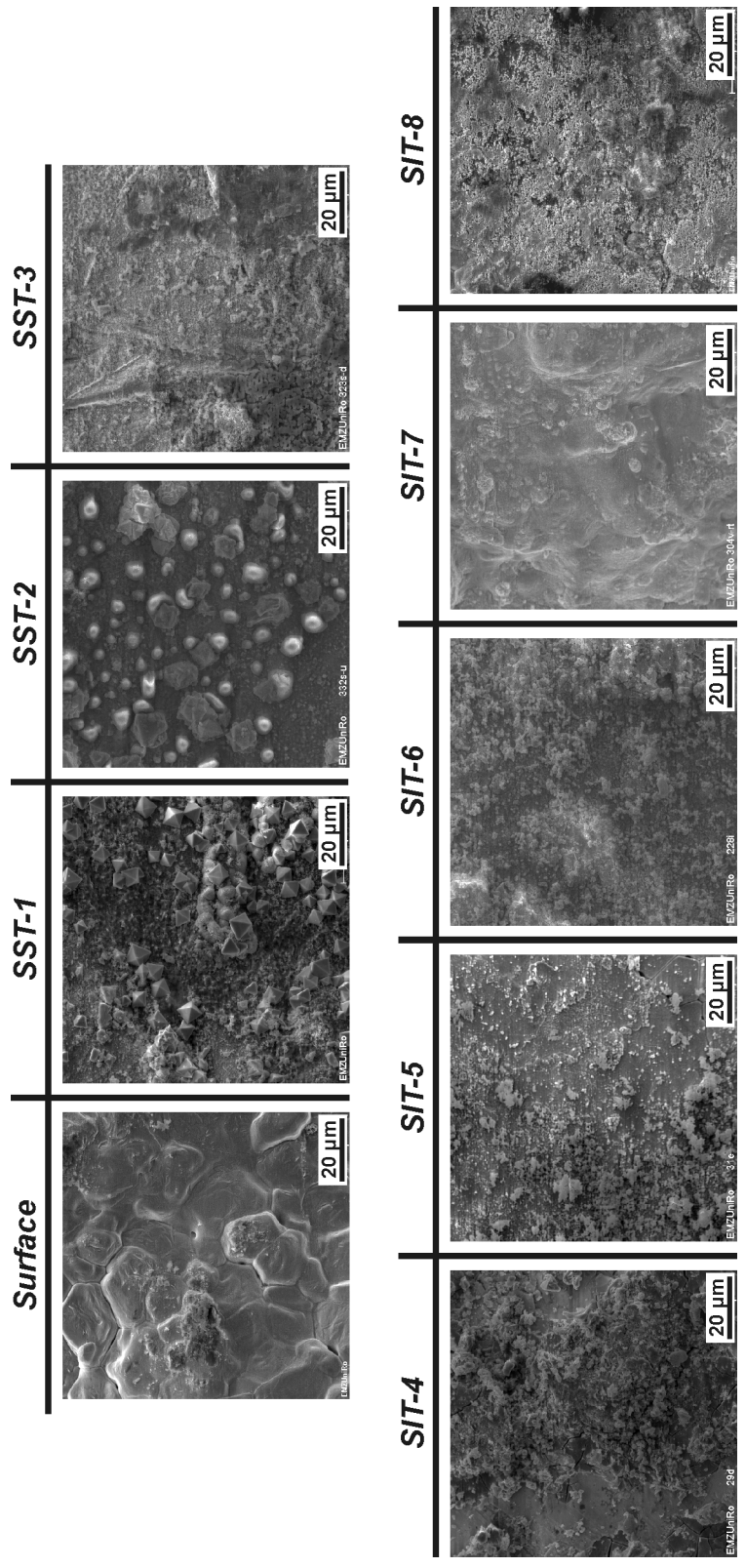**Figure A.8:** Metallic surface and cluster deposition on tin.

**Figure A.9:** Metallic surface and cluster deposition on zinc.